Carbon Intelligent Framework for Handling Uncertainty in Smart Energy Systems

GARG, ANKITA

Carbon Intelligent Framework for Handling Uncertainty in Smart Energy Systems

Ankita Garg

A thesis presented for the degree of

Doctor of Philosophy

Department of Computer Science

Durham University

United Kingdom

February 2025

Abstract

Carbon emissions are becoming a global concern responsible for climate change. The renewable energy sources (RESs) such as wind, solar, biomass are gaining importance to reduce emissions in the energy sector. However, these sources depend highly on various technical, economical, and environmental conditions and hence, a planned strategy is required to place different RESs based on their suitability. The thesis presents a detailed analysis on energy purchased/sold, costs associated with installing new RESs and the operational costs of existing electricity sources to reduce the total carbon emissions in the UK's residential sector.

The inherent intermittency in RESs introduces significant uncertainties, demanding robust uncertainty modelling. Most of the existing works fail to capture the dynamic fluctuations in the renewable integrated energy networks especially under extreme weather conditions. Therefore, a time-coordinated strategy is proposed to capture temporal correlations among uncertain parameters dynamically. The proposed method is compared with the traditional Markov Chain Monte Carlo technique, showing a notable shift in the probability density function under adverse weather events. Testing this approach on an IEEE 33-bus system results in an improved voltage profile and reduced power losses. Furthermore, renewable reliance and carbon emission factors are introduced to evaluate our method's performance, and these metrics reveal the network's sustainability and resilience.

Additionally, with the integration of RESs into modern power systems, energy consumers participate in the energy market making the entire network more complex and uncertain. Various strategies exist in the literature to address the real-time uncertainties in the distribution networks. However, the existing works do not consider the overall carbon emissions of the network under such uncertainties that need further attention. In this research, an integrated two-fold approach is proposed that combines competitive market mechanisms with cooperative strategies to enhance reliability and resilience in

distribution networks under uncertainty. In the normal operational stage, a competitive approach is adopted wherein an optimal price is determined to meet the required consumer demand, facilitating energy sharing among areas and minimising reliance on the grid, thereby reducing carbon emissions associated with conventional energy generation. To detect and identify an uncertain event within the network, a heuristic algorithm is proposed, which determines the hidden inter-dependencies among the different network input parameters. Finally, to mitigate the impact of these identified uncertainties, a cooperative approach is introduced wherein all areas leverage the battery storage facilities to ensure continuity of energy supply and minimise overall losses. During an uncertain event, a maximum reduction of 97% is observed in the carbon footprints for the proposed scheme while maintaining the overall profit.

Supervisors: Dr. Gagangeet Singh Aujla and Prof. Hongjian Sun

Acknowledgements

A PhD journey is more of a marathon than a sprint, and as I cross the finish line, I would like to thank everyone who has supported me along the way. I want to express my foremost gratitude to the almighty God for giving me strength throughout my PhD. I would like to start with a sanskrit shloka:

वक्रतुण्ड महाकाय सूर्यकोटि समप्रभ।
निर्विघ्नं कुरु मे देव सर्वकार्येषु सर्वदा॥

I would like to extend my sincerest thankfulness to my respected supervisors, Dr. Gagangeet Singh Aujla and Prof. Hongjian Sun. Your mentorship, patience and insights have provided me with invaluable support and guidance throughout my journey. Your thorough feedback has helped me to improve my research and your belief in my potential gave me the courage to face any hardships head-on and emerge stronger.

No words can express my heartful adoration towards my parents (Sanjay Garg and Ekta Garg), for providing their boundless love and support that has been the foundation of my success, and to my brother, Varun Garg, whose encouragement has been a strong source of strength. During the difficult times, your faith in me has been a beacon of hope. I want to extend my profound thanks to my parents-in-law, Dr. Ashok Jindal and Dr. Anita Jindal, for their unwavering understanding, as well as for fostering a supportive and peaceful environment that allowed me to concentrate on my PhD. I am fortunate to have the blessings of my late grandparents, as their wisdom and values have given me the courage to move forward with confidence and conviction. To my husband, Anish Jindal, I am extremely grateful for being my anchor, my cheerleader, and my greatest supporter during turbulent times. Your firm belief in me, your patience during long research

discussions during days and nights, and your love have been the bedrock upon which this achievement stands. I was blessed to carry a new life blossom within me, which has made the journey of my PhD extremely special. Now, as I write down these final words, my adorable daughter, Amyra, is here in this world with us. She has been one of my greatest sources of motivation, reminding me every day of the importance of resilience, perseverance and the joy of new beginnings.

This acknowledgment is incomplete without mentioning the contributions of Dr. Prasenjit Basak (my Masters' academic mentor), who have always guided me in the right direction; Dr. Jeyabalan Velandy (my Masters' Industrial mentor), who exposed me to the practical aspects of the theoretical engineering and Dr. Arijit Baral, who along with being a great mentor, encouraged my decision to pursue the PhD from Durham University.

I would like to thank all my friends (especially Akshay Kapoor) and family who have encouraged me directly or indirectly to follow my passion.

Thank you all!

Ankita

Contents

Declaration

The work in this thesis is based on research carried out at the Department of Computer Science, Durham University, England, UK. No part of this thesis has been submitted elsewhere for any other degree or qualification, and it is the sole work of the author unless referenced to the contrary in the text.

Some of the work presented in this thesis has been published in journals and conference proceedings - the relevant publications are listed below.

Publications

- **A. Garg**, G. S. Aujla and H. Sun, "Techno-Economic-Environmental Analysis for Net-Zero Sustainable Residential Buildings," in ***IEEE PES Innovative Smart Grid Technologies Europe (ISGT EUROPE)***, Grenoble, France, 2023, pp. 1-5. (**Chapter 3**)
- **A. Garg**, A. Singh, G.S. Aujla, and H. Sun, "Two-fold Strategy Towards Sustainable Renewable Energy Networks When Uncertainty is Certain," ***IEEE Transactions on Consumer Electronics***, 2024, DOI: 10.1109/TCE.2024.3475581. (**Chapter 5**)
- **A. Garg**, G. S. Aujla and H. Sun, "Analyzing Impact of Data Uncertainty in Distributed Energy Resources using Bayesian Networks," in ***IEEE International Conference on Communications, Control, and Computing Technologies for Smart Grids (SmartGridComm)***, Glasgow, United Kingdom, 2023, pp. 1-6. (**Chapter 5**)

Published papers that are not included in this thesis:

- M.A. Santana, I. Stefanakos, X. Fang, **A. Garg**, H. Sun and A. Osman, "Weather Impact on DER Long-term Performance: A Formal Verification Approach", in ***IEEE PES Innovative Smart Grid Technologies Asia (ISGT ASIA) 2024***, India, pp. 1-5.

Forthcoming Publications:

- **A. Garg**, G. S. Aujla and H. Sun, "Temporal Energy Scheduling of Smart Energy Systems under Weather Uncertainty," to be submitted in IEEE Transactions on Smart Grid. (Under Preparation) (**Chapter 4**)

List of Figures

List of Tables

Nomenclature

ABC Artificial bee colony

AC Alternating current

ACO Ant colony optimisation

AI Artificial intelligence

AMI Advanced metering infrastructure

BESS Battery energy storage system

BN Bayesian network

CE Carbon emission

CEF Carbon emission factor

CF Carbon footprint

CHP Combined heat and power

CPT Conditional probability table

DC Direct current

DER Distributed energy resource

DG Distributed generation

DN Distribution network

DSO Distribution system operator

EV Electric vehicle

GA Genetic algorithm

GAMS General algebraic modelling system

GC Global controller

GHG Greenhouse gas

HSA Harmony search algorithm

HOMER Hybrid optimisation of multiple energy resources

HVAC Heating, ventilation, and air conditioning

IC Intelligent control

IGDT Information gap decision theory

LC Local communities

LCOE Levelised cost of energy

LSF Least square fitting

LSTM Long short-term memory

MCMC Markov chain Monte Carlo

MCS Monte Carlo simulation

MILP Mixed-integer linear programming

MODE Multi objective differential evolution

MOMSOS Multi objective multi swarm optimisation strategy

MOP Multi-objective optimisation problem

MF Membership function

NPC Net present cost

NR Newton Raphson

NSGA Non-dominated sorting genetic algorithm

PDF Probability density function

PSO Particle swarm optimisation

PSOGSA Particle swarm optimisation gravitational search algorithm

PV Photovolatics

RC Regional controller

RES Renewable energy source

RIDES Renewable interconnected distributed energy systems

RL Reinforcement learning

RQ Research questions

SAC System annual cost

SOC State of charge

TCS Time-coordinated strategy

VD Voltage deviation

WCSS With-in-cluster sum of squares

WT Wind turbine

Chapter 1

Introduction

Approximately 35 billion barrels of oil are being used worldwide every year to provide for the energy needs of our planet [1]. This huge dependence scale on fossil fuel pollutes the Earth and will not last forever. The researchers estimate about 40% of the world's oil has been consumed [1]. According to the latest studies, the world will run out of oil and gas in the next 50 years and about a century for coal [1]. On the other side, there are abundant clean and green renewable energy sources (RESs) such as the sun, water, and wind. What if we could exchange the dependence on fossil fuels for an existence based solely on renewables? Researchers have been working to answer this question for decades, yet renewable energy still provides only about 13% of the total energy needs [2]. The sun continuously radiates about 173 quadrillion watts of solar energy on the Earth, which is almost 10,000 times our present needs [3]. So why cannot there be a complete reliance on renewables? This is because there are other hurdles, such as efficiency, intermittency, and energy transportation. To maximise efficiency, solar plants must be in areas with many days of sunshine a year, such as deserts. However, these are far from densely populated regions with high energy demand. Other forms of renewable energy from which we could draw power, such as hydroelectric, geothermal, and biomass, have their own limits based on availability and location.

Moreover, with the advent of digitisation and urbanisation, greenhouse gas (GHG)

emissions are increasing, leading to climate change, impacting the physical environment and life on this planet. Therefore, there is an urgent need to reduce GHG emissions, control global warming, and alleviate climate change. According to the Paris Climate Agreement, to maintain the global warming temperature below 1.5°C and to achieve net zero carbon emissions by 2050, the investment in renewable energy would increase by 25% over the next decade [4]. The conventional power system consists of large generating stations scattered throughout the nations, usually in remote areas. These produce electricity using coal, gas, nuclear, and renewable sources. Electricity generated is delivered to the end user through a complex transmission and distribution network, which appears seamless to the end user. However, sometimes, there are abnormal events such as thunderstorms, heavy rains, that could result in power system failures, the cascading of which could lead to complete interruption in the electricity supply to the end user [5]. Furthermore, with the world's increasing electricity demand each year, the conventional grid technology of one-way connection of generation, transmission and distribution is getting old. The global electricity demand is expected to rise by 75% by 2030, which would make it even harder for the grid to cater to this load demand [6]. To overcome this challenge, distributed generation (DG) is gaining importance. Distributed energy resources (DERs), such as solar panels, wind turbines, and battery storage systems, enable localised energy generation, reduce transmission losses, and enhance energy security by mitigating dependence on centralised power plants [7]. With the increasing penetration of DERs, the traditional uni-directional power system is becoming bi-directional as shown in Fig. 1.1. Enabled by communication technologies, the consumers are participating in the energy market by selling and purchasing energy from the power grid, allowing a two-way flow of power [8].

The integration of DERs into distribution networks (DNs) offers numerous advantages, including enhanced grid resilience, improved energy efficiency, and increased use of RESs, which collectively contribute to reducing carbon emissions and achieving sustainability goals. RESs such as solar energy are also cost-effective to meet

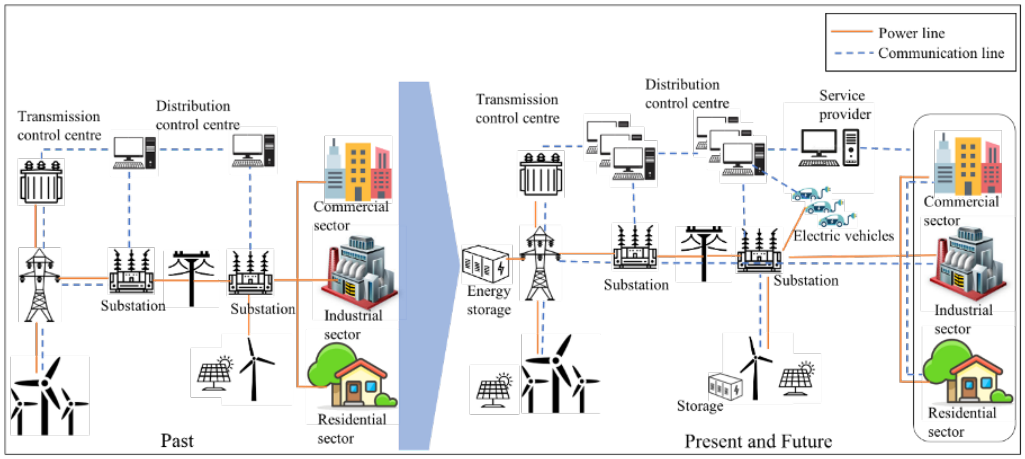

Figure 1.1: Change in energy system over the years

part of the energy needs. The fundamental driver of this change is that renewable energy technologies follow learning curves, which means that with each doubling of the cumulative installed capacity, their price declines by the same fraction. However, the price of electricity from fossil fuel sources does not follow learning curves, so we should expect that the price difference between expensive fossil fuels and cheap renewables will become even larger in the future [2]. However, the inherent uncertainties involved with RESs, such as power fluctuations and intermittence, may deteriorate the stability and security of power grids. For instance, the power output of renewable energy systems (say solar energy) reaches a peak at noon, which coincides with the off-peak loading period and leads to a power imbalance in the electric network. Therefore, there is a need to handle these uncertainties in the energy network for its reliable, efficient and stable operation.

1.1 Trends Towards Net-Zero

To achieve the global net zero emission targets in the energy sector by 2050, a transition from fossil fuel to clean energy technologies such as offshore wind, rooftop solar panels and nuclear power is needed. Fig. 1.2 and Fig. 1.3 show renewable energy generation (solar, wind, and hydro) [9] and per capita carbon emissions [10] for major economies such as India, the United States, the UK and China since

1970. Over the decades, the US and the UK have shown a reduction in per capita carbon emissions and increased renewable energy generation. On the contrary, an increasing trend in emissions and renewable generation is observed in both India and China.

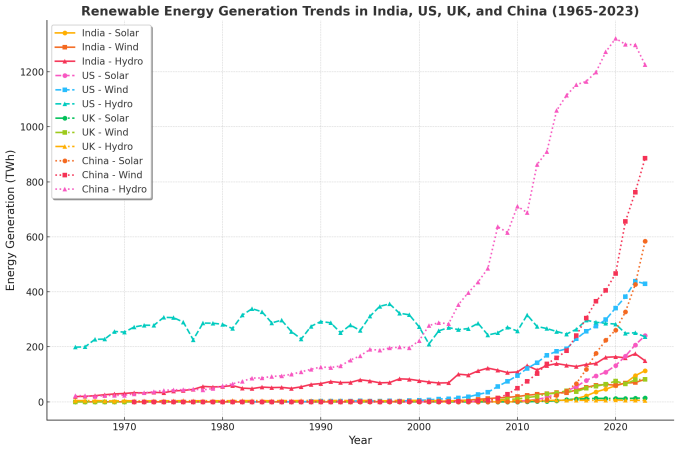

Figure 1.2: Renewable energy generation trends of different countries

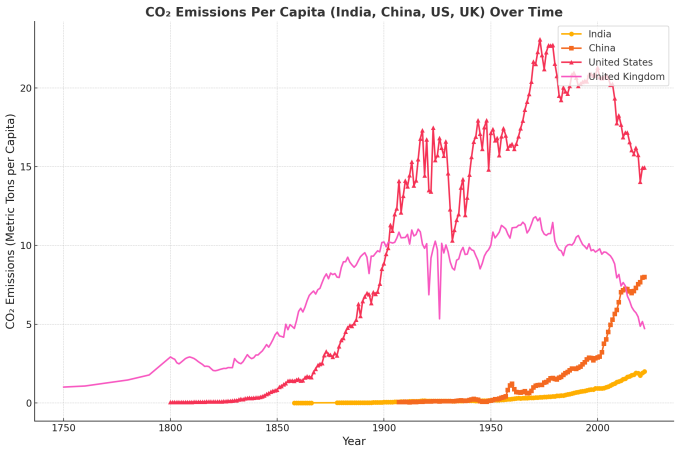

Figure 1.3: Per-Capita carbon emissions in different countries

Approximately 50% of the total GHGs are being emitted in China, USA, Russia, and European countries [11]. The UK became the first G7 country to legally commit the net-zero emissions in all the sectors of UK's economy by 2050 and successfully cut the emissions by 48% from 1990 to 2021 [12]. Many initiatives are being carried out by different utilities and industries to understand the scope and effect of these emissions. Figure 1.4 highlights the different sectors responsible for the emissions and the cohort of 32 UK companies [13] taking part in this world-wide

rally to achieve net-zero emissions by 2050.

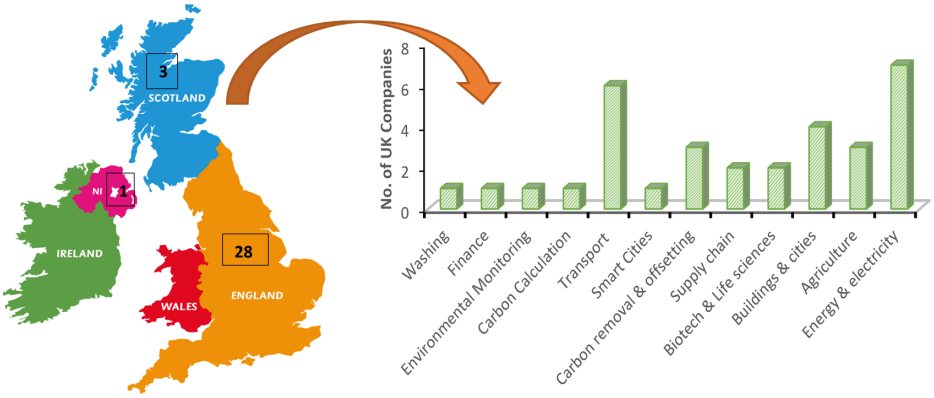

Figure 1.4: UK companies working in different sectors for net-zero emissions

The energy sector contributes about 34% of the global emissions, wherein the contribution of UK's energy sector is approximately 1% of the global emissions [14]. There has been a notable reduction in coal-based energy in the UK over the past two decades to achieve the net-zero goals. The energy generation from coal dropped from 40% in 2012 to 2% in 2020 and finally the UK shut down its last coal based plant on 30^{th} September 2024 [15]. The UK has invested significantly in offshore wind with the aim to increase the installed offshore wind capacity to 50GW and floating offshore wind to 5GW by 2030 [16].

1.2 Uncertainty in Energy Systems

DERs involving RESs provide flexibility in grid management, allowing for more effective demand response and peak load management. The global growth in renewable energy capacity has almost doubled in 2023 as compared to 2022 reaching above 500 gigawatts with solar panels alone accounting for one-third of the additions [17]. In addition to renewables, other emerging technologies such as green hydrogen, carbon capture, utilisation and storage are used to reduce emissions in the transportation and industrial sectors [17]. However, the integration of DERs in the energy sector presents several challenges and uncertainties. These include

technical issues such as maintaining grid stability and reliability amidst intermittent renewable energy outputs [18], ensuring effective communication and control systems for real-time coordination [19,20], and addressing the complexities of bidirectional power flows [21].

Uncertainty, in simple terms, is defined as the variation in the system characteristics (input or output) that may affect the system response [22]. In this work, uncertainty in energy systems refers to the degree of unpredictability and variability in the factors that control energy generation, distribution, and consumption. Fig. 1.5 depicts the holistic view of a renewable integrated decentralised power system with the bi-directional flow of power (power lines) and information (communication lines). It highlights the technical and operational uncertainties associated with different stages in the energy network (generation, transmission, distribution and consumer end) which are discussed as follows.

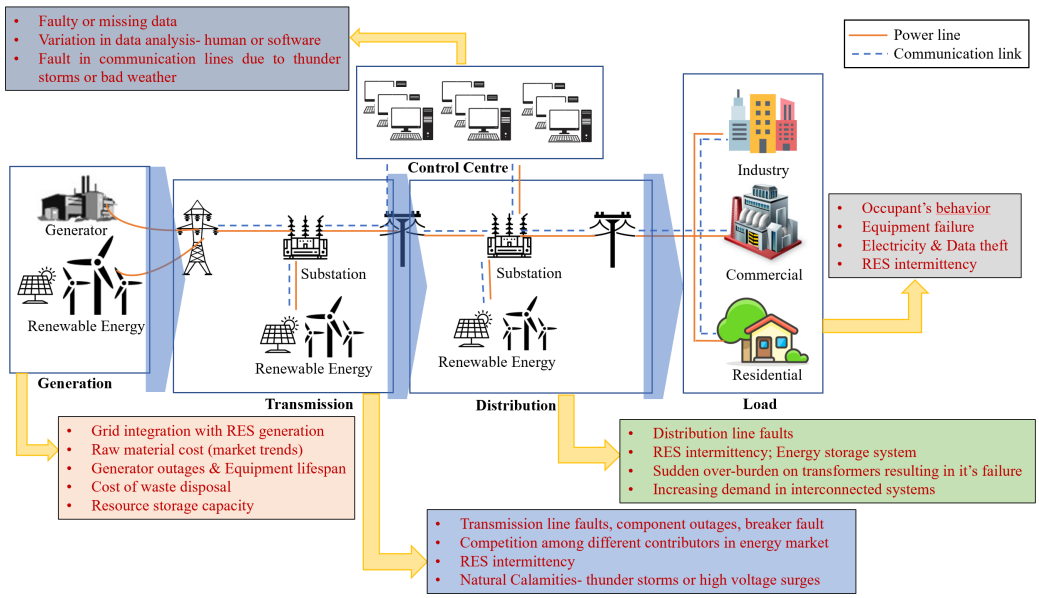

Figure 1.5: Uncertainties associated with different stages of energy systems

- ***Generation Stage Uncertainty:***

  The integration of RESs with the grid is the biggest challenge due to the intermittent nature of RESs, making it difficult to predict the renewable generation, hence, unbalancing the real-time generation and demand. Energy

generation is also affected by global market trends in terms of raw material costs, particularly in terms of the equipment required for renewable and traditional energy sources. There are other significant uncertainties, such as the lifespan of equipment and generator outages, as aging or unexpected breakdowns can result in power failures. Further, there are environmental and regulatory challenges associated with the disposal of waste created by traditional sources of energy, such as fossil fuels and nuclear power. Finally, the storage of surplus renewable generation is a critical issue and if not managed wisely would go to waste, making the long-term energy planning more complex.

- ***Transmission Stage Uncertainty:***

  Energy generated is transmitted to the far distant substations, which makes the transmission network prone to various uncertainties. Transmission line faults and component outages can occur due to equipment aging, environmental factors, and natural disasters such as thunderstorms. Such faults can lead to power outages which may lead to grid blackouts. Moreover, it is difficult to maintain network stability with the integration of RESs due to their fluctuating power generation. There is increased competition among the energy suppliers in the transmission market, making energy trading more complex. Furthermore, the transmission infrastructure such as transmission lines and insulators is susceptible to natural calamities like high-voltage impulses and thunderstorms which can lead to disruption in the power delivery across the energy network.

- ***Distribution Uncertainty:***

  There are technical and operational challenges associated with the uncertainties in the DN (that connects substations to the energy users). The distribution lines are prone to various faults due to the environmental calamities, and wear and tear of the equipment with time, which can impact their reliable power delivery. The local generation and integration of RESs with the DNs

is another challenge that could result in equipment failure. The distribution transformers can face the issues of overburden (leading to potential outages) with sudden impulses in demand or supply due to weather events in the renewable integrated DNs. Moreover, the interconnection of electric vehicles and energy storage puts more burden on the existing DN that needs to be restructured to meet the growing energy demand.

- ***Consumer End Uncertainty:***

  The major uncertainty associated with the consumer end (residential, commercial, industrial) is the unpredictability of occupant's behavior. Consumer demand depends on internal (economic conditions, changing consumption patterns) and external (environmental, holidays) parameters, making it difficult to predict energy consumption accurately. Hence, maintaining the balance between energy demand and supply becomes more complicated. In addition, sudden ripples caused by appliance failures at the consumer end disrupt the normal operation of the entire energy network. For example, a sudden increase in the load of a building can cause an outage at the local level, which may affect the stability of the distribution network. Also, with fluctuating renewable energy generation, the load demand is not always met and areas that rely primarily on RESs face outages for longer periods. Another type of uncertainty at the consumer end is energy theft leading to economic losses.

- ***Control Center Uncertainty:***

  With decentralization, the control center has become the brain of the energy network responsible for managing the power flow across generation, transmission, and distribution networks. The control center relies on the data from various sensors across the network for real-time energy operation, control and management. Therefore, faulty or missing data can lead to inaccurate decision-making of energy delivery, making the network unstable and more prone to outages. Moreover, errors in the data analysis and measurement

either due to human negligence or faulty equipment, is another uncertainty faced at this stage. Further, the communication lines that link various parts of the grid are vulnerable to external factors such as weather conditions that can disrupt the ability to monitor the network operations.

1.3 Problem Statement

Addressing the climate change challenge, researchers are aiming toward carbon neutrality through RES using carbon-intelligent computing [23]. However, different types of uncertainties, as discussed above, hampers this integration. To analyse this problem in more depth, a case study has been performed wherein a domestic load with solar photovoltaic (PV) panel is installed at its rooftop as depicted in Fig. 1.6. A basic MATLAB Simulink model has been implemented to realise this scenario that highlights the uncertainties at different stages in this energy system. Electricity produced by solar is DC (direct current) in nature so it is passed through the inverter which converts it into AC (alternating current) required to feed the load. The system is connected with both PV and grid, so that if PV is unable to meet load demand, it can be fed through the grid. During sunny days, the entire demand is being fulfilled by a carbon-free source of energy, i.e., solar. However, during nighttime or bad weather, the load demand exceeds the PV generation, therefore, electricity flows from the grid to meet the load demand as shown in Fig. 1.6. It can be seen that from t=0.5 mins to t=0.75 mins, the solar power becomes zero and hence, no power flows through the load. Therefore, the grid supplies the required power in order to supply 24/7 reliable power to the load.

However, the grid dependency again hinders the aim towards net-zero carbon emissions. When the load is dependent completely on RESs, there are no carbon emissions. However, due to the uncertain nature of renewable energy sources, load dependency on grid increases leading to more carbon emissions (shown in Fig. 1.6).

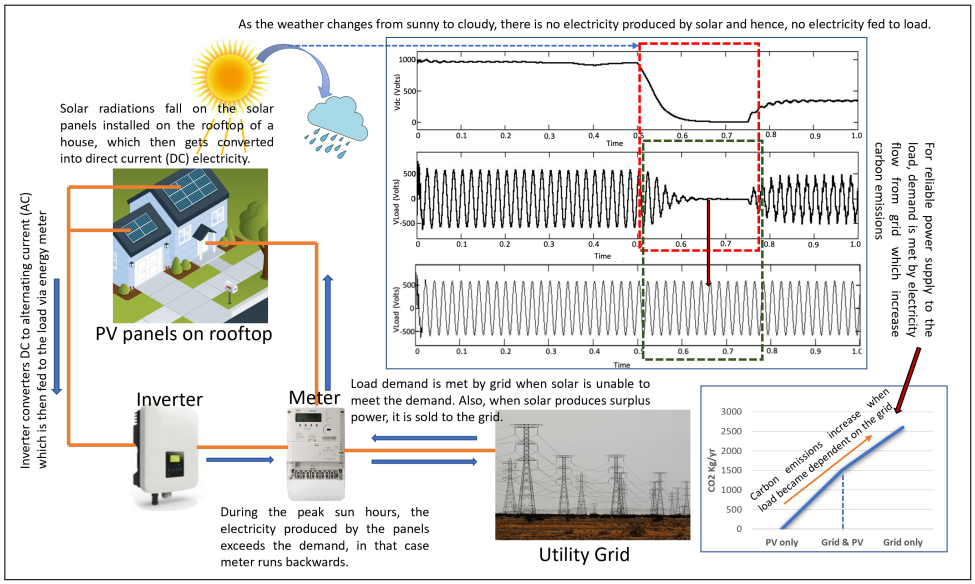

Figure 1.6: Effect of uncertainty on load profile and carbon emissions of a household

1.3.1 Case 1: Uncertainty at Consumer End: sudden load is added

Human nature is unpredictable, which leads to uncertainty in the energy systems. When a sudden load is added to the system operating with a renewable energy source, there is a sudden dip in the source voltage (as seen in Fig. 1.7 from t=0.35 mins to t=0.4 mins). In this case, PV is capable of feeding both the loads, as seen in Fig. 1.7; however, if the load rises above the capacity of the PV panel, it will lead to failure in the system and dependency on the grid would increase.

1.3.2 Case 2: Uncertainty at Generation End: no Sun/ zero Irradiance

With sudden changes in the weather (from sunny to cloudy), the sun's radiations take a sudden dip, and in that case, the PV panel becomes incapable of supplying any power to the load; thereby, the voltage across the load becomes zero (as shown Fig. 1.8 from t=0.5 mins to t=0.75 mins). Therefore, the load relies either on the battery storage (expensive) or the grid (carbon emitter).

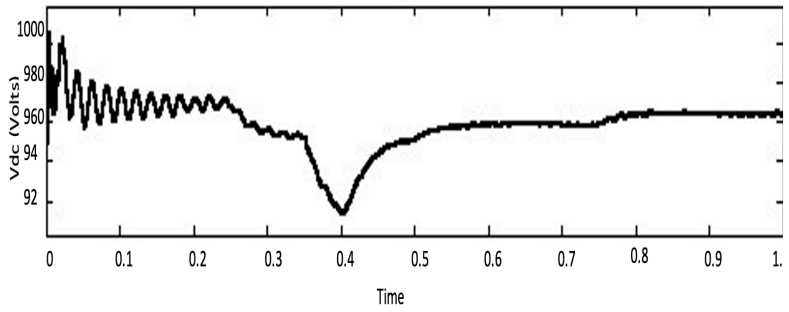

(a)

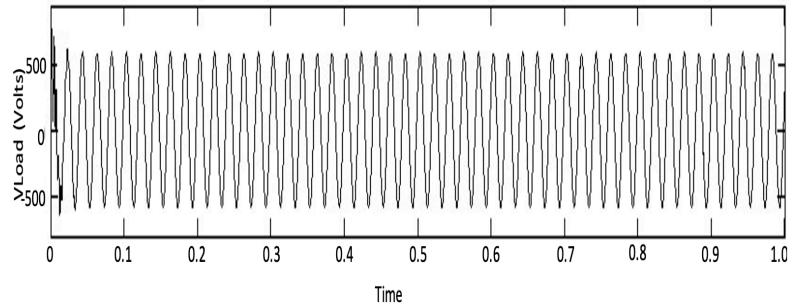

(b)

Figure 1.7: Effect on voltage profiles of (a) source (b) load, in case of uncertainty at consumer end

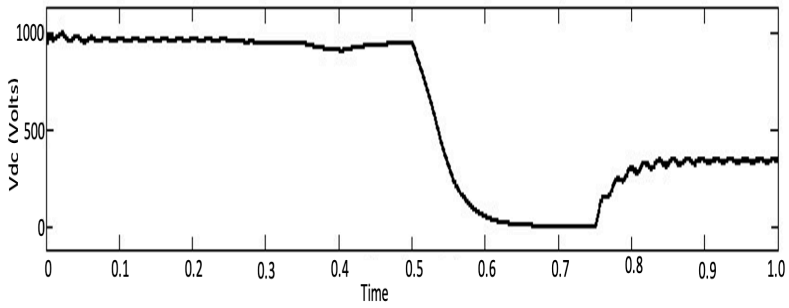

(a)

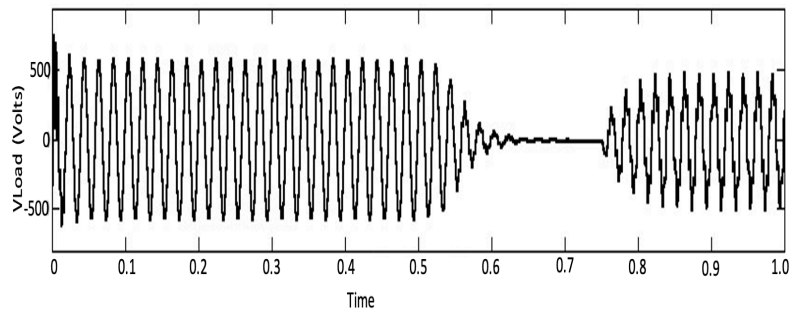

(b)

Figure 1.8: Effect on voltage profiles of (a) source (b) load, in case of uncertainty at generation end

1.3.3 Case 3: Uncertainty at Transmission/Distribution End: distribution line fault

When the load is disconnected from the PV source due to some fault in the distribution line, the PV will work on its maximum power point as there is no load. In this case, the load becomes dependent on the grid, thereby contributing to carbon emissions. The voltage profiles of both the PV panel and the load can be analysed through Fig. 1.9.

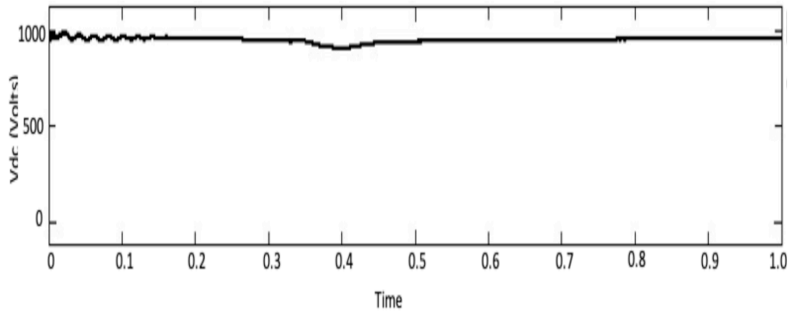

(a)

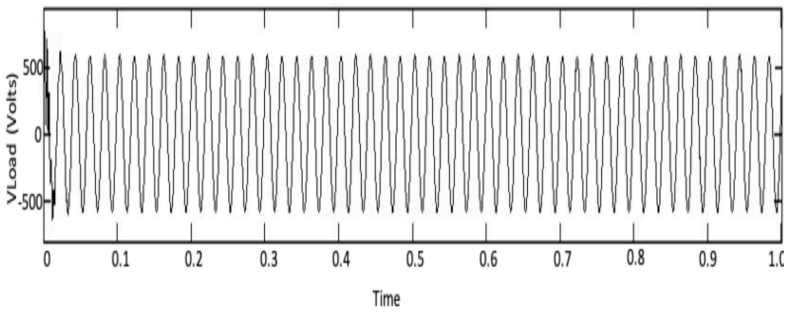

(b)

Figure 1.9: Effect on voltage profiles of (a) source (b) load, in case of distribution end uncertainty

1.4 Research Questions

Carbon-intelligent computing is the key to mitigating the deviations in the expected energy demand due to the uncertainties associated with renewable energy through the intelligent control of carbon-neutral energy [24–26]. To completely rely on

renewable energy generation, the following key research questions (RQs) need to be investigated.

- **RQ1:** How do we compute (and understand) the uncertainties associated with renewable energy generation and model (or analyse) these for the reliable operations of the energy systems?
- **RQ2:** How can the impact of uncertain parameters on system performance be accurately measured and mitigated in real-time for reliable DN operation?
- **RQ3:** What novel methods can be developed to decarbonise energy networks by effectively managing the uncertainties in the DERs and enhancing the sustainability of the DNs?

These questions aim to comprehensively explore the effects of uncertainties on power systems in order to develop robust strategies ensuring stable and sustainable energy network operations.

1.5 Research Objectives

Based on the discussed challenges, problem statement and research questions, the proposed research aims to handle the uncertainties associated with renewable energy generation so that we can rely on carbon-free energy without interruption. Therefore, the following key objectives are formulated in the present research:

- ***Objective 1:*** Study and understand the uncertainties associated with renewable energy generation, transmission, and distribution. The real-time data will determine the factors (such as temperature, market conditions, and human behaviour) that affect these uncertainties.
- ***Objective 2:*** Develop an optimisation model leading towards developing a prototype that can be used by various utilities to efficiently manage their

carbon emissions and shift their energy demand from conventional energy to renewable energy. Hence, the aim is to take a miniature step to save the planet Earth from global warming and make it greener and cleaner.

- ***Objective 3:*** Design and develop a carbon-intelligent computing framework by leveraging AI to understand and model the uncertain parameters and finally mapping the tasks with low-carbon energy supply intelligently (learn, align, and reinforce).

1.6 Significance of the Work

Keeping in mind the UN sustainable development goals, and the UK's aim for net-zero emissions by 2050, this research focuses on proposing a novel energy efficiency optimisation mechanism based on artificial intelligence (AI) for managing smart energy systems. AI enables a system to learn by itself without being explicitly programmed. Various companies like Google and Facebook are already using this concept in speech and image recognition [7-9]. In the present research, we will be extending this idea to meet the global climate change challenge and contribute to a greener environment. A dynamic carbon intelligent framework is developed for smart energy infrastructure which can be extended to smart building, smart grid, or a smart city, to handle uncertainties associated with renewable-based energy systems. This involves predicting the energy demand of infrastructure at a particular time of the day using historical data of that infrastructure that further controls and optimises the energy usage intelligently to reduce the dependency on the grid. Further, the proposed framework accounts for the 6Ws' of uncertainty (What, Who, Where, When, Why, and hoW) as shown in Fig. 1.10. It means WHAT uncertainty (Definition) is, WHEN it is generated (Probability), WHERE is it present (Possibility), WHO is responsible for its generation (Sources), WHY it needs to be evaluated (Consequences) and HOW it can be reduced (Mitigation) for the efficient, reliable and sustainable operation of the energy systems.

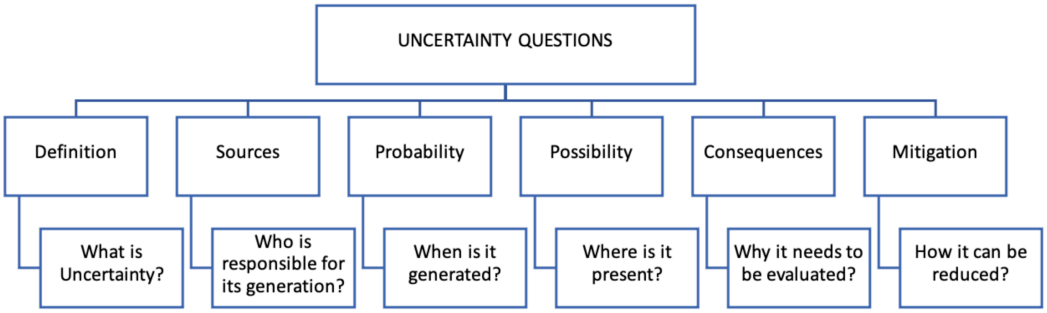

Figure 1.10: 6 W's of uncertainty

The relationship of 6Ws of uncertainties with the thesis chapters is discussed as follows:

- *WHAT is uncertainty:* Addressed in Chapter 2, where various uncertainty modelling techniques for energy networks are mentioned.
- *WHEN uncertainty arises:* Discussed in Chapter 4, where a novel time-coordinated uncertainty modelling technique is introduced to predict the intermittent behaviour of RESs for optimal energy scheduling.
- *WHERE is uncertainty present:* Investigated in Chapter 3, which optimises the placement and sizing of hybrid RESs in a network to minimise emissions and costs.
- *WHO is responsible for uncertainty generation:* Tackled in Chapter 5, where different types of uncertainties are detected using a Bayesian network-based approach to identify hidden interdependencies among weather parameters affecting real-time system operation.
- *WHY uncertainty requires evaluation:* Covered in Chapter 1 and Chapter 2, where the impact of uncertainty on energy planning and operational performance is discussed.
- *HOW uncertainty can be mitigated:* Handled in Chapters 4 and 5, where intelligent control strategies are proposed for planning and real-time uncertainty mitigation.

1.7 Thesis Organisation

After introducing the global trends to achieve the net-zero emissions and the need to model the uncertainty in the renewable integrated energy networks, the thesis has been organised into the following chapters:

- **Chapter 2: Literature review**

  This chapter provides information on relevant research works to model and handle various types of uncertainties in energy networks. It further discuss the uncertainty modelling techniques to address different uncertainties at the operational and planning stage.

- **Chapter 3: Optimal planning of renewable energy systems**

  This chapter discusses the different combinations of RESs in a hybrid energy system to minimise the associated costs and emissions. Further, a techno-economic-environmental analysis is performed for the optimal placement of RESs in the energy network.

- **Chapter 4: Uncertainty modelling for temporal energy planning**

  This chapter introduces an intelligent framework that manages and controls the uncertainty for short-term energy management. A novel uncertainty modelling technique is proposed in this chapter for the accurate prediction of the intermittent behavior of RESs for optimal energy planning.

- **Chapter 5: Energy system operation under real-time uncertainty**

  This chapter provides a two-fold strategy to handle the real-time operational uncertainty in DNs. This Bayesian network-based approach identifies the hidden interdependencies among the various weather parameters which is then used to detect the type of uncertainty and then finally mitigate it maintaining the low carbon emissions throughout the operation.

- **Chapter 6: Conclusion**

  This chapter concludes the entire thesis that focuses on proposing a carbon intelligent framework for the efficient and reliable operation of the energy network. Moreover, it provides future research directions for the work carried out in this thesis.

The mapping of the research objectives with the thesis chapters and the publications is highlighted in Fig. 1.11.

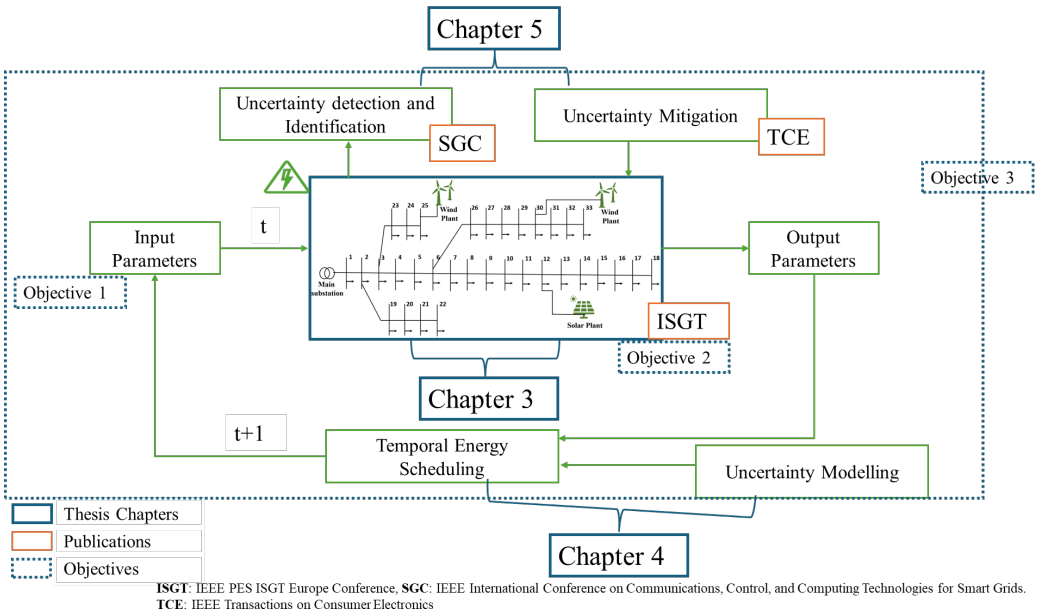

Figure 1.11: Mapping of thesis objectives with chapters and publications

Chapter 2

Literature Review

Renewable energy contributed approximately 46.02% of the total electricity generation in the UK in 2023 [9]. As per the Paris Climate Agreement, to maintain the global warming temperature below 1.5 degree Celsius and to meet net-zero carbon emissions by 2050, the investment on renewable energy would increase by 25% over the next decade [4]. These RESs, however, come with inherent uncertainties (such as intermittency in generation) that need to be evaluated and therefore, optimal planning for renewable energy plants is required to replace conventional fossil fuel-based plants and maintain energy security. In this chapter, we will discuss the work done by various researchers to find out the optimal number of RESs in an energy system. Further, the different types of uncertainties associated with renewable integrated energy systems are discussed along with the various modelling techniques proposed in the literature to handle those uncertainties. The research questions are then derived from the open problems in the literature, and a small motivation study is carried out to further refine these questions to create research objectives. The list of symbols used in this chapter are shown in Table 2.1.

2.1 Optimal Planning of Renewable Energy Systems

Solar and wind constitute the largest part of the total renewable energy generation. Interestingly, these clean sources of energy individually are sufficient to power the

Table 2.1: Table of symbols used in chapter 2

Symbol	Description
f(x)	Probability density function (PDF).
α	Scale parameter in Weibull PDF
β	Shape parameter in Weibull PDF
μ	Mean value in normal PDF
σ	Standard deviation in normal PDF.
E(y)	Expected value of output uncertain variable
x	Random variable
X	Input uncertain variable vector
X_c	Input uncertain variable vector at counter C = c
Y	Output variable dependent on uncertain inputs
Y_c	Output uncertain variable vector at counter C = c
X^α	α-cut of uncertain input variables
$\pi_X(x)$	Membership function (MF) in fuzzy logic.
U	Universe of discourse for the uncertain input variables.
$\overline{X^\alpha}, \underline{X^\alpha}$	Lower and upper bounds of α-cut.
$\overline{Y^\alpha}, \underline{Y^\alpha}$	Lower and upper bounds of output α-cut.
$G^\alpha_{X_i}$	α-cut of the i-th input variable in possibilistic analysis.
Z^e	Value of probabilistic variable sampled from its PDF.

entire mankind. However, due to their intermittent nature and expensive initial investment, currently, it is not possible to rely completely on only a single type of RES. For instance, solar energy is unevenly distributed across the planet therefore, some areas have more irradiance than others. Moreover, less solar energy is available on cloudy days or at night. Further, the efficiency of a solar cell itself is a challenge [27]. Moreover, in addition to the fluctuation in wind energy generation, no matter how large or efficient a turbine is, there is a limit to how much wind it can convert into electricity [28]. Therefore, different energy sources are integrated to form a hybrid energy system to maintain energy security.

To leverage the available natural resources, smarter and more efficient ways of deploying renewable energy plants needs to be employed and decentralised generation is one of them. Solar and wind plants can be built near urban areas to provide affordable energy to local households. This would reduce the dependency on the utility grid contributing to a reduction in fossil fuel-based energy generation and

stepping towards a greener environment. In this regard, many researchers [29–34] are working on finding out the optimal combination of various renewable energy plants resulting in a reduction in carbon footprints and cost per kWh based on constraints such as location, weather, market trend, and other economic parameters (initial investment, payback period, etc.) as shown in Table 2.2. For instance, in [32], a new model was proposed to reduce Iran's carbon footprints by considering different scenarios on renewable energy subsidies, and tariff variations. In [33], the effect of carbon emissions on agriculture and the role of RESs in reducing this problem was analysed. An eco-industrial park scheme was discussed in [34] to encourage industries to rely on renewable energy generation wherein the excess energy could be given to the nearby urban areas.

Based on the literature, the optimisation methods to find the optimal placement of RESs can be classified as analytical and numerical methods. The analytical methods are further categorised into classic and basic search methods, that involves solving complex mathematical formulations to find the exact solution. Numerical methods are iterative methods and provide an approximate solution to the problem. A complete hierarchical flowchart of different optimisation methods is shown in Fig. 2.1. Out of the various methods highlighted in Fig. 2.1, some of the commonly used AI-based optimisation methods defined in the literature [35–44] to find the optimal location and capacity of RESs are NSGA-III (Non-dominated Sorting Genetic Algorithm III) [35], MOMSOS (Multi-Objective Multi-Swarm Optimisation Strategy) [36], GA + PSO (Genetic Algorithm + Particle Swarm Optimisation) [37], ABC (Artificial Bee Colony) [38], HSA (Harmony Search Algorithm) [39], LSF + PSOGSA (Least Square Fitting + Particle Swarm Optimisation Gravitational Search Algorithm) [40], GA GAMS (Genetic Algorithm in General Algebraic Modelling System) [41], MODE (Multi-Objective Differential Evolution) [42] and Hybrid ACO-ABC (Hybrid Algorithm combining Ant Colony Optimisation and Artificial Bee Colony) [44]. The researchers have used these methods to find the size and location of hybrid RESs while minimising total power loss, voltage deviation,

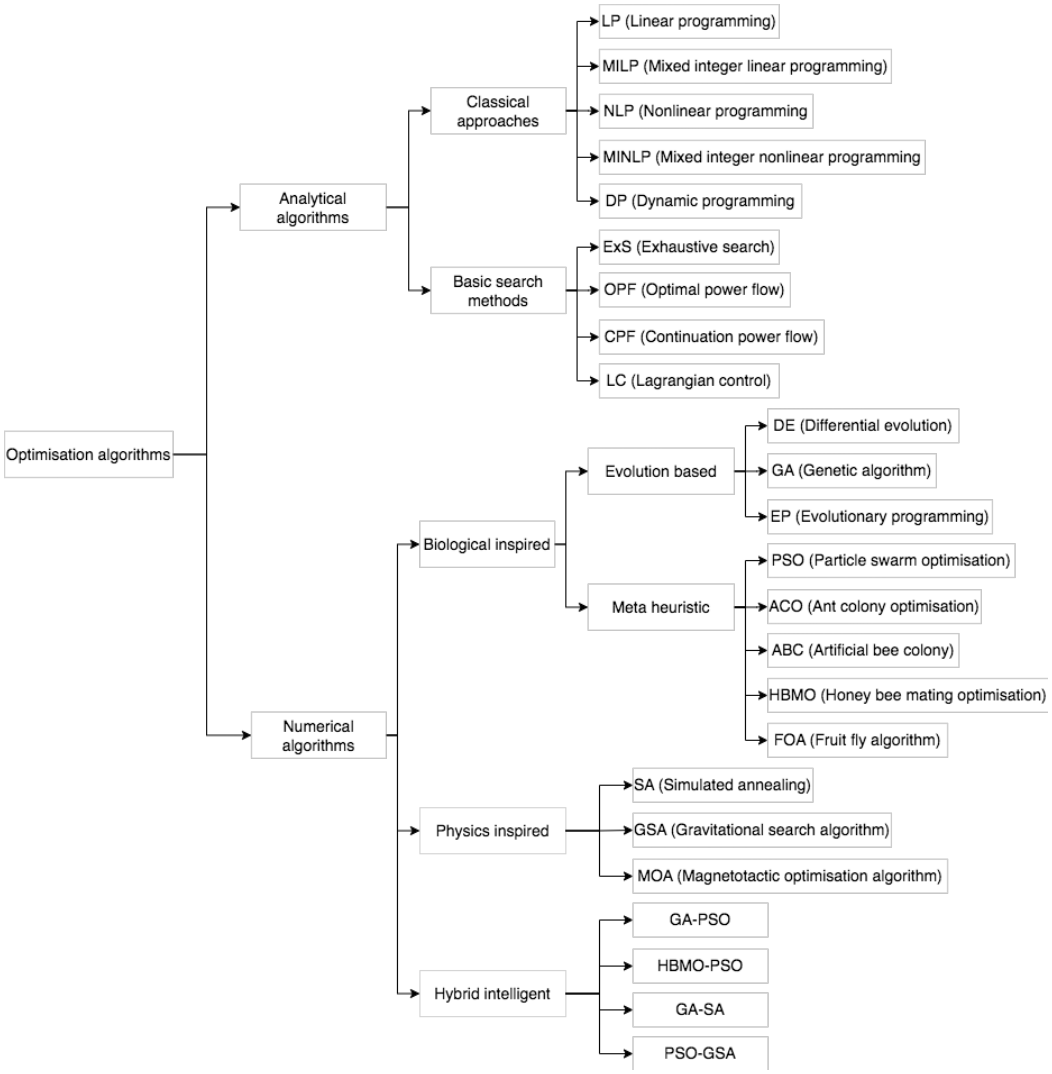

Figure 2.1: Most commonly used optimisation algorithms for optimal placement of RESs

cost, carbon emission and improving the system reliability as depicted in Table 2.2. Although the above-mentioned methods are widely used to determine the optimal location and capacity of RESs, however, they need high power and computation time, making them difficult to implement in real-time scenarios. Moreover, there is still a gap in deciding on a combination of different algorithms (hybrid approach) that is robust to RESs uncertainties, has a high convergence rate and takes less computational time.

Moreover, the UK government energy act aims to change the energy utilisation

Table 2.2: Summary of research on optimal placement and sizing of DG in the distribution system

Ref.	Capacity	Location	Type	Objective Function	Optimisation Algorithm
[35]	✓	✓	WT+PV	Ploss, VD	NSGA-III
[36]	✓	✓	WT+PV+Biomass	Cost, Ploss, VD	MOMSOS
[37]	✓	✓	PV	Ploss, VD	Analytical method
[38]	✓	✓	PV+WT	Cost, Emissions, Ploss, VD	Water Cycle
[39]	✓	✓	PV+WT	Ploss, Cost, Emissions	Improved HSA
[40]	✓	✓	PV+WT	Ploss, VD, Cost	LSF+PSOGSA
[41]	✓	✓	PV	Ploss, VD	GA
[42]	✓	✓	WT	Ploss, VD, Reliability, Cost	GA GAMS
[43]	✓	×	Small Hydro	Ploss	MODE
[44]	✓	✓	Fuel Cell, WT	Ploss, VD, Cost, Emissions	Hybrid ACO-ABC

WT: Wind turbine; PV: Solar panel; Ploss: Power loss; VD: Voltage deviation

paradigm from supply-side management to demand-side management. To realise national energy security, the need for renewable energy has become a priority that balances fossil energy which still serves as the main energy resource. Moreover, exploration and exploitation of energy resources should be done as part of national energy security [45]. With the time-varying behaviour of renewable energy sources and flexible loads, the unit commitment and dispatch problem can change significantly [46, 47]. In that regard, there is a need for methodologies that leverage supplementary power plant capacities and provide additional flexibility to compensate for real-time imbalances [48]. To cope with unforeseen increases in demand, losses of power plants and transmission lines, and other contingencies [49], enhanced feed-in management, re-dispatch measures, planning and forecasting methods, and efficient energy management strategies with appropriate optimisation techniques are required [50]. The authors in [24] implement deep reinforcement learning for designing an optimisation algorithm for computer-intensive jobs using a computational model based on the power and thermal dynamics of the long–and short–term memory networks. Another statistical correlation technique reported in [25] wherein energy consumption is predicted based on climatic conditions and then utilised to optimise the power usage of the electricity utilities. In [26], a deep rein-

forcement learning framework has been utilised to achieve an 11% reduction in the cooling cost of the smart infrastructure compared to the baseline algorithms. A new AI-based optimisation methodology has been reported in [51] for planning energy in smart infrastructures. This technique achieved a 51.4% reduction in energy cost compared with the unplanned smart infrastructure model. Few researchers, such as in [52], computed a carbon index for a server to shift the incoming requests to other servers (when exceeding a certain threshold) based on static parameters. However, most studies do not include the dynamic nature of the requests being handled, nor do they have an automated process that considers the system's uncertainties. So, to make carbon-intelligent decisions in smart energy systems such as smart cities, smart buildings, smart homes, smart hospitals, smart grids etc., by incorporating such uncertainties is still lacking in the literature.

2.2 Classification of Uncertainty

Various models in the literature [53] have been reviewed to manage and optimise energy. These energy models are classified as energy planning models, energy supply-demand models, forecasting models, renewable energy models, emission reduction models and optimisation models. These days, energy system optimisation models are one of the main areas of research that provide integrated, technology-rich implementation of the entire energy system for its analysis, management, and optimisation for short- and long-term energy planning. With renewable energy-grid integration, these models are becoming complex, and various uncertainties are associated.

Uncertainty in renewable integrated energy systems is a complex and multifaceted issue, given the dynamic and interconnected nature of these systems. With the increasing integration of RES such as solar, wind, and hydropower into the power grid, uncertainties can arise at various stages of system design, operation, and management. These uncertainties are generally classified into three broad categories:

power system uncertainty, communication system uncertainty, and technological uncertainty as illustrated in Fig. 2.2 [54–58]. Each of these categories has specific implications for the stability, efficiency, and reliability of renewable integrated energy systems.

Power system uncertainty could be defined as the variations during the power flow stage of the energy system. It can further be categorised as design uncertainty (changes in physical properties and computational analysis of the system model under different conditions), operational uncertainty (fluctuations in the electrical and mechanical properties during the operating stage of the energy system), environmental uncertainty (system variations due to unpredictable climatic conditions), and regulatory uncertainty (volatility in market conditions and economic regulations). The smart energy systems deal with a lot of information that is received using the communication network. Therefore, any fluctuations or disturbances in the flow of information lead to communication uncertainty. There could be uncertainty in data (which is measured inappropriately or any error in the data analysis), security (related to the privacy of the entire energy network, which is interconnected with other energy networks) and socio-economic (due to unpredictable weather and economic conditions of the state/ country/world). Another form of uncertainty arises with the advancement of new technologies and is termed technological uncertainty. Each day, researchers come across new materials (such as natural ester oil in place of conventionally used mineral oil in the transformers) and new software or devices (like the use of machine learning to replace traditional statistical methods). There could be an up-gradation in the entire system (renewable energy systems replacing the conventional grid is the best suitable example of system uncertainty).

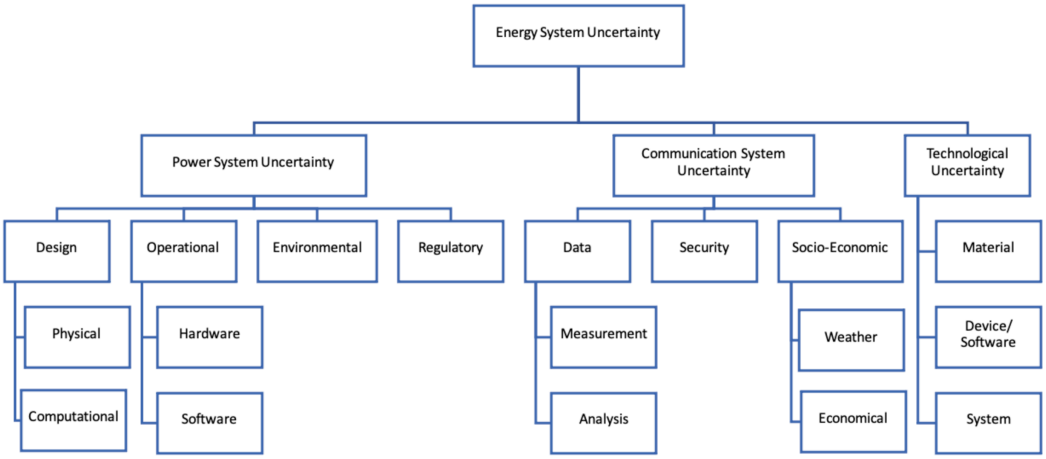

Figure 2.2: Classification of uncertainties associated with the energy system

2.3 Uncertainty Modelling Techniques

The traditional deterministic concepts used in power system operation and planning do not consider the uncertainties in DNs due to the inherent variability of RESs, unpredictable consumer demands, and data quality issues [59]. These models cannot handle the complexities of DER integration, regulatory changes, and cybersecurity risks [19, 60].

The existing stochastic methods (as shown in Fig. 2.3) such as probabilistic approaches [61], possibilistic approaches [62], hybrid approaches [63], information gap decision theory [64], and robust optimisation [65], have been well explored in the literature. The main purpose of these methods is to measure the impact of uncertain input parameters on the system output parameters. However, the main difference between these methods is to utilise different approaches implemented to describe input parameters' uncertainty [66–68]. For instance, the probability density function (PDF) is used in probabilistic methods, while in the fuzzy approach, a membership function (MF) is assigned for modelling uncertain parameters. The optimisation objectives can be divided into Economy, environmental protection, reliability, flexibility, or combination.

Out of these six commonly used optimisation methodologies, this research will

focus on hybrid optimisation techniques to handle different types of uncertainties associated with renewable energy systems. Techniques mentioned in Fig. 2.3 are used to solve single uncertain parameters, whereas using hybrid optimisation, it is possible to consider multiple uncertain parameters at a time [69, 70]. Hybrid optimisation is nothing but a combination of other optimisation techniques such as probabilistic and possibility optimisation (as described below) that combines both optimisation techniques through two loops. These loops can be defined as an outer loop that evaluates the uncertainty of the possibility variable and an inner loop that evaluates the uncertainty of the probability variable.

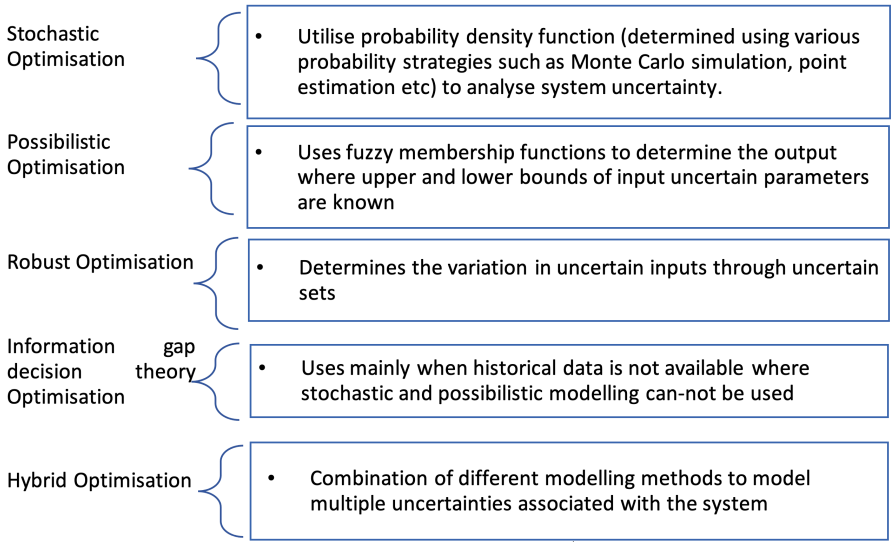

Figure 2.3: Uncertainty modelling techniques

2.3.1 Probabilistic/ Stochastic Optimisation

In probabilistic optimisation, system uncertainty is characterised based on the PDFs of the random uncertain variables. The uncertain input variables sometimes follow PDF; for example, wind speed patterns follow Weibull PDF [69], [70]. A brief mathematical calculation is shown below.

$$f(x) = \frac{\beta}{\alpha^{\beta}} x^{(\beta-1)} exp\left[-\left(\frac{x}{\alpha}\right)^{\beta}\right] \tag{2.1}$$

Using normal PDF, the load uncertainty can be modeled as:

$$f(x) = \frac{1}{\sigma\sqrt{2\pi}} e^{\frac{(x-\mu)^2}{2\sigma^2}} \tag{2.2}$$

Here, y $= f(x)$ has been considered as a multivariate function whereas $x = \{x_1, x_2, ..., x_n\}$ is an input uncertain variable vector.

The aim is to determine the PDF of the output variable (y), assuming the PDF of the input variable (x) is known. To determine the PDF of y, various probability strategies are used, out of which Monte Carlo simulations (MCS) [69] are well-known due to their capability to deal with non-linear, complex or systems with multiple uncertain variables. MCS is an iterative process, and the flowchart of its calculation procedure is shown in Fig. 2.4.

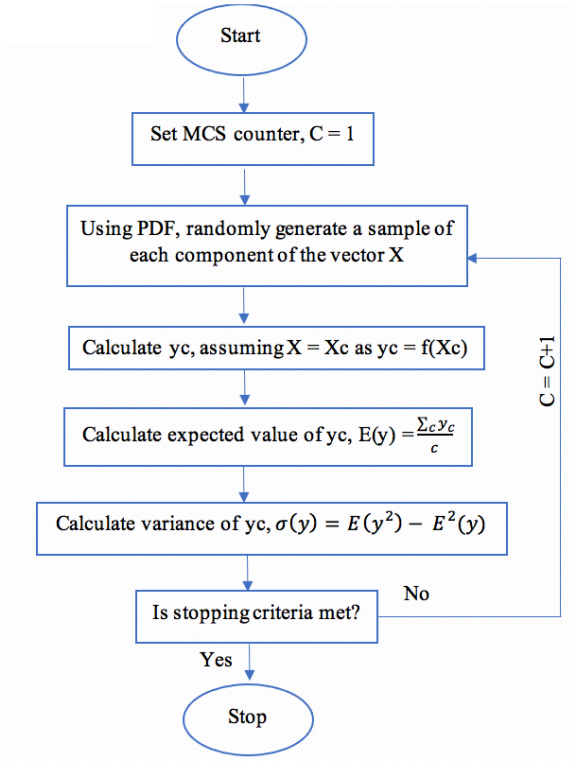

Figure 2.4: Flowchart for Monte Carlo simulation

2.3.2 Possibilistic/ Interval Optimisation

This method of uncertainty modelling uses linguistic categories to describe the uncertain variables with fuzzy boundaries. To model the renewable energy uncertainty, the possibilistic output variable Y of the energy system model with the vector of uncertain variables X is represented as $Y = f(X_1, X_2, ..., X_N)$. It is assumed that the possibility distribution of X is known; therefore, the possibility distribution of Y can be evaluated using the α-cut method [70] as follows:

The α-cut of input uncertain variables, X is calculated using the following equations:

$$X^{\alpha} = \{x \in U \mid \pi_X(x) \geq \alpha; 0 \leq \alpha \leq 1\} \tag{2.3}$$

$$X^{\alpha} = \left[\underline{X}^{\alpha}, \overline{X}^{\alpha}\right] \tag{2.4}$$

where, U is universe of discourse of X (range of its possible values), $\overline{X}^{\alpha}$ and $\underline{X}^{\alpha}$ represents upper and lower limits of X^{α} respectively.

Evaluating the α-cut value of each uncertain input variable, α-cut of output variable Y is evaluated as below:

$$Y^{\alpha} = \left[\underline{Y}^{\alpha}, \overline{Y}^{\alpha}\right] \tag{2.5}$$

$$\underline{Y}^{\alpha} = inf\left[f(G^{\alpha}_{X_1}, G^{\alpha}_{X_2}, ..., G^{\alpha}_{X_N})\right] \tag{2.6}$$

$$\overline{Y}^{\alpha} = sup\left[f(G^{\alpha}_{X_1}, G^{\alpha}_{X_2}, ..., G^{\alpha}_{X_N})\right] \tag{2.7}$$

where $G^{\alpha}_{X_N}$ represents the α-cut of Nth possibilistic input variable.

2.3.3 Hybrid Optimisation

In real-time problems, such as smart energy systems, there are a variety of uncertain parameters; some may be possibilistic, or some may be probabilistic. In such scenarios, the system's output could be represented as a multivariate function, $y = f(X, Z)$, where X represents a vector of possibilistic uncertain parameters

and Z is a vector of probabilistic uncertain parameters. Therefore, combining the methods, a hybrid optimisation method [69]- [70] can be modeled by considering Monte Carlo simulation (probabilistic approach) in the outer loop and α-cut method (possibilistic approach) in the inner loop. The following steps are employed in the hybrid optimisation approach:

Step1: For each Z_i *in* Z, generate value using its PDF, Z_i^e.

Step2: Calculate Y^α and $\overline{Y}^\alpha$

$$\underline{Y}^\alpha = \min f(Z^e, X^\alpha) \tag{2.8}$$

$$\overline{Y}^\alpha = \max f(Z^e, X^\alpha) \tag{2.9}$$

where,

$$X^\alpha = \left[\underline{X}^\alpha, \overline{X}^\alpha\right] \tag{2.10}$$

The above steps are repeated to obtain the statistical data of the parameters of the output's MF, such as PDF or expected values.

A brief procedure on how to decide which modelling methods suit best in a system under consideration is shown in Fig. 2.5. First, sensitivity analysis is carried out to determine the impact of input uncertain parameters on the output, and then the parameters with more impact on the system's output are scrutinised. In the next stage, dimensions, or the number of different sources of uncertainty, are analysed based on which the modelling techniques are selected. For example, a system with multiple uncertain parameters is more likely to be modeled using hybrid optimisation techniques. Table 2.3 highlights various uncertainty modelling approaches using different formulations and concepts to analyse and model the uncertainties.

The main purpose of the above methods was to measure the impact of uncertain input parameters on the system output parameters based on historical data. However, prior knowledge of an uncertain input's pre-defined probability distribution

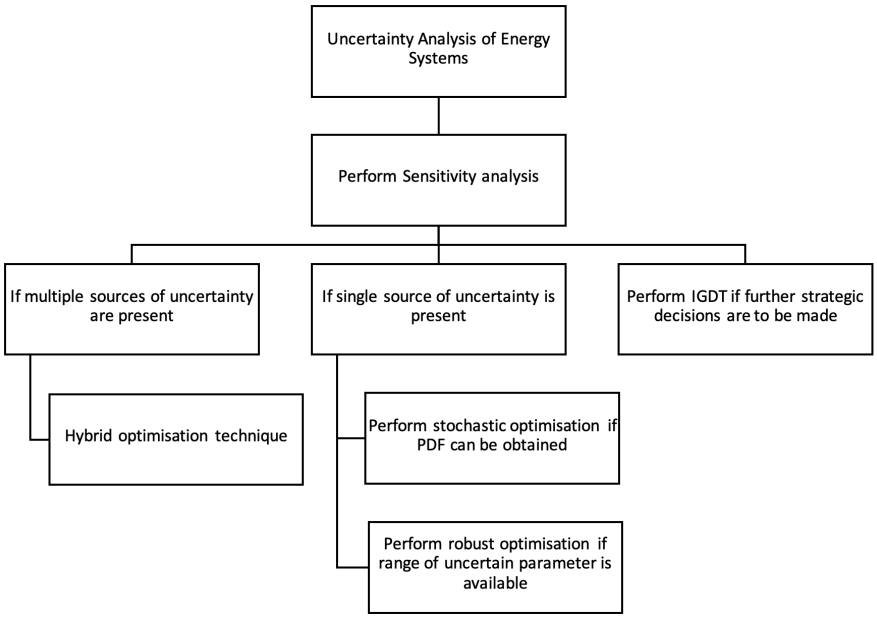

Figure 2.5: Detailed procedure to perform uncertainty analysis

function is required in these methods. To overcome this limitation, a data-driven two-stage stochastic optimisation algorithm was proposed in [72] to model the uncertainty in DN output parameters. In this article, the authors used the decomposition method for the parallel computation of uncertain parameters to reduce the dependence on prior knowledge for both stages. An optimisation algorithm based on the concept of Conditional Value at Risk that models the uncertainty in demand and energy prices was proposed in [73] to enhance renewable energy generation while minimising operational costs. All these methods have considered no correlation among the different uncertain parameters, which is not feasi-

Table 2.3: Types of uncertainty modelling techniques used by various researchers

Ref.	**Modelling approach**	**Method**	**Key-concept used**	**CO2 estimation**
[61]	Probabilistic	Monte-Carlo Simulation, Point estimation	Probability density function	Yes
[62]	Possibilistic	α – cut, defuzzification	Membership function	Yes
[64]	Interval	Interval optimisation	Intervals	No
[65]	Information Gap Decision Theory	Risk averse, Risk seeker	Forecasted values	No
[63]	Robust	Distributed model, Engineering game model	Uncertain sets	No
[71]	Hybrid	α cut – Monte Carlo	Multiple sources of uncertainty	Yes

ble in a complex power system network, where parameters are correlated to each other. Many researchers have used AI-based methods to identify the hidden inter-dependencies among the uncertain parameters in the DNs. For instance, in [74], a physics-informed probabilistic graph convolution network was proposed to predict the voltages within the DNs integrated with solar panels and electric vehicles. In this article, the Bayesian network (BN) was used to quantify the uncertainty in the network topology at the planning stage.

Despite the accurate predictions in the planning stage, real-time (or operational) uncertainties can impact the power system operations. So, further research is required to uncover the potential of addressing these uncertainties. The BN's ability to model complex inter-dependencies and update beliefs based on new data makes it advantageous for real-time uncertainty detection and management. BNs are being used in various applications due to their ability to provide reliability in uncertainty estimations. Many researchers have used BNs in the energy sector for various applications including energy forecasting, optimisation risk assessment, O&M planning, etc. [75, 76]. However, modelling the data uncertainty using BNs in DERs is still an unexplored research area.

To predict weather-induced power outages, another AI-based approach, namely long short-term memory (LSTM), was used by [77] to identify weather patterns and their impact on power system reliability. However, robust probabilistic methods are needed to handle and model sudden uncertainties and maintain the power system performance of DNs. In this regard, Pan *et al.* in [78] proposed a probabilistic approach to model the uncertain reserve capacity of wind generators considering the operational uncertainties. Other studies carried out in [79] and [80] used nested Markov Chain Monte Carlo (MCMC) and joint raw moments-based analytical methods respectively for the probabilistic power flow analysis. While these methods demonstrate better efficiencies as compared to traditional MCMC methods under normal conditions, they do not fully account for the real-time variations of weather-dependent RESs under extreme weather events.

In [81], an optimal strategy for mitigating voltage imbalances in DERs was proposed through the joint allocation of energy storage systems. This approach aimed to stabilise voltage profiles by strategically deploying storage devices. Similarly, [82] explored a mitigation strategy designed to address congestion in multi-operator flexible market systems for energy trading. However, both studies did not address the impact of uncertainty on carbon emissions associated with these systems. The potential for reducing carbon footprints through these uncertainty mitigation strategies remains unexplored.

In a nutshell, an intelligent and robust framework is required because existing methods for uncertainty modelling in power systems rely on static probability distributions, which limits their adaptability to real-time fluctuations. Therefore, a carbon-intelligent framework is proposed that extends existing research by integrating Bayesian networks with the stochastic energy scheduling for uncertainty-aware decision-making to optimise renewable energy scheduling, improve grid resilience, and minimise carbon emissions.

Chapter 3

Optimal planning of renewable energy systems

The energy sector contributed around 73.2% (24.2% by Industries, 16.2% by transportation, 17.5% by the residential buildings) of the total global carbon emissions in 2020 [83]. Often the residential sector is overlooked as it deals directly with consumer-end, however, it is important to reduce its emissions as it accounts for approximately one-fifth of the global emissions in the world [83]. RESs such as wind, solar, biomass are gaining importance to reduce emissions in the energy sector. However, these sources depend highly on various technical, economical, and environmental conditions and hence, a planned strategy is required to place different RESs at different locations based on their suitability in order to efficiently meet the required load demand while reducing the total carbon emissions. Taking this into account, this chapter presents a hybrid energy system model designed to optimise the integration of RES within different types of energy systems within the planning stage to meet the user load demand. It comprehensively discusses the combination of various parameters to consider for decision-making while planning such an integration. These parameters include technical parameters (such as the amount of energy generated from different sources, electricity purchased and sold to the grid), economic parameters (including costs associated, lifetime, and pay-

back period of the specified configuration), and finally environmental parameters (carbon emissions) for different combinations of RESs along with the utility grid. Fig. 3.1 shows the overall research approach used to find the optimal combination of RESs.

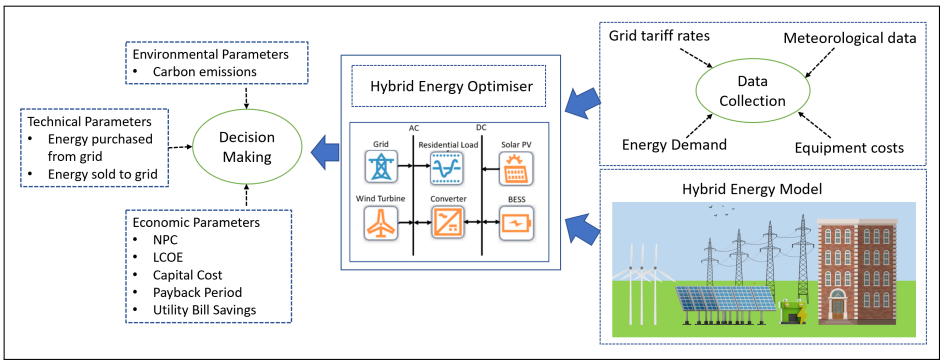

Figure 3.1: Techno-economic-environmental analysis process in a hybrid energy system

The first step involves the collection of various types of data, which is critical for the accurate simulation and optimisation of the energy system. This data includes energy demand profiles, weather patterns, economic factors, and technological specifications, all of which are fed into the hybrid energy system model. The model is designed to simulate different configurations of renewable energy plants— such as solar panels, wind turbines, and battery storage systems— alongside traditional electricity grid (or utility). Through simulation, the model seeks to identify the optimal combination of these energy sources that can meet the load demand while balancing technical, economic, and environmental objectives. The main contributions of this chapter are:

- Determination of optimal combination of RESs in terms of capacity and location to meet the load demand using PSO while reducing the cost and carbon emissions.
- Comparative analysis of different combinations of renewable energy generation and utility grid based on the technical, economic, and environmental parameters to meet the load demand.

The nomenclature used in this chapter for the symbols is presented in Table 3.1.

Table 3.1: Table of symbols used in chapter 3

Symbol	Description
BG	Budget for the installation (£)
c_1, c_2	Acceleration constants to control influence of *pbest* and *gbest*
CE_{sys}	System carbon emissions (kg CO_2)
CE_{per}	Permissible carbon emissions (kg CO_2)
C_{pv}	Solar power generation cost (£/kWh)
C_w	Wind power generation cost (£/kWh)
C_b	Battery operational cost (£/kWh)
C_{in}	Invertor operational cost (£/kWh)
C_{pv}	Costs (Capital, replacement, operational, maintenance) for solar panels (£)
C_w	Costs (Capital, replacement, operational, maintenance) wind turbines (£)
C_{in}	Costs (Capital, replacement, operational, maintenance) for inverters (£)
Cap_{pv}, Cap_w, Cap_b	Capacities of solar panels, wind turbines and batteries (kW)
D_{pv}	Derating factor (%)
f	Discount rate (%)
$gbest$	Global best solution
$G_T(t)$	Solar irradiance incidence at time t (kW/m^2)
G_{STC}	Solar irradiance incidence under standard testing conditions (kW/m^2)
L_{pv}, L_w, L_b	Location of solar panels, wind turbines and batteries (kW)
LT	Project lifetime (years)
$pbest_i$	Particle i^{th} best score
$P_B(t)$	Battery power at time t (kW)
$P_g(t)$	Power fed by the utility grid at time t (kW)
$P_{load}(t)$	Instantaneous load demand at time t (kW)
$P_{pv}(t)$	Power of PV panel at time t (kW)
P_{peak}	Peak PV module output power (kW)
$P_{pv}^{min}, P_{pv}^{max}$	Lower and upper solar power capacity (kW)
$P_w(t)$	Power of wind turbine at time t (kW)
P_w^r	Rated power of wind turbine (kW)
P_w^{min}, P_w^{max}	Lower and upper wind power capacity (kW)
P_o^i	Power output from the inverter (kW)
P_o^r	Rectified inverter output to the battery (kW)
P_{dc}, P_{ac}	DC and AC powers of converter (kW)
r_1, r_2	Random numbers between 0 and 1
r_n, r	Nominal and real discount rate (%)
SOC^{min}, SOC^{max}	Lower and upper state of charge (SOC) of battery (%)
T_C	PV cell temperature (°C)
$T_{C,STC}$	PV cell temperature under standard testing conditions (°C)
$vel_i(t)$	Velocity of i^{th} particle at time t (m/s)
$v(t)$	Wind speed at time t (m/s)
v_i, v_o	Cut-in and Cut-off wind speed (m/s)
v_r	Rated wind speed (m/s)
J	Inertia weight to balance global and local exploration
N_w	Number of wind turbines installed
α_p	Power temperature coefficient
w_1, w_2	weights that balance the importance of cost and emissions
N_{pv}	Number of solar panels
N_b	Number of batteries
$x_i(t)$	Position of i^{th} particle at time t
η_{ch}, η_{dch}	Battery charging and discharging efficiencies
η_i, η_r	Inverter and rectifier efficiencies of converter (%)
ω	inertia weight to balance the global and local exploration

3.1 Model Description

The model described in this chapter as depicted in Fig. 3.1 is a comprehensive hybrid energy system designed to optimise the integration of RESs. It combines multiple data inputs, including energy demand profiles, weather data, and economic parameters, to simulate various configurations of solar, wind, and battery storage systems alongside grid electricity. Each of these are discussed briefly below:

3.1.1 Load

In the model, two distinct types of loads have been considered to evaluate the performance and optimisation of the hybrid energy system. The first load type is a *residential load*, which represents the energy consumption patterns of a typical residential area consisting of multiple households. The second load type is a *hybrid load*, which encompasses a more complex and diverse set of energy demands. This includes not only residential consumption but also commercial, industrial, and possibly institutional loads within a broader distribution network. A detailed description of both the loads along with their daily energy demand profiles is described as follows.

3.1.1.1 Residential Load:

The residential load considered in this study consists of approximately 150 households in London [84]. Each household contributes to the overall load profile, which is characterized by daily and seasonal variations. The load profile is predominantly influenced by factors such as occupancy patterns, weather conditions, and energy consumption behaviors. For the purpose of this analysis, the aggregated load of the residential complex is modeled as a time-varying demand curve, representing the hourly energy consumption of all households for an entire year for these houses based on [84]. Figure 3.2 depicts the monthly power demand for the residential

sector where January month contributes towards the highest consumption and September towards the lowest.

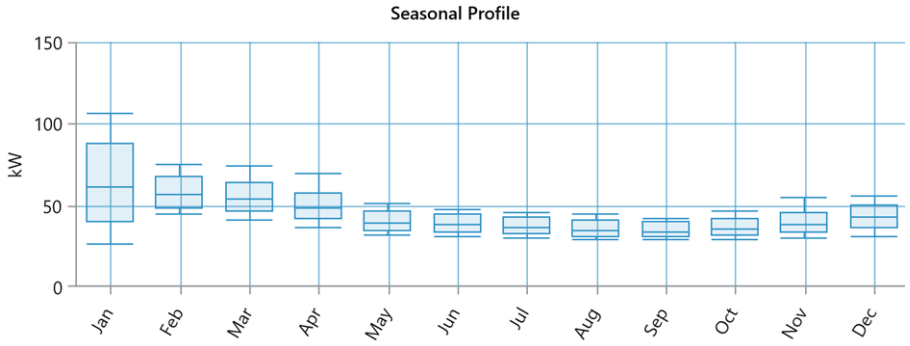

Figure 3.2: Monthly profile of the residential sector

Moreover, it has been found that the largest annual peak demand occurred on 13^{th} January as shown in Fig. 3.3. The reasons behind that are: 1) weekend during which people prefer to spend time with their families at home 2) the lowest temperature went to -1^oC with high wind speeds. Therefore, instead of going out, residents must be at home most of the time doing household chores, watching movies, etc. which increases the electricity consumption.

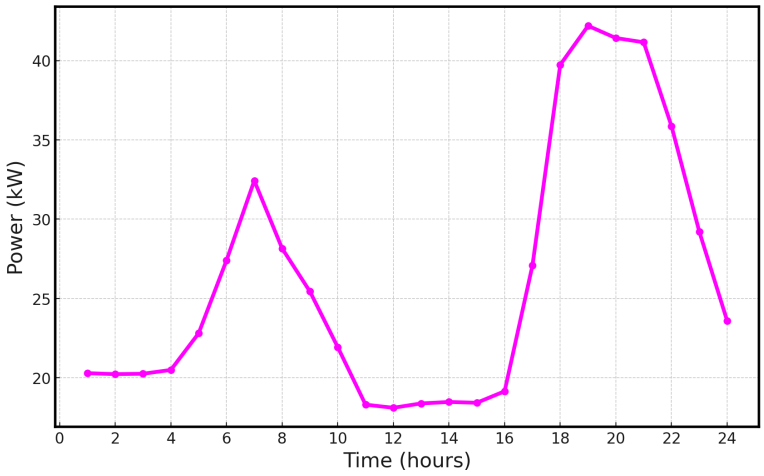

Figure 3.3: Energy profile of the peak demand day

3.1.1.2 Hybrid Load:

A mixed load environment, including residential, commercial, retail, and hospital loads is considered for the analysis [85]. The residential loads within the network typically follow a similar pattern to the previously described residential complex, with peak demand in the evening. However, the commercial, retail, and hospital loads introduce additional complexities.

- **Commercial Loads:** These include office buildings, educational institutions, and small businesses, with a load profile that peaks during standard business hours (8 AM to 6 PM) as shown in Fig. 3.4. Commercial loads are generally more stable throughout the day but can vary depending on the type of business and occupancy levels.

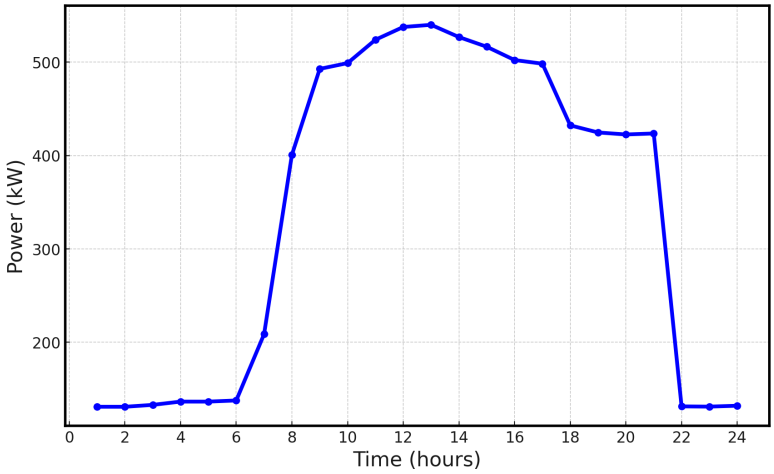

Figure 3.4: Energy profile for the commercial load

- **Retail Loads:** Retail loads, encompassing shops, supermarkets, and malls, tend to have a slightly later peak, typically in the late morning to early evening. These loads are influenced by consumer behavior, operational hours, and special events or sales periods. Figure 3.5 shows the typical daily load of a medium-sized supermarket.

- **Hospital Loads:** Hospital loads are critical and less variable, with a relatively constant demand throughout the day and night as depicted in Fig. 3.6.

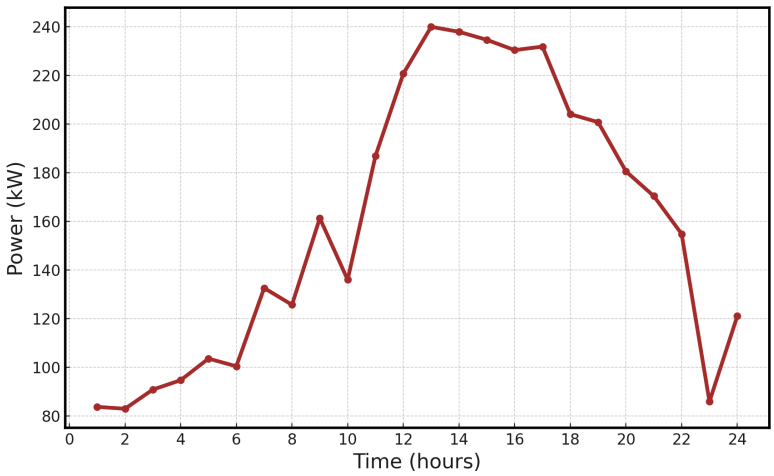

Figure 3.5: Energy profile for the retail load

These loads include essential services such as lighting, HVAC (Heating, Ventilation, and Air Conditioning), medical equipment, and emergency power systems. Due to the critical nature of hospital operations, these loads have high reliability and power quality requirements.

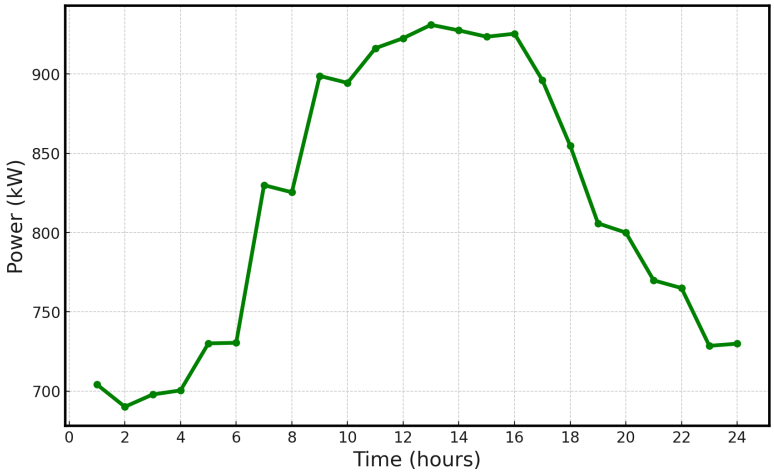

Figure 3.6: Energy profile for the hospital load

3.1.2 Solar Panels

Solar panels are made up of small units called solar cells. The panels are connected in series and parallel to harness the solar energy and convert it into power. Light from the sun (also called solar irradiation) stimulates electrons on a solar panel

that creates direct current. However, the derating factor and the temperature of the PV panels have a negative effect on the DC produced in proportion to the solar irradiation. Taking this into account, the power produced by the PV can be mathematically calculated as [31]:

$$P_{pv}(t) = N_{pv} P_{peak} D_{pv} \left[\frac{G_T(t)}{G_{STC}}\right] [1 - \alpha_p (T_C - T_{C,STC})] \tag{3.1}$$

where P_{peak} is the peak PV module output power, D_{pv} is the derating factor (%), α_p is the power temperature coefficient, $G_T(t)$ and G_{STC} are solar irradiance incident on PV module at time t (kW/m^2) and under standard testing conditions respectively, T_C and $T_{C,STC}$ are PV cell temperature at time t and under standard testing conditions respectively, $N_{pv} = N_s \times N_p$, i.e., number of panels connected in series and parallel respectively.

Fig. 3.7 represents the average hourly profile of solar irradiation and corresponding energy output by the PV panels for January and September.

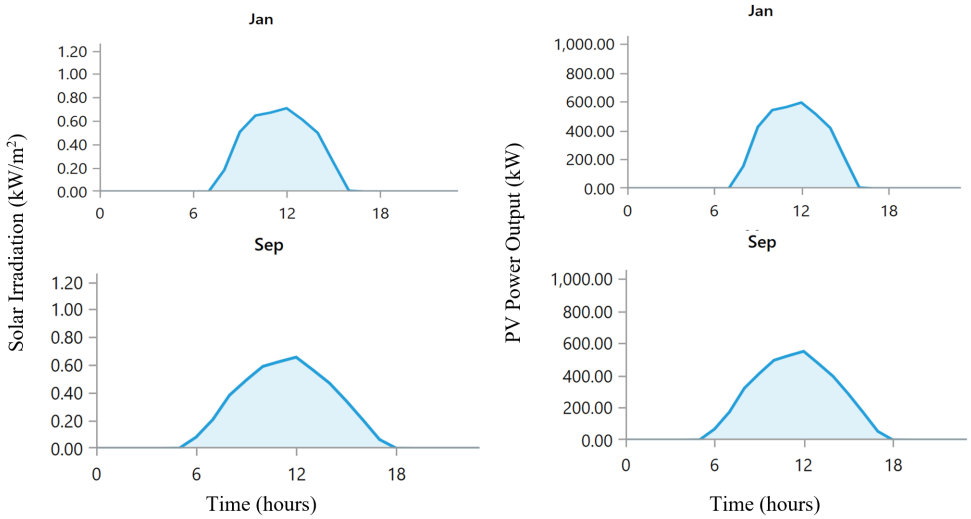

Figure 3.7: Average hourly profile of solar irradiation and corresponding energy output by the PV panel

3.1.3 Wind Turbine

The wind energy can be modeled as a series of blades mounted around a rotor catch the wind and translate its kinetic energy into rotational energy. Traditional windmills use this concept to grind wheat or pump water; whereas modern wind turbines turn a generator that creates electricity. This conversion from wind's rotational energy to electricity can be calculated as [30]:

$$P_w(t) = N_w P_w^r \begin{cases} 0 & ; \quad v(t) \leq v_i \ or \ v(t) \geq v_o \\ \frac{v(t)-v_i}{v_r-v_i} & ; \quad v_i \leq v(t) \leq v_r \\ 1 & ; \quad v_r \leq v(t) \leq v_o \end{cases} \tag{3.2}$$

where $v(t)$ is wind speed at time t, v_i and v_o are cut-in and cut-off wind speed respectively, v_r is rated wind speed, and P_w^r is rated power of wind turbine. N_w is the number of wind turbines installed. There are three primary factors that determine just how much energy turbines can produce: size and orientation of the blades, aerodynamic design of the blades, and the amount of wind turning the rotor. Figure 3.8 represents the average hourly profile of wind speed and corresponding energy output by the wind turbine for January and September.

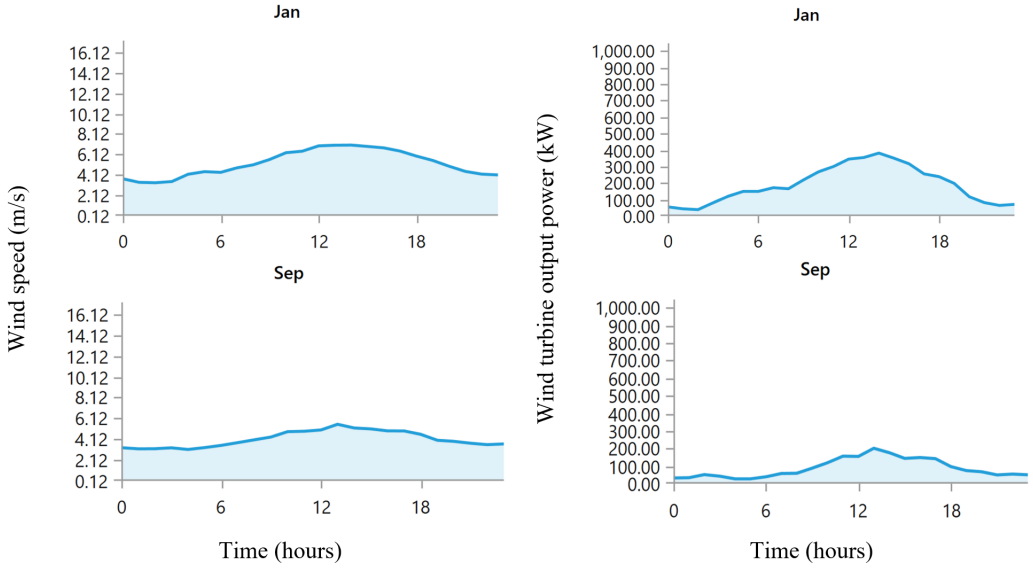

Figure 3.8: Average hourly profile of wind speed and corresponding energy output by the wind turbine

3.1.4 Battery Energy Storage System

The energy generated from the RESs gets stored in the battery during the off-peak period and could be used during the peak demand hours. BESS maximises the utilisation of energy generated by RESs and hence, contributes towards stable operation during the situation of mismatch between the energy generation and demand. The instantaneous power of the battery $P_B(t)$ can be defined as [31, 86]:

$$P_B(t) = P_B(t-1) - \begin{cases} \eta_{ch}(P_{load}(t) - \frac{P_{pv}(t)+P_w(t)}{\eta_r}) \text{ ; charging} \\ \eta_{dch}(\frac{P_{load}(t)}{\eta_c} - (P_{pv}(t) + P_w(t))) \text{ ; discharging} \end{cases} \tag{3.3}$$

where P_{load} is the load demand, η_r is the converter efficiency, η_{ch} and η_{dch} are the battery charging and discharging efficiencies, respectively.

3.1.5 Converter

Power converters are employed to convert DC power to AC and vice-versa. For instance, DC electricity generated by PV panels is converted to usable electricity before sending to the consumer. In addition to this, AC power is converted into DC by the converter to charge the battery. The power conversion can be determined as follows [29]:

$$P_o^i = \eta_i P_{dc} \tag{3.4}$$

$$P_o^r = \eta_r P_{ac} \tag{3.5}$$

where, P_o^i is the power output from the inverter (kWh), P_o^r is the rectified inverter output to the battery, P_{dc} and P_{ac} are the DC and AC powers respectively, η_i and η_r are the inverter and rectifier efficiencies respectively.

3.1.6 Utility Grid

It represents the local utility company that supplies electricity to the residential load. The tariff rates, demand charges and consumption charges are considered as per the standard UK energy rates [87].

3.2 Problem Formulation

The optimal placement and sizing of RESs forms a mixed-integer linear programming (MILP) problem. In this section, the optimisation problem is formulated using PSO to determine the optimal size of wind turbines, solar panels and energy storage required to meet the energy demand.

This subsection will focus on the optimisation of a residential load, which typically involves simple load balancing and basic equations for energy generation and consumption. The goal here would be to minimise costs and emissions while meeting the energy demand of the residential area using different energy sources (grid, solar, wind, etc.).

The objective is to minimise the total cost and carbon footprints of the system with more penetration of RESs while ensuring a reliable and sustainable power supply. The decision variables in this MILP optimisation problem are the number of solar panels (N_{pv}), wind turbines (N_w) and batteries (N_b) needed for the optimal operation to minimise the system annual cost (SAC) and carbon emissions of the residential buildings over the time period T.

The multi-objective function for SAC can be formulated as:

$$\min(SAC) = \sum_{t=1}^{T}(N_{pv}C_{pv}(t) + N_wC_w(t) + N_bC_b(t) + P_o^iC_{in}(t)) \tag{3.6}$$

The above equation is subjected to various constraints as listed below.

- Power Balance Constraint

$$\sum_{t=1}^{T}(P_{pv}(t) + P_w(t) + P_b(t) + P_g(t)) \geq P_{load}(t) \tag{3.7}$$

- Capacity Constraints

$$P_{pv}^{min} \leq P_{pv}(t) \leq P_{pv}^{max} \tag{3.8}$$

$$P_w^{min} \leq P_w(t) \leq P_w^{max} \tag{3.9}$$

$$SOC^{min} \leq SOC(t) \leq SOC^{max} \tag{3.10}$$

- Economic Constraints

$$\sum_{t=1}^{T}(N_{pv}C_{pv}(t) + N_wC_w(t) + N_bC_b(t) + P_o^iC_{in}(t)) \leq BG \tag{3.11}$$

- Environmental Constraints

$$\sum_{t=1}^{T} CE_{sys}(t) \leq CE_{per}(t) \tag{3.12}$$

The values of C_{pv}, C_w, C_b and C_{in} include the capital, replacement, salvage, operational and maintenance costs of solar panels, wind turbines, battery units and inverters respectively. N_{pv}, N_w and N_b are the functions of their respective locations (L_{pv}, L_w and L_b) and capacities (Cap_{pv}, Cap_w and Cap_b) which is optimised by the PSO. The description of these variables is presented in Table 3.1.

3.3 Optimisation Methodology

The strategic placement and sizing of Distributed Generation (DG) is critical for achieving optimal performance in power networks. Improperly sized or located DG units can result in a range of complex technical, economic, and environmental issues, including system inefficiencies, increased operational costs, and adverse environmental impacts. This problem is characterised by a mixed-integer, non-linear formulation with a high degree of constraints, making it a highly complex optimisation challenge. It encompasses multiple objectives, often conflicting, such as minimising active power losses, improving voltage profiles, enhancing voltage stability margins, increasing system reliability, and reducing both operational costs and emissions. To address this multi-objective optimisation problem effectively, advanced multi-objective algorithms are frequently employed. In our case, we have used particle swarm optimisation (PSO) to solve the multi-objective optimisation problem associated with DG placement and sizing. In addition to its simplicity, PSO has the ability to converge quickly to a near-optimal solution while handling complex and multi-dimensional problems in the energy network as compared to the other optimisation methods.

PSO is a swarm-based meta-heuristic method based stochastic optimisation technique, used for solving optimisation problems by simulating the social behavior of the particles. It is a type of evolutionary algorithm and is particularly useful for finding approximate solutions to complex problems where the search space is large and traditional optimisation methods may struggle. It can be effectively used for the optimal placement of RESs with the objective of reducing carbon emissions and minimising overall energy costs. The problem involves determining the best locations and capacities for installing RES such as wind turbines and solar panels, taking into account both environmental and economic factors. The working of the PSO algorithm is depicted in Algorithm 3.1 and briefly explained as follows.

- **Particle initialisation:** Particle is the basic unit in PSO, representing potential solutions to the optimisation problem. The particle's position encodes variables such as the number of RES units at each potential site and their respective capacities. They are randomly distributed in the search space.

- **Swarm:** It is a collection of particles that move through the search space, such as representing different configurations of RES placements, while sharing information about the best-found solution with each other. This allows the swarm to converge towards an optimal solution.

- **Optimisation/Fitness function:** It evaluates how good a particle's position is with respect to the overall optimisation objective. Once the fitness of each particle's solution is evaluated, the global best solution (*gbest*) is updated to reflect the particle with the best score (*pbest*). This global best solution then guides the search process by serving as a target for the other particles to aim for. The fitness function for this problem can be written as:

$$fitness = w_1\ SAC + w_2\ CE \tag{3.13}$$

  where w_1 and w_2 are weights that balance the importance of cost and emissions.

Algorithm 3.1 Particle Swarm Optimisation Algorithm

Initialise the population (particles) x_i randomly for $i = 1, 2, \ldots, N$
Initialise the velocity vel_i of each particle randomly
Set parameters: inertia weight ω, acceleration constants c_1 and c_2
Evaluate the fitness of each particle $f(x_i)$ using eq. (3.13)
Set the personal best $pbest_i = x_i$ for each particle
Set the global best $gbest$ to the position of the best particle in the population
while stopping criterion is not met **do**
    for each particle i **do**
        Update velocity vel_i using eq. (3.14)
        Update position x_i using eq. (3.15)
        Evaluate the fitness of the new position $f(x_i(t+1))$
        if $f(x_i(t+1)) < f(pbest_i)$ **then**
            Update personal best: $pbest_i = x_i(t+1)$
        end if
        if $f(pbest_i) < f(gbest)$ **then**
            Update global best: $gbest = pbest_i$
        end if
    end for
end while
Return global best solution $gbest$

- **Parameter tuning:** Each particle's (i) parameters such as velocity (vel_i) and position (x_i) are updated iteratively based on its own best-known position and the best-known position of any particle in the swarm. The velocity at time $t+1$ is updated as follows:

$$vel_i(t+1) = \omega vel_i(t) + c_1 r_1(pbest_i - x_i(t)) + c_2 r_2(gbest - x_i(t)) \quad (3.14)$$

  where ω is the inertia weight to balance the global and local exploration, c_1 and c_2 are acceleration constants that control the influence of $pbest$ and $gbest$, r_1 and r_2 are random numbers between 0 and 1. The position of particle is updated as:

$$x_i(t+1) = x_i(t) + vel_i(t+1) \quad (3.15)$$

- **Convergence:** The above step is repeated until the swarm converges around the best-found solution. The process continues for a specified number of iterations or until a stopping criterion is met (e.g., the fitness value changes by less than a threshold).

Figure 3.9 shows the operational strategy used to find the optimal placement of RESs in the distribution network using PSO and Newton Raphson (NR) method [88]. NR method is used to carry out the load flow analysis of the energy network, wherein the currents, voltages and power flow within the network are calculated. These parameters are used to establish the initial network's performance which is a crucial step to solve the optimisation problem.

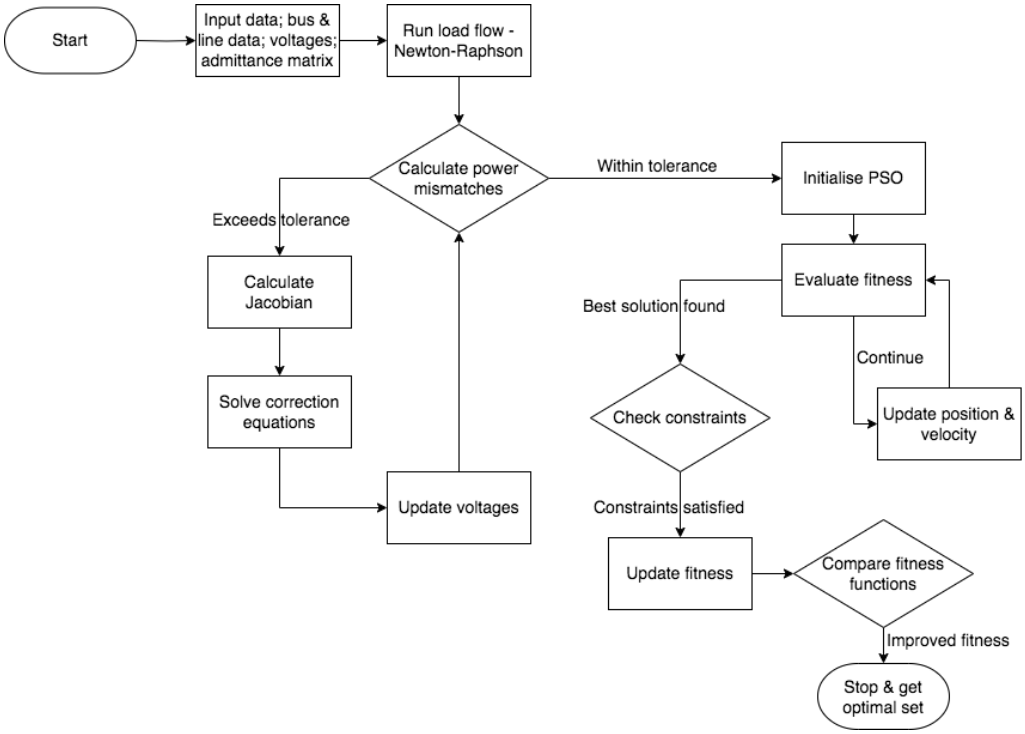

Figure 3.9: Operational Strategy for the optimal operation of renewable integrated DNs

3.4 Results & Discussion

In this work, the MILP is solved using PSO to obtain the results for various configurations of energy generation sources (Grid, Solar, and Wind) which were validated using HOMER (Hybrid Optimisation of Multiple Energy Resources) [89] for both the type of loads mentioned in the section 3.1. The decision-making for the optimal placement of RESs involves evaluating technical, economic, and environmental pa-

rameters to determine the feasibility of each scenario, allowing consumers to choose between cost and emissions for their electricity needs. The optimisation problem using PSO is converged in 10 and 60 iterations for residential and hybrid loads respectively as shown in Fig. 3.10. The key concept used to decide the feasibility of the result was that at every time step, the load demand was being met under the specified conditions.

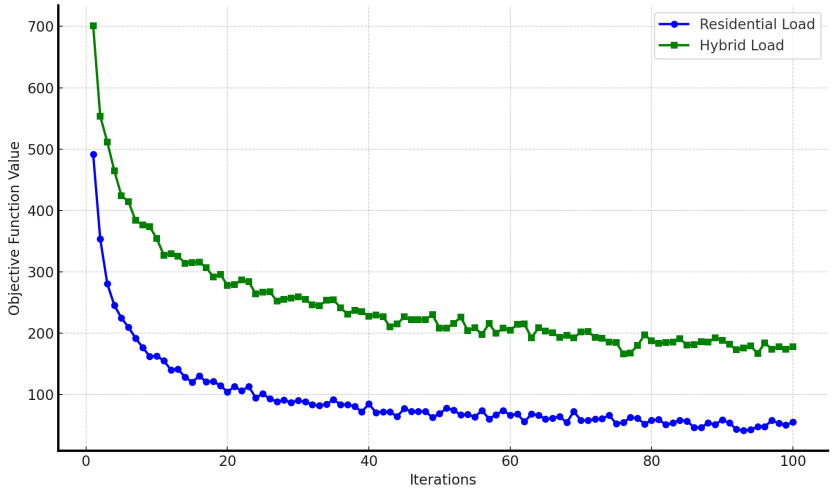

Figure 3.10: Convergence curve using PSO for the residential and hybrid load

The simulation results are analysed and classified into three main categories: technical, economic, and environmental parameters.

- **Technical Parameters:** These include the amount of energy generated from each source (solar, wind, and grid), the total electricity purchased from the grid, and the electricity sold back to the grid. These parameters provide insight into the efficiency and reliability of different system configurations, highlighting their ability to meet the residential load demand and contribute excess energy to the grid.

- **Economic Parameters:** The economic analysis covers several key financial metrics associated with the different energy configurations. These include:

  - *Net Present Cost (NPC):* NPC is defined as the difference between the total costs incurred by the project (including capital expenditure, opera-

tional, and maintenance costs) and the total revenue generated over the project's lifetime. It offers a comprehensive measure of the long-term financial viability of the system and is calculated as [89]:

$$NPC = \frac{SAC}{(1-(1+r)^{-LT})/r} \tag{3.16}$$

where, LT is the project lifetime (years), r is the real discount rate.

$$r = \frac{r_n - f}{1+f} \tag{3.17}$$

where, r_n is nominal discount rate and f is the inflation rate.

- *Levelised Cost of Energy (LCOE):* This metric represents the average cost per kilowatt-hour (kWh) of electricity produced by the system, taking into account all costs incurred during the project's lifecycle. LCOE is a crucial factor in comparing the cost-effectiveness of different energy sources which is mathematically formulated as:

$$LCOE = \frac{SAC}{Energypurchased + Energysold} \tag{3.18}$$

- *Utility Bill Savings:* This parameter quantifies the reduction in energy costs for the consumer, achieved by generating a portion of their electricity on-site rather than relying entirely on grid electricity. It is an important consideration for consumers looking to reduce their long-term energy expenditures.

- **Environmental Parameters:** The environmental impact of each energy configuration is assessed by measuring the total carbon emissions associated with the system. This analysis is essential for understanding the ecological footprint of the energy systems and for guiding decisions toward more sustainable energy practices.

The top six combinations resulted from PSO which are able to satisfy the optimisation constraints given in Eqs. (3.7) - (3.12) are depicted in Fig. 3.11. Figure 3.12

and Fig. 3.13 shows the results of simulation for these combinations with respect to carbon emissions, LCOE, energy sold and energy purchased from the grid for residential and hybrid loads respectively.

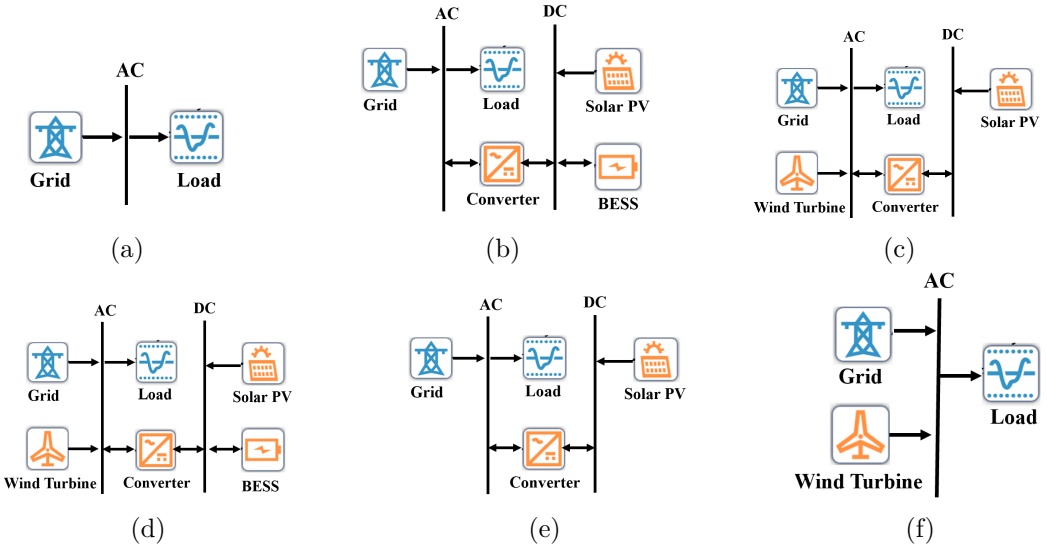

Figure 3.11: Different configurations of RESs with and without the grid for the optimal operation of the energy network

The following points could be inferred from Fig. 3.12 and Fig. 3.13:

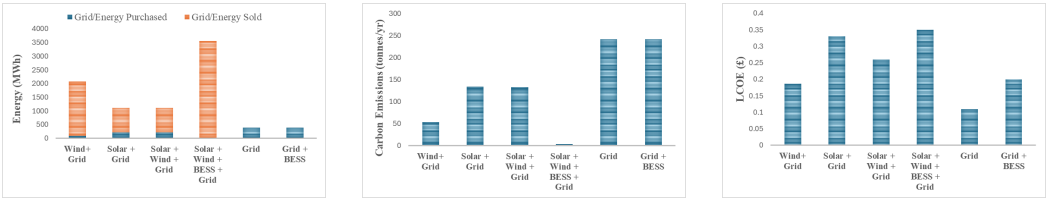

(a) (b) (c)

Figure 3.12: Comparison among different configurations based on carbon emissions, utility bill savings, energy sold & purchased for residential load

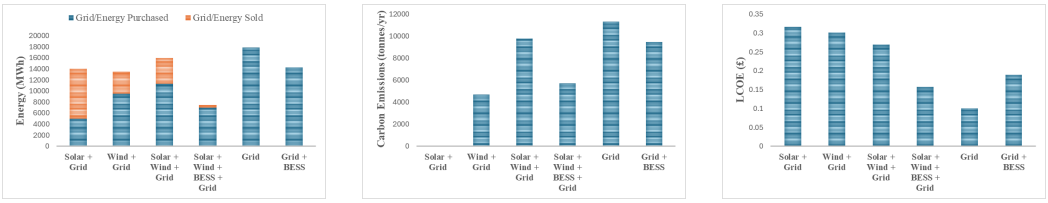

(a) (b) (c)

Figure 3.13: Comparison among different configurations based on carbon emissions, utility bill savings, energy sold & purchased of Hybrid load

- **Solar+wind+BESS+grid system** results in the lowest carbon emissions compared to other systems. After meeting its local load demand, this system generates the most surplus energy that is sold back to the grid. This indicates that the system is highly efficient in producing more energy than it consumes locally. High energy sales to the grid imply that this system not only covers its local energy needs effectively but also contributes significantly to the overall grid supply. This could be especially beneficial in balancing grid demand, particularly during peak times or when renewable generation is high. Despite its environmental benefits and high energy production, the system has the highest LCOE. Renewable energy sources, while cleaner, are expensive to deploy, especially when coupled with battery storage.

- **Grid and Grid+BESS systems** account for the highest carbon emissions, as they rely entirely on electricity purchased from the grid, which is often generated from fossil fuels. This dependency not only contributes to increased emissions but also leads to higher utility bills for consumers due to the consistent need to buy electricity from the grid. However, these systems benefit from a lower LCOE, primarily because they avoid the upfront costs and maintenance associated with renewable energy installations and storage systems, making them more economically feasible in terms of immediate costs despite their environmental drawbacks.

- **Wind+grid, solar+grid Solar+wind+grid systems** represent trade-off solutions, balancing environmental impact with economic considerations. These systems integrate renewable energy sources (wind, solar, or both) with grid electricity, which helps reduce carbon emissions compared to a grid-only system. By generating a portion of electricity locally, reliance on grid power is decreased, leading to lower utility bills. However, these systems still depend on grid electricity, especially during periods when renewable generation is insufficient, which keeps emissions higher than fully renewable setups. Despite this, their LCOE remains relatively low, as the use of grid power reduces

the need for expensive energy storage solutions, making these configurations a more affordable yet environmentally conscious option.

Out of the various feasible solutions obtained after simulating the energy system with a distinct combination of energy resources, three best possible solutions (or cases) were selected based on minimum emissions, minimum cost and trade-off between emissions and cost. These cases are shown in Table 3.2 and Table 3.3 for residential and hybrid loads respectively, and are explained as follows:

Table 3.2: Techno, Economic and Environmental analysis for residential load

		Case A: Grid only	**Case B: Solar+Wind +BESS+Grid**	**Case C: Wind+Grid**
Architecture			PV capacity- 1046 kW Wind Capacity - 600 kW BESS - 580 strings each 1kWh	Wind Capacity - 800 kW
Technical Parameters	Energy purchased (kWh/yr)	381,516	4,000	84,000
	Energy Sold (kWh/yr)	0	3,544,514	1,991,185
Economic Parameters	NPC (£)	0.5M	8.2M	3.1M
	LCOE (£/kWh)	0.11	0.35	0.187
	Capital Cost (£)	0	8.95M	1.8M
	Payback Period (yr)	–	18	6.2
	Utility Bill Savings (£/yr)	-38,151	176,285	91,159
Environmental Parameters	Carbon Emissions (Kg/yr)	241,118	3870	53,000

Table 3.3: Techno, Economic and Environmental analysis for hybrid load

		Case A: Grid only	**Case B: Solar+Wind +BESS+Grid**	**Case C: Solar+Grid**
Architecture			PV capacity- 2042 kW Wind Capacity - 781 kW BESS - 3401 strings each 1kWh	PV Capacity - 10,673 kW
Technical Parameters	Energy purchased (MWh/yr)	17,888	7039	4986
	Energy Sold (MWh/yr)	0	425	9020
Economic Parameters	NPC (£)	23M	35M	80M
	LCOE (£/kWh)	0.1	0.157	0.316
	Capital Cost (£)	0	15M	73M
	Payback Period (yr)	–	21	12
Environmental Parameters	Carbon Emissions (tonnes/yr)	11,305	5700	0.243

3.4.1 Case A: Minimum Cost

In this scenario, there is no renewable generation to avoid the initial capital investment and the residential load is solely dependent on the utility grid to meet its load demand. There is only one-way flow of energy, i.e., electricity is purchased from the grid. From an economic standpoint, the Grid-only system is the most cost-effective configuration, achieving the lowest LCOE across both load scenarios. In the first load scenario, the Grid-only system delivered an LCOE of just £0.11/kWh, with an associated NPC of £0.5M. This system's simplicity—relying entirely on grid-supplied electricity—eliminates the need for capital-intensive infrastructure,

such as solar panels, wind turbines, and battery storage, thereby reducing upfront costs to zero. Similarly, in the second load scenario, the LCOE further dropped to £0.1/kWh, despite the NPC increasing to £23M due to the higher energy demand. However, this economic advantage comes with a significant environmental cost, as this configuration resulted in the highest carbon emissions: 241,118 kg per year in the first scenario and 11,305 tonnes per year in the second. The Grid-only system, while economically appealing, highlights the trade-off between cost efficiency and environmental sustainability, demonstrating the limitations of relying solely on grid electricity.

3.4.2 Case B: Minimum Emissions

In order to minimise carbon emissions, the Solar+Wind+BESS+Grid system stands out as the most environmentally sustainable configuration. Particularly under the first load scenario, this hybrid system achieved a remarkable reduction in carbon emissions, down to a mere 3,870 kg per year. This significant reduction is attributed to the strategic integration of 1,046 kW of PV capacity, 600 kW of wind capacity, and a robust BESS consisting of 580 strings, each with a capacity of 1 kWh. The system's reliance on renewable energy sources allowed it to minimise energy purchases from the grid to just 4,000 kWh per year, while efficiently selling 3,544,514 kWh of excess energy back to the grid. Similarly, under the second load scenario, this system demonstrated its superior environmental performance with carbon emissions reduced to 5,700 tonnes per year, even with a higher load. This setup not only exemplifies the potential for near-zero emissions but also showcases the capability of modern energy systems to drastically cut down on fossil fuel dependence by maximising the use of renewable resources. This is a zero-emissions case that considers a low-carbon energy system having both solar and wind in addition to the grid connectivity as a backup.

3.4.3 Case C: Tradeoff between cost and emissions

As reflected in Table 3.2 and Table 3.3, this case discussed a trade-off between cost and emissions, to provide a practical solution for solving the energy needs in the present scenario of rising energy prices. Under the first load scenario (as shown in Table 3.2), the Wind+Grid system achieved a substantial reduction in carbon emissions to 53,000 kg per year, while maintaining a relatively low LCOE of £0.187/kWh and an NPC of £3.1M. This setup utilised 800 kW of wind capacity, effectively reducing grid dependency and enabling the sale of 1,991,185 kWh of surplus energy back to the grid. This configuration represents a pragmatic compromise, offering significant environmental benefits at a moderate cost.

In the second load scenario depicted in Table 3.3, the Solar+Grid system exemplified an even more aggressive reduction in emissions, achieving near-zero carbon output at 0.243 tonnes per year, thanks to its substantial PV capacity of 10,673 kW. Despite this impressive environmental performance, the economic trade-off is evident in its higher LCOE of £0.316/kWh and an NPC of £80M, driven by the substantial capital cost of £73M. This system's ability to sell 9,020 MWh of excess energy to the grid further enhances its financial viability, offering considerable utility bill savings over time.

Both the Wind+Grid and Solar+Grid configurations illustrate the feasibility of achieving a balance between environmental and economic objectives. They provide residential complexes with flexible solutions that align with varying priorities—whether it is reducing carbon footprint or managing long-term energy costs—making them attractive options in the transition toward sustainable energy systems.

The above-mentioned cases highlight the fact that reduction in carbon emissions can be achieved by increasing the renewable energy penetration in the existing energy systems, resulting in increasing investment costs. In contrast, with the existing grid, the load demand can be met, however, the target of zero emissions

can not be achieved. Therefore, a trade-off between emissions and cost provides an optimal solution (as discussed in Case C) while designing the capacity of renewable plants in a residential sector. Fig. 3.14 and Fig. 3.15 represent all the feasible solutions obtained after running the PSO, and the tradeoff solution is selected by taking the average values for both cost and emissions.

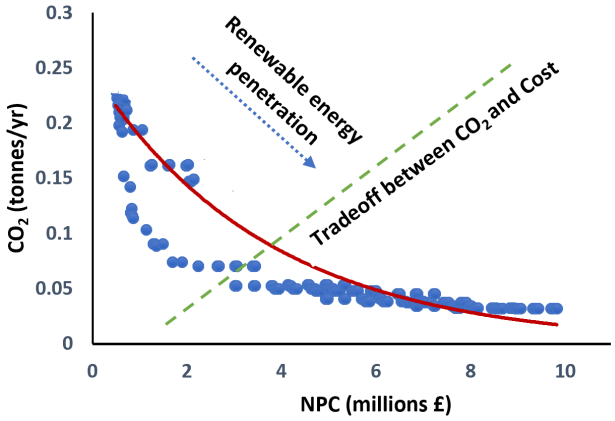

Figure 3.14: Relationship between carbon emissions and NPC (residential load)

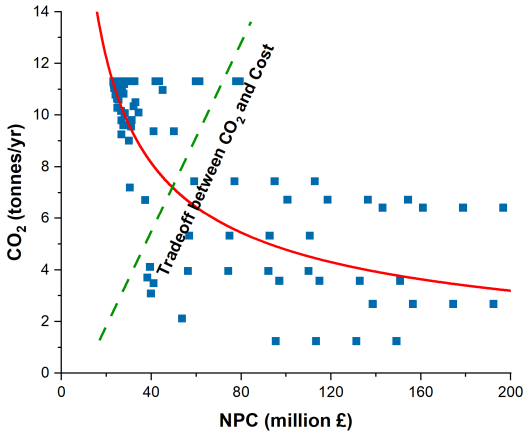

Figure 3.15: Relationship between carbon emissions and NPC (hybrid load)

Figure 3.16 and Fig. 3.17 shows the contribution of different sources of energy to meet the demand under the optimal conditions (Case C) obtained after MILP optimisation. As winds were stronger in London (as compared to solar irradiation), wind energy contributed the largest amount to meet the load demand. Therefore, the results obtained suggest that wind energy alone was able to supply the load, and the investment costs for installing other renewable energy plants (such as solar

panels and BESS) should be avoided. However, there is a need for backup (either grid or other RES) to meet the load demand whenever winds are not strong enough to generate enough energy.

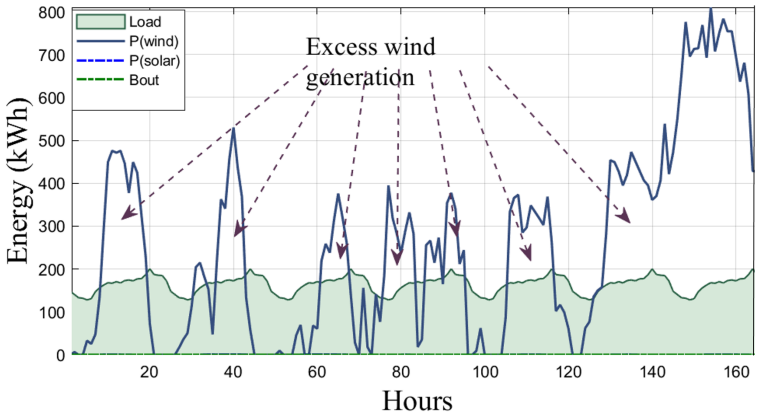

Figure 3.16: Energy generation by RESs to meet demand (residential load)

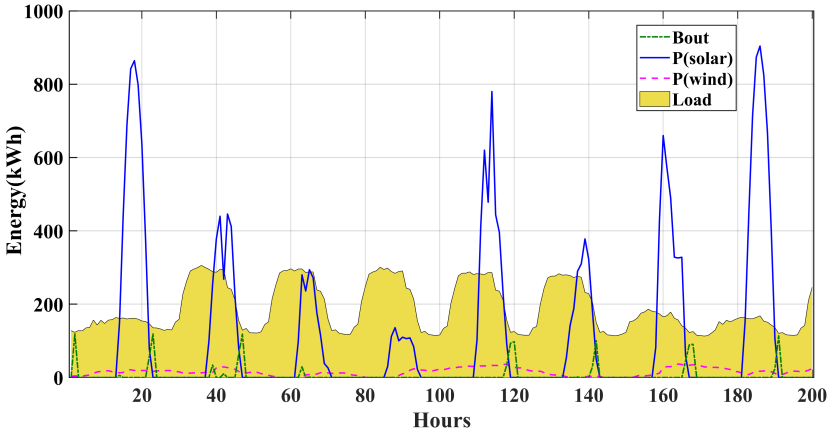

Figure 3.17: Energy generation by RESs to meet demand (hybrid load)

Furthermore, the energy sold by the households was higher than the energy purchased from the grid (as depicted in Fig. 3.18 and Fig. 3.19) resulting in the overall profit to the energy user and simultaneously contributing towards the greener environment.

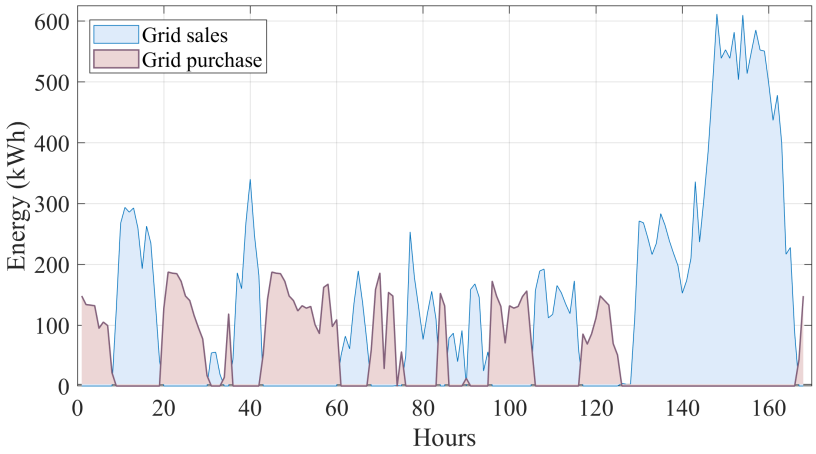

Figure 3.18: Hourly energy sold and purchased from the grid (residential load)

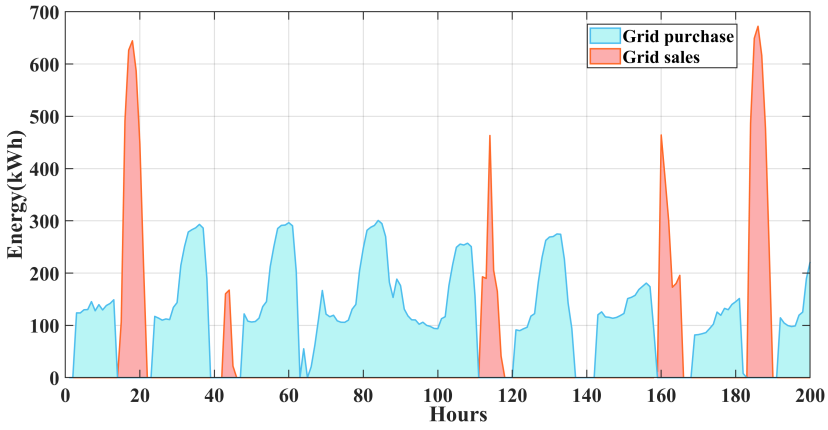

Figure 3.19: Hourly energy sold and purchased from the grid (hybrid load)

3.5 Summary

The techno-economic-environmental analysis presented in this chapter highlighted different feasible combinations of distinct energy sources to reduce the overall costs and carbon emissions. Given the renewable energy penetration in the energy systems and the cost associated to replace the existing energy system with renewable energy systems, the thesis presented an optimal planning solution – a trade-off between cost and emissions for the considered residential load. The environmental analysis carried out in this work suggested the dominance of installing wind turbines or solar panels based on the weather profile of the area. Technical analy-

sis deduced the amount of energy exchange between the households and the grid, whereas economic parameters advised the energy users about the profit and the pay-back period for the optimal case.

Chapter 4

Uncertainty modelling for temporal energy planning

The high reliance of RESs on weather conditions poses certain challenges such as the risk of power outages leading to blackouts especially during extreme weather events [90]. For instance, California experienced around 70% fall in solar generation during the cyclone Hurricane Hilary in August 2023 [91]. Adverse weather conditions like cyclones, thunderstorms, and heatwaves significantly affect renewable power generation, resulting in power disruptions. To mitigate these impacts and enhance DN resilience by reducing power outages due to these uncertainties, a more robust and dynamic approach to model uncertainty is required. The previous chapter used the techno-economic-environmental analysis to decide the optimal location and capacity of renewable energy generation such that the overall cost and carbon emissions are minimised. However, it does not considered the uncertainties associated with the RESs. In this chapter, the temporal variations and complex interdependencies of uncertain parameters in power systems are identified to capture their real-time fluctuations. Based on this, our main contributions are as follows:

- The dynamic probability density functions for uncertain parameters at each time interval are generated to capture temporal variations.
- A two-stage time coordinated Bayesian approach is proposed to identify the

complex interdependencies among uncertain parameters and improve the accuracy of generated samples, especially during extreme weather events.

- An intelligent two-stage stochastic energy scheduling is proposed for the efficient operation and control of the energy system.
- Two performance metrics are proposed to validate the effectiveness of the method by integrating the impacts of carbon footprints and RES in DNs.

The symbols used in this chapter are depicted in Table 4.1.

Table 4.1: Table of symbols used in chapter 4

Symbol	**Description**
$C_{gen}(t)$	Cost of generating power at time t (£)
$C_{grid}(t)$	Cost of purchasing or selling power from/to the grid at time t (£)
$C_{recourse}(t)$	Expected cost of recourse actions under different uncertainty scenarios (£)
$C_b(t)$	Cost associated with charging or discharging the energy storage system (£)
P_{load}	Total energy demand (kW)
$CE(t)$	Carbon emissions associated with power generation at time t (kg CO_2)
$E^f_{dis}(t)$	Energy discharged from battery in area f at time t (kWh)
$E_{total\_sup}(t)$	Total energy supplied by all areas at time t (kWh)
e	Elasticity coefficient
E_G	Total energy generated by the main substation over a time period (kWh)
μ_i	Emission factor of non-renewable energy source i (kg CO_2/kWh)
$g_{ij,n}$	Conductance of branch n between buses i and j (Siemens)
K	Number of renewable energy sources (RESs) in the network
$P^i_{gen}(t)$	Power generated by energy source i at time t (kW)
$P_{grid}(t)$	Power exchanged with the grid at time t (purchased or sold) (kW)
$P_{load}(t)$	Power demand at time t (kW)
P_{loss}	Total power loss in all branches of the network (kW)
$P_{res,k}(t)$	Renewable power generation of each RES at time t (kW)
$P_b(t)$	Power charged/discharged from storage at time t (kW)
ϵ	Allowable deviation for load demand
δ	Uncertain parameter
w_t	Shape parameters of a PDF
θ_i, θ_j	Voltage angles at buses i and j (Radians)
V_{dev}	Voltage deviation (V)
V_{ref}	Reference voltage (V)
V_i, V_j	Voltages at buses i and j (V)
w_1, w_2, w_3, w_4	Weighting factors for each objective in optimisation
SOC_i	State of charge for energy storage system at time i (%)

4.1 Proposed framework

An intelligent framework is proposed (as shown in Fig. 4.1) for the optimal operation of hybrid renewable energy integrated DN. It aims to efficiently tackle uncertainties associated with the RESs generation, storage and distribution to the end-user. The framework comprises three main components: Data Analyser, Uncertainty Modeler and Energy Scheduler, each of them performing a number of tasks critical for the decision-making of energy scheduling. The novelty of this framework lies in the uncertainty modeler that uses the dynamic distributions to predict real-time uncertainties and the energy scheduler that balances the computational efficiency and accurate energy scheduling by intelligently triggering the quarterly scheduling. As a result of combining these elements, the system aims at optimising the operational costs and the amount of carbon emitted during power generation, and still provides a constant supply of energy to users making the whole energy management smart and flexible to the system's operating environment. The detailed functionality of each component is explained below.

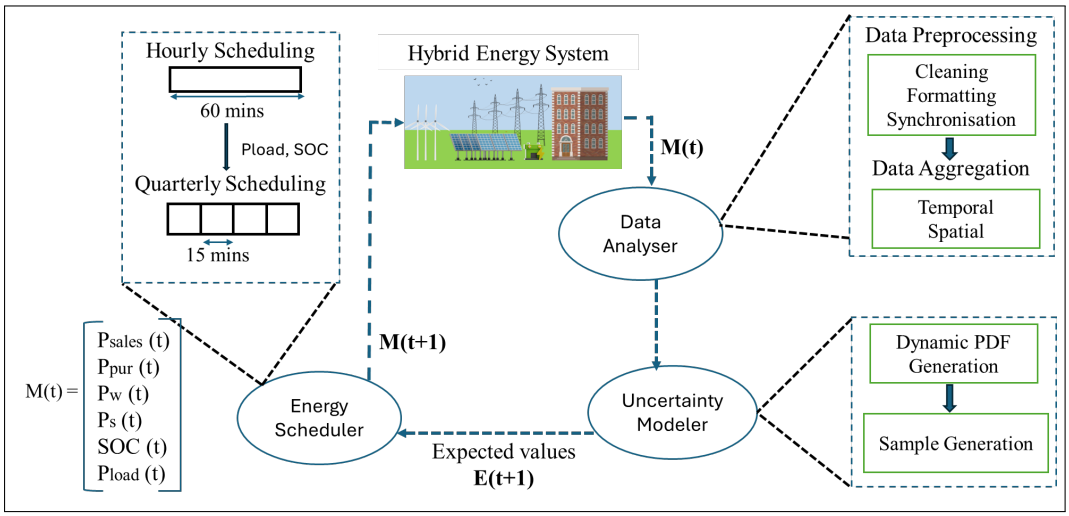

Figure 4.1: Framework for intelligent scheduling of energy systems under uncertainty

4.1.1 Data Analyser

The Data Analyser plays a key role in gathering and processing data from different sources within an energy network. These sources include internal inputs such as generation units (renewable and non-renewable), battery storage, consumer load, sensors, and external inputs like meteorological data, energy prices etc [92], [93]. The process followed by data analyser is as follows:

- **Data Preprocessing:**

  To ensure the quality, reliability and compatibility of data with the system model and optimisation methods, data pre-processing is important. The raw data gathered from various sources is preprocessed before fetching insights for the analysis. The following steps are done after collecting the data:

  - ***Data Cleaning:*** The raw data may contain missing values, noise, and errors, that need to be cleared. Therefore, data cleaning involves:
    - The missing or incomplete data is handled using various methods such as linear interpolation and statistical averaging.
    - Errors due to faulty sensors or communication issues from the raw data are filtered during the data cleaning process.
    - The outliers such as sudden energy surges due to equipment malfunctioning are eliminated.
  - ***Data Formatting:*** The data is gathered from various sources, such as smart meters, weather sensors, and generation units, that have different formats (time-series data, categorical data, etc.). With the data formatting, the entire data is converted to a common format making it consistent and compatible for the analysis.
  - ***Data Synchronisation:*** The data analyser synchronises the entire data gathered from different sources (with different time stamps). This

is a crucial step for the proper alignment of data especially for the time-sensitive tasks such as real-time energy management.

- **Data Aggregation:**

  After preprocessing the data, the complexity of the data is further reduced by aggregating it to extract useful information. It involves combining the data based on common features such as time and location as follows:

  - ***Temporal Aggregation:*** Data can be summarised over various time periods (e.g., hourly, daily, weekly) to provide a high-level view of trends and patterns. For example, aggregating power outputs from solar PV systems on an hourly basis to detect daily generation patterns and summarising consumer energy consumption over a month to analyse billing and usage trends.
  - ***Spatial Aggregation:*** In geographically distributed systems, data can be aggregated based on location, such as aggregating wind generation data from multiple turbines in a wind farm and aggregating energy consumption data across different buildings or neighborhoods to assess regional demand patterns.

- **Data Output and Communication:**

  After the data preprocessing and aggregation, the data analyser communicates the processed and analysed data insights to the other components of the energy network framework. This data is processed in a structured format that can be used by the uncertainty modeler and energy scheduler to make decisions.

  - Real-time data on renewable generation and demand forecasts are passed to the Uncertainty Modeler to quantify and model uncertainties.
  - Aggregated data and insights are shared with the Energy Scheduler to optimise energy distribution and demand response strategies.

4.1.2 Uncertainty Modeler

A novel time-coordinated strategy (TCS) based on the BN and MCMC approach is proposed to model the uncertainty in DNs. This modified MCMC approach provides more accurate estimation of real-time uncertainties, helping the energy scheduler to make more robust decisions. The approach involves two stages that utilise the dynamic behaviour of uncertain variables while modelling these parameters in DNs and are described as follows:

4.1.2.1 Stage 1: Temporal Probability Density Function generation

The dynamic distributions offer numerous advantages such as more adaptive scheduling and improves real-time forecasting errors by capturing the temporal variations in the uncertain parameters. In renewable integrated DNs, instead of using static distributions for the uncertain parameters (e.g., Weibull for wind speed or binomial for solar irradiance), we fit the PDFs at each time interval based on historical data using Eq. (4.1). Let $\delta(t)$ represent an uncertain variable (e.g., wind speed) at time t. The PDF $f(\delta(t))$ is dynamically generated using the observed data $\{\delta(t)\}_{t=0}^{T}$ over past intervals:

$$f(\delta(t)) = \mathrm{PDF}(\delta(t); \alpha_t) \tag{4.1}$$

where α_t represents the set of parameters that define the PDF at each time step t. Further, these dynamic PDFs are updated using Bayesian networks to incorporate the hidden inter-dependencies among the different time intervals of an uncertain variable. Using Bayes formula, the conditional probability ($Pr(X|Y)$) of the occurrence of an event X given the probability of an event Y is calculated. Here X represents the value of an uncertain parameter at time t and day d of a year and Y represents the historical values of the uncertain parameter (at time steps, $t = t-1, t-2, \ldots$ and days, $d = d-1, d-2, \ldots$). To consider the real-time impact of the intermittent nature of RESs in the network and to enhance the robustness of the network model to operational uncertainties, we compute the correlation of

uncertain variables across different time steps. For instance, we analyse how wind speed ($v(t,d)$) at time t on the day d of the year is correlated with wind speed at different times on the current and previous days. Hence, we compute the conditional probabilities for the wind speed as

$$Pr(v(t,d) \mid v(t-1,d), v(t-2,d), \ldots, v(t,d-1), \ldots). \tag{4.2}$$

Based on the established conditional probabilities, the new PDF, $q(\delta(t))$ of the uncertain variable δ at any time t, is calculated as

$$q(\delta(t)) = f(\delta(t); \omega_t) \tag{4.3}$$

where ω_t determines the updated PDF shape parameters obtained from the correlation among the real-time values and predicted values of the uncertain parameters.

4.1.2.2 Stage 2: Sample Generation using modified MCMC

The dynamically generated PDFs (obtained in Eq. (4.1)) from stage 1 are used to generate samples. The basic MCMC approach (where at any time t and i^{th} iteration, the current state of a sample depends on its previous state) is utilised for the sample generation, with a modification that the PDF obtained in Eq. (4.3) is used as a proposal distribution. For each current state ($\delta_i(t)$), a sample y is generated from the proposal distribution obtained in stage 1 ($q(y, \delta_i(t))$). The probability of acceptance of the current state is given as

$$\gamma(\delta_i(t), y(t)) = \min\left(1, \frac{f(y(t))q(\delta_i(t)|y(t))}{f(\delta_i(t))q(y(t)|\delta_i(t))}\right). \tag{4.4}$$

The new state of the sample at time t, $\delta_i(t)$ is given by

$$\delta_i(t) = \begin{cases} \delta_i(t), & u \leq \gamma(\delta_{i-1}(t), \delta_i(t)) \\ \delta_{i-1}(t), & u > \gamma(\delta_{i-1}(t), \delta_i(t)) \end{cases} \tag{4.5}$$

where u is a random number drawn from the uniform distribution over the interval $(0,1)$.

Therefore, following the above steps, samples are generated and are then fed to the DN model for the probabilistic power flow using Eq. (4.6) to Eq. (4.13). The TCS ensures that the generated samples accurately reflect the dynamic behaviour and interdependencies of uncertain variables in DNs, leading to more robust and resilient network models.

4.1.3 Energy Scheduler

The energy scheduler is a key component for the optimal allocation of energy while reducing the operational cost and emissions of the hybrid renewable energy DN. The deterministic approaches for energy scheduling do not capture the inherent uncertainties associated with the RESs and the unpredictable load demand. Therefore, in this chapter, we have employed two-stage stochastic optimisation to model the various uncertainties in the DN. In two-stage stochastic optimisation, the decisions are made in two stages as [94], [95], [96]:

- **First Stage:** This stage decisions are called "*Here-and-now*" decisions which are made based on the forecasts before the uncertainties are revealed.
- **Second Stage:** These are "*Recourse*" actions that are taken after uncertainties (such as actual renewable energy generation or demand) are revealed, making adjustments to the first-stage decisions.

The energy scheduling problem in this framework involves optimising the power generation, storage management, and grid interaction to minimise both operational costs and carbon emissions [97], [98]. The goal of the energy scheduler is to minimise the total operational costs (involving energy generation and storage) and carbon emissions (due to the non-renewable sources of energy). The multi-objective problem (MOP) is framed as:

$$\min\ (MOP) = (w_1 P_{loss} + w_2 V_{dev} + w_3 E_G + w_4 C_{tot}) \tag{4.6}$$

where w_1, w_2, w_3, w_4 are the weighting factors of each objective. P_{loss} represents the total power loss in all the branches (N) and is given by [99]

$$P_{loss} = \sum_{n=1}^{N} g_{ij,n}[V_i^2 + V_j^2 - 2V_iV_jcos(\theta_i - \theta_j)] \tag{4.7}$$

where $g_{ij,n}$ is conductance of branch n between the buses i and j, V_i, V_j and θ_i, θ_j represents the voltage and angle of buses i and j respectively.

V_{dev} is the voltage deviation representing the difference between the voltage at i^{th} bus V_i and the reference voltage V_{ref}:

$$V_{dev} = \sum_{i=1}^{B} |V_i - V_{ref}| \tag{4.8}$$

where B is the total number of buses in the network.

E_G is the total energy generated by the main substation over the time period (T). It is calculated by the summation of power generation from the substation ($P_{grid}(t)$) at each time step t:

$$E_G = \sum_{t=1}^{T} P_{grid}(t)\Delta t \tag{4.9}$$

where Δt is the time interval between successive power measurements.

$$C_{tot} = C_{\text{gen}}(t) + C_{\text{grid}}(t) + C_{\text{b}}(t) + C_{\text{recourse}}(t) \tag{4.10}$$

where $C_{\text{gen}}(t)$ is the cost of generating power from renewable and non-renewable sources at time t, $C_{\text{grid}}(t)$ is the cost of purchasing or selling power from/to the grid at time t, $C_{\text{b}}(t)$ is cost associated with charging or discharging the energy storage system, $C_{\text{recourse}}(t)$ is the expected cost of recourse actions based on different uncertainty scenarios.

While solving the optimisation problem in Eq. (4.6) at time t, the following linear and non-linear constraints are considered as given in Eq. (4.11), Eq. (4.12) and Eq. (4.13) representing the power balance, voltage and thermal constraints, respectively:

$$P_{grid}(t) + \sum_{k=1}^{K} P_{res,k}(t) = \sum_{i=1}^{B} P_{load,i}(t) + \sum_{n=1}^{N} P_{loss,n}(t) \tag{4.11}$$

$$V_{min,i}(t) \leq V_i(t) \leq V_{max,i}(t) \tag{4.12}$$

$$I_i(t) \leq I_{max,i}(t) \tag{4.13}$$

where $P_{res,k}$ is the renewable power generation of each RES such that $k = 1, 2, \ldots, K$ (K is the number of RESs in the network) and $P_{load,i}$ is load connected at each bus 'i' ($i = 1, 2, \ldots, B$).

In the *first-stage decisions*, before uncertainties are revealed, decisions about the energy generation (including renewable and non-renewable energy sources), energy storage and energy trading with the grid are taken, which are represented as:

$$\text{First-stage decisions} = \left\{ P^i_{\text{gen}}(t), P_{\text{b}}(t), P_{\text{grid}}(t) \right\}_{t=1}^{T} \tag{4.14}$$

The *second-stage decisions* (recourse actions) are made after the uncertainty is realised (e.g., actual renewable generation and demand). The adjustments are made in the first stage decisions such as increasing/decreasing reliance on grid and load shedding.

The overall recourse cost C_{recourse} in the second stage is calculated as the expected value of the recourse cost at each scenario ($C_{\text{recourse},s}(t)$) and is expressed as:

$$C_{\text{recourse}}(t) = \mathbb{E}\left[\sum_{s=1}^{S} \pi_s C_{\text{recourse},s}(t) \right] \tag{4.15}$$

where:

- S: Number of uncertainty scenarios.
- π_s: Probability of scenario s.

Additionally, carbon emissions incurred in the second stage, primarily from non-renewable sources, are calculated as:

$$CE(t) = \sum_{i \in \text{Non-Renewable Sources}} \mu_i P^i_{\text{gen}}(t) \tag{4.16}$$

where:

- μ_i: Emission factor (in $kgCO_2/kWh$) of non-renewable energy source i.

Further, to improve scheduling accuracy and reducing computational efforts, the energy scheduler performs stochastic optimisation in two phases, i.e., hourly (60 minutes) and quarterly (15 minutes). The hourly scheduling is conventionally performed due to the slow response time of the large power plants. However, with the integration of RESs and fast-changing loads, modern energy markets (including those of Germany, Australia, etc.) have moved to quarterly scheduling for higher flexibility [100]. In our work, we have performed hybrid energy scheduling taking hourly and quarterly intervals.

The energy scheduler performs energy allocation decisions every hour based on the forecasted values and makes adjustments after 15 minutes whenever significant deviations in generation or demand are detected. Hourly scheduling allows less computational efforts when the fluctuations in uncertain parameters are within the permissible limits. However, the sudden fluctuations in the uncertain parameters remain unnoticed in hourly scheduling, because of which quarterly scheduling is triggered. In quarterly scheduling, more frequent adjustments in the decision variables are done, keeping a balance between demand and supply, thereby maintaining the network stability. However, simulating the entire system after every 15 minutes is computationally extensive, therefore, in this chapter, we are using a blend of hourly and quarterly scheduling.

The energy scheduler keeps on simulating the network on an hourly basis until the signal for quarterly scheduling is triggered. The energy scheduler decides when to trigger quarterly scheduling to balance computational efficiency with the need for fast responses to capture real-time fluctuations. Triggering too frequently results in high computational costs while triggering too infrequently can lead to higher emissions or operational costs.

The following criteria are used for triggering quarterly scheduling:

- **Renewable Generation Volatility**: If renewable energy generation fluctu-

ates significantly from predicted values, the ES triggers quarterly simulations to avoid excess reliance on fossil-fuel-based generation. The volatility threshold is defined as:

$$\Delta_{\text{renew}} = \left| \frac{P_{\text{renew}}^{\text{actual}} - P_{\text{renew}}^{\text{forecast}}}{P_{\text{renew}}^{\text{forecast}}} \right| \times 100 \tag{4.17}$$

If Δ_{renew} exceeds a certain threshold (5%), the system switches to quarterly scheduling.

- **Demand Spike**: When the demand increases beyond the forecasted range, there is a need to purchase more power from the grid, thereby increasing the reliance on the grid. The energy scheduler triggers quarterly scheduling if:

$$P_{\text{load}}^{\text{actual}} > P_{\text{load}}^{\text{forecast}} + \epsilon \tag{4.18}$$

where ϵ is an allowable deviation for load demand.

- **Carbon Emission Threshold**: If the overall carbon emissions exceed a predefined threshold, the ES triggers the quarterly scheduling to reduce the reliance on the grid and thereby reducing the carbon emissions. Therefore,

$$E_{\text{CO}_2}^{\text{threshold}} < CE(t) \tag{4.19}$$

4.2 Results and Discussion

We consider a 33-bus DN (as shown in Fig. 4.2) integrated with optimally placed RESs of optimal capacity to minimise power losses, voltage deviation, and energy generation from the main substation. The optimal combination (location and capacity) of RESs into the DN is decided using Chapter 3 and is shown in Table 4.2. Based on this, Table 4.3 shows the line and branch data for the considered DN [101]. The historical, real-time and forecasted data is sent to the uncertainty modeler by the data analyser. The hourly profiles for wind speed, solar radiation and temperature of Durham, UK are shown in Fig. 4.3, Fig. 4.4 and Fig. 4.5 respectively [102].

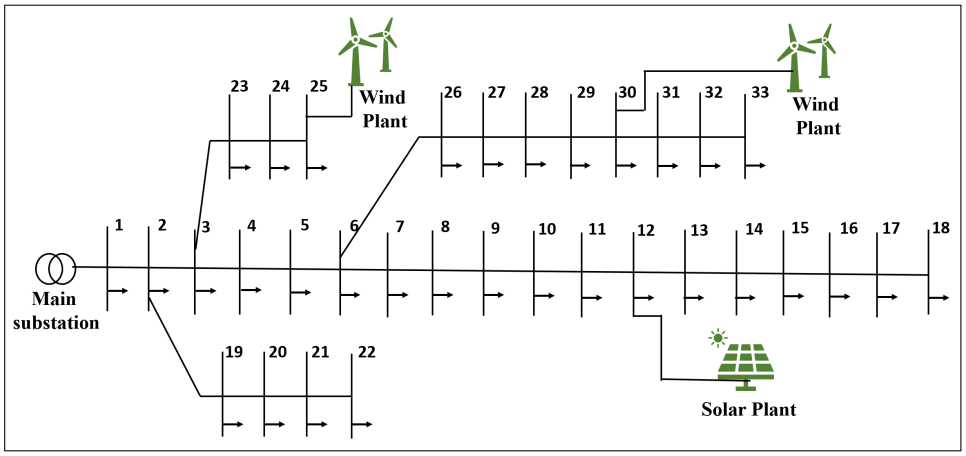

Figure 4.2: RESs interconnected IEEE 33-bus DN

Table 4.2: Optimal placement of RESs in DNs

	WT1	WT2	PV
Capacity (kW)	1254	1043	834
Bus No	25	30	12

Table 4.3: Line and Branch data for 33 Bus DN

Branch No.	**From bus**	**To bus**	**R (Ω)**	**X (Ω)**	**P (kW)**	**Q (kW)**
1	1	2	0.0922	0.0477	0	0
2	2	3	0.4930	0.2511	100	60
3	3	4	0.3660	0.1864	90	40
4	4	5	0.3811	0.1941	120	80
5	5	6	0.8190	0.7070	60	30
6	6	7	0.1872	0.6188	20	20
7	7	8	1.7114	1.2351	200	100
8	8	9	1.0300	0.7400	200	100
9	9	10	1.0400	0.7400	60	20
10	10	11	0.1966	0.0650	60	20
11	11	12	0.3744	0.1238	45	30
12	12	13	1.4680	1.1550	60	35
13	13	14	0.5416	0.7129	60	35
14	14	15	0.5910	0.5260	120	80
15	15	16	0.7463	0.5450	60	10

16	16	17	1.2890	1.7210	60	20
17	17	18	0.7320	0.5740	60	20
18	2	19	0.1640	0.1565	90	40
19	19	20	1.5042	1.3554	90	40
20	20	21	0.4095	0.4784	90	40
21	21	22	0.7089	0.9373	90	40
22	3	23	0.4512	0.3083	90	40
23	23	24	0.8980	0.7091	90	50
24	24	25	0.8960	0.7011	420	200
25	6	26	0.2030	0.1034	420	200
26	26	27	0.2842	0.1447	60	25
27	27	28	1.0590	0.9337	60	25
28	28	29	0.8042	0.7006	60	20
29	29	30	0.5075	0.2585	120	70
30	30	31	0.9744	0.9630	200	600
31	31	32	0.3105	0.3619	150	70
32	32	33	0.3410	0.5302	210	100

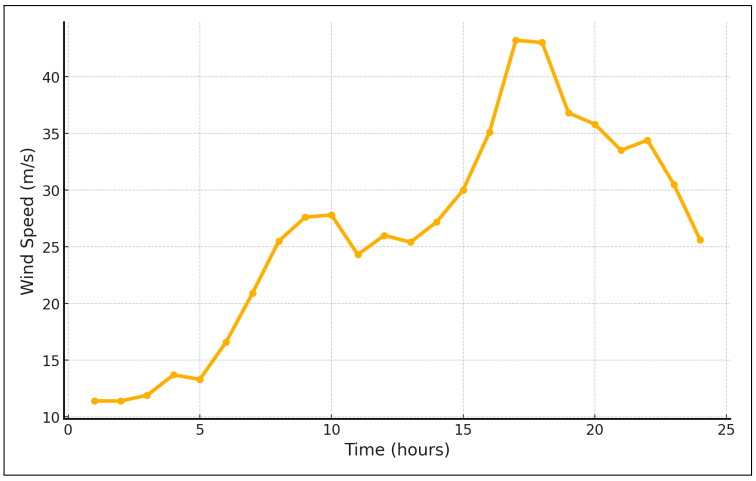

Figure 4.3: Hourly wind speed profile of Durham during the extreme weather

To validate the proposed framework, we analysed data from Storm Debi, which affected North-East England on November 13, 2023 [103]. Due to significant variations in wind speed, solar irradiance, and temperature, these are considered uncer-

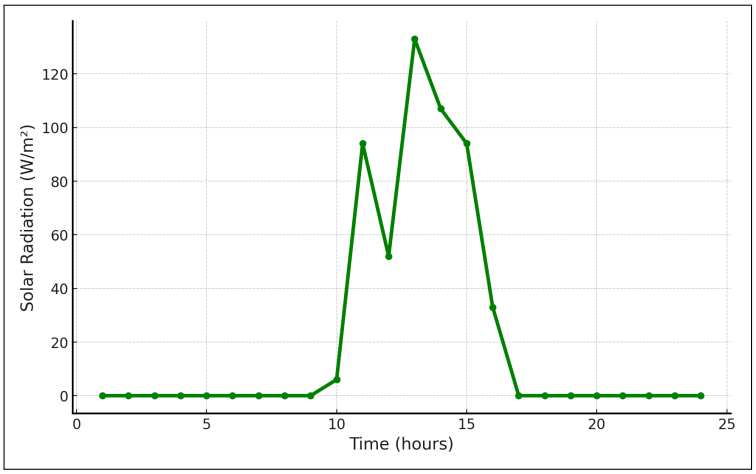

Figure 4.4: Hourly solar radiation profile of Durham during the extreme weather

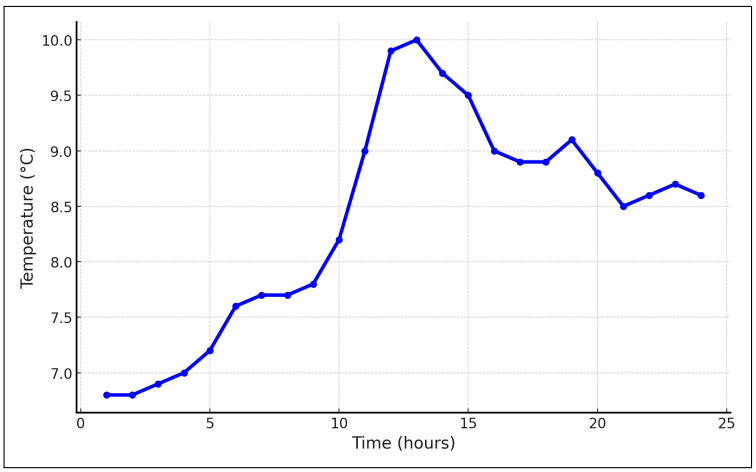

Figure 4.5: Hourly temperature profile of Durham during the extreme weather

tain variables impacting power system operations. We modeled their PDFs using our proposed methodology and compared them with those generated by standard MCMC methods. Figures 4.6–4.7 show the comparison, highlighting a shift in the standard PDFs due to our method's ability to capture real-time fluctuations more accurately.

Table 4.4 presents the average values of uncertain parameters from the generated samples, showing that MCMC results deviate significantly during extreme weather, leading to inaccurate uncertainty modelling. These results are obtained using commonly used MCMC methods, i.e., Metropolis Hastings, Gibbs and Hamilton [104], which are compared with their corresponding modified time-coordinated

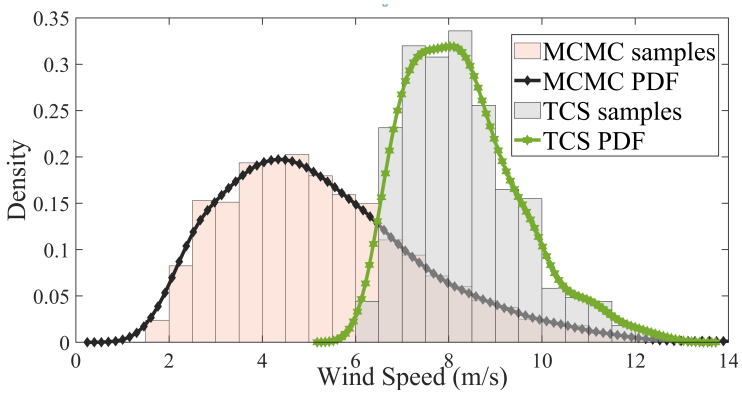

Figure 4.6: PDFs of wind speed using MCMC and TCS

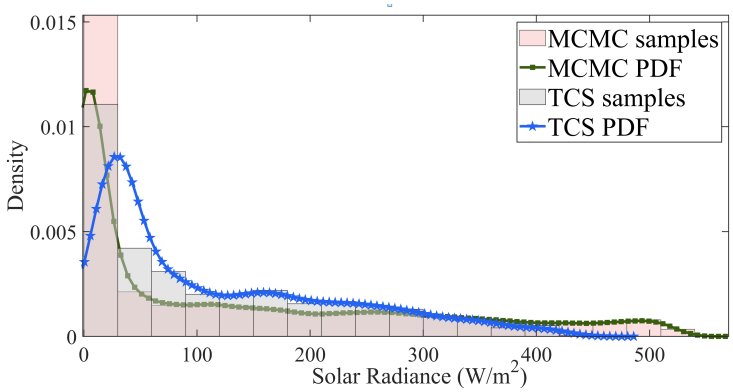

Figure 4.7: PDFs of Solar radiance using MCMC and TCS

Table 4.4: Average values of uncertain parameters using MCMC and TCS sampling methods

Parameter	**Real-time**	**MCMC Methods**			**TCS Methods**		
		Metropolis	Gibbs	Hamilton	Mod-Metropolis	Mod-Gibbs	Mod-Hamilton
Windspeed (m/s)	9.5	4.39	4.76	4.74	9.93	8.89	8.98
Error (%)		53.79	49.89	50.10	4.53	6.42	5.47
Solar Radiance (W/m^2)	94	126	100	133	85	87	90
Error (%)		34.04	6.38	41.48	9.57	7.45	4.25
Temperature (°C)	9.5	5.72	5.68	6.6	7.67	8.34	8.68
Error (%)		39.79	40.21	30.52	19.26	12.21	8.63

approaches. It is observed that different MCMC methods give almost the same results with both the conventional and modified approaches. Henceforth, the Hamilton MCMC method is used in this chapter for comparison with the proposed TCS.

Using the PDFs from Fig. 4.6 and Fig. 4.7, we generated scenarios for solar and wind power respectively which are then utilised for the optimal power flow analysis [99]. Figure. 4.8 shows the voltage profile of the 33-bus DN under normal and

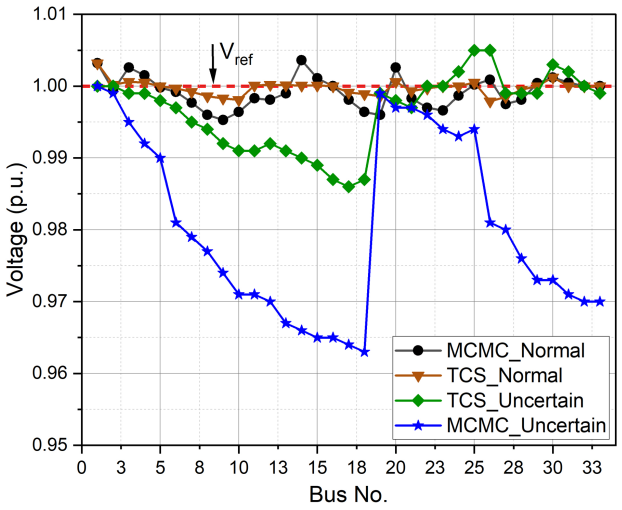

Figure 4.8: Voltage profile of a DN under normal and uncertain conditions using MCMC and TCS

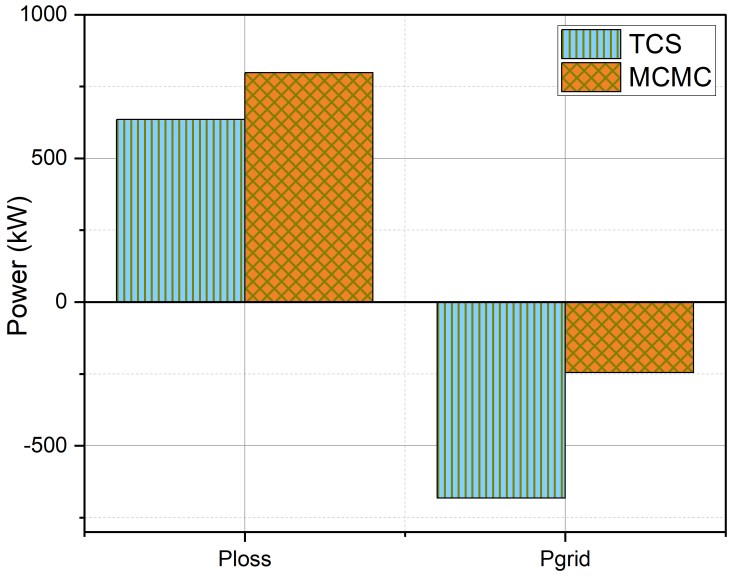

Figure 4.9: Power loss and grid generation of a DN using MCMC and TCS

extreme conditions. As inferred from this figure, the proposed approach maintains minimal voltage deviation during extreme weather, ensuring stable network operation, while both methods yield similar profiles under normal conditions. Fig. 4.9 presents power losses (P_{loss}) and grid power generation (P_{grid}) for both TCS and

MCMC approaches. A negative P_{grid} indicates excess renewable generation sold to the grid, reducing carbon footprints. Accurate weather parameter modelling with TCS increases energy sold to the grid, enabling precise energy scheduling, enhancing network robustness, and reducing power outages, thereby improving resilience during extreme weather.

The information about the uncertain event (increased wind speed due to storm) predicted by the uncertainty modeler is passed to the Energy Scheduler, which takes the following actions (as depicted from Fig. 4.10). In Fig. 4.10, the results for energy scheduling at 15-minute and 60-minute intervals are shown, where the horizontal axis represents the time intervals of 15 minutes (4 intervals of 15 minutes in an hour, therefore, $4 * 24 = 96$ intervals for a day).

- **Prevention of dynamic load curtailment**: There would be more wind power generation due to increased wind speed. However, the load demand increased suddenly from t = 60 to t = 70 which is captured using quarterly scheduling. Therefore, the scheduler sends the signal to discharge the batteries to meet the load demand. Due to surplus wind generation, the batteries are further charged while meeting the load demand. If not forecasted and managed accurately, the excess renewable energy would be wasted due to an imbalance in load and generation.

- **Real-time Grid management**: After detecting the extreme weather event (or increase in wind generation), the scheduler sends a signal to the grid to initiate the energy sales based on the market conditions from t = 60 to t = 70. It implies that energy is sold to the grid when prices are high, thereby maximising the revenue. Overall, the quarterly scheduling showed 30% more energy sales to the grid which remained unnoticed in hourly scheduling.

- **Demand-side Management**: During the periods of high renewable generation, there is around (30-40)% increase in load demand. Fig. 4.10(c) shows an increase in grid sales during that period, indicating a balance between load

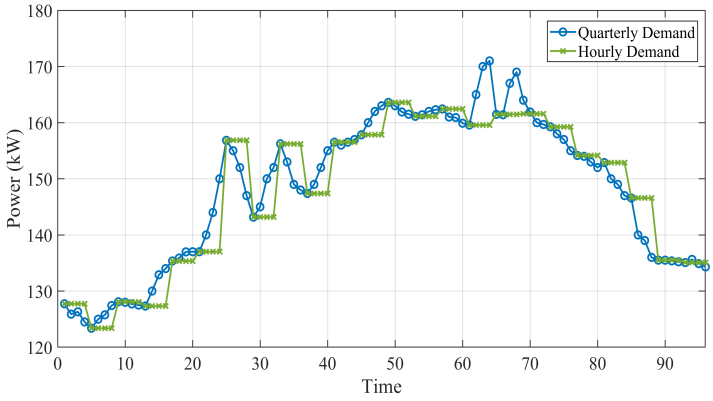

(a)

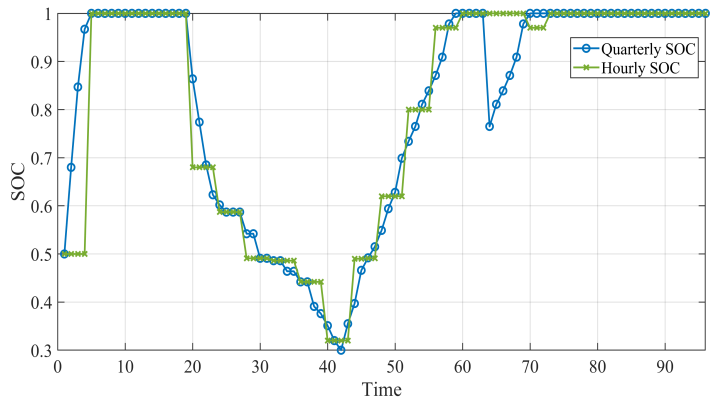

(b)

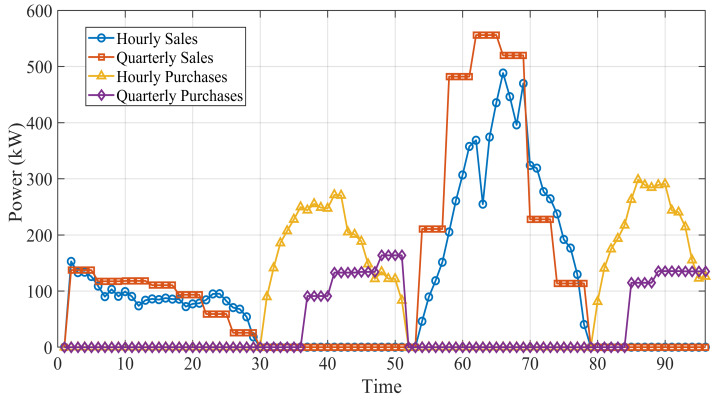

(c)

Figure 4.10: (a) Load demand, (b) SOC and (c) Grid sales and purchase profiles

and generation with quarterly scheduling. The scheduler shifts the flexible loads to the events of surplus renewable energy generation. By feeding the non-critical loads during the surplus generation period, the scheduler reduced the dependency on the grid, thereby establishing a balance between demand and supply and reducing carbon emissions.

- **Uncertainty resilience**: With the quarterly energy scheduling, the energy system takes preventive actions before the uncertain event hits its peak. In this case, during the storm, the wind speed can exceed the cut-off speed and the wind power plant would then need to be shut down. Therefore, based on this information, the scheduler would pre-charge the batteries such that the critical load is fed even during the period of outages.

Further to evaluate the performance of the network in terms of its resilience and carbon footprints, we introduce two new metrics:

- *Renewable reliance factor* ($\Re$): It determines the percentage of load being met by the renewable generation with respect to the total load over a period of time (T). Its value closer to 1 indicates more reliance on RESs.

$$\Re = \sum_{t=1}^{T} \frac{P_{load}(t) - P_{grid}(t)}{P_{load}(t)}; 0 \leq \Re \leq 1 \tag{4.20}$$

- *Carbon emission factor* (CEF): Based on the $\Re$, CEF determines the carbon footprints in the considered network. It is calculated as below and a value closer to 0 indicates lesser carbon emissions.

$$CEF = \xi(1 - \Re); 1 \geq CEF \geq 0 \tag{4.21}$$

where ξ is percentage of emissions from grid generation*.

Table 4.5 presents the values of $\Re$ and CEF using MCMC and TCS under normal and extreme weather conditions. Results are similar under normal conditions

*https://www.nationalgrid.com/stories/energy-explained/how-much-uks-energy-renewable

Table 4.5: Comparison of performance metrics using MCMC and TCS under normal and uncertain conditions in a DN

	Normal		Extreme	
	TCS	MCMC	TCS	MCMC
$\Re$	**0.680**	0.659	**0.976**	0.751
CEF	**0.182**	0.194	**0.0136**	0.142

but vary under extreme conditions. Using TCS, $\Re$ is nearly 1, indicating wind turbines generate power close to their installed capacity during storms, and the corresponding CEF is near zero, indicating minimal carbon emissions.

4.3 Summary

To reduce the impact of extreme weather events on real-time power system operations, we proposed a robust and time-coordinated uncertainty modelling strategy (i.e., TCS) based on Bayesian networks. TCS dynamically adapts to time-varying distributions and incorporates temporal correlations, offering improvements over traditional MCMC methods. Results show that TCS maintains minimal voltage deviation during extreme weather, increases energy sold to the grid, and accurately models weather parameters for better energy scheduling. This enhances system resilience and stability during uncertain events obtained from the proposed performance metrics, ensuring real-time robustness and reduced carbon emissions.

Chapter 5

Energy system operation under real-time uncertainty

In chapter 4, we discussed the impact of modelling uncertainty in the planning stage and how we can minimise it. However, even after this, there may still arise uncertainty in the operation stage which can hamper the working of the energy network. Researchers have employed advanced AI methods to predict real-time power generation in the energy networks [105]. However, sometimes there are abnormal events or operational uncertainties in such networks due to grid congestion, equipment failure, natural disasters, overloading, or other environmental factors. If left unattended, these could lead to cascading failures or outages resulting in power system blackouts or interrupting the reliability of supply [63]. One of the biggest blackouts occurred in Bangladesh in Oct. 2022 due to the 3% rise in the peak energy demand from the forecasted value, which resulted in the grid failure [106]. Therefore, there is a need to develop intelligent and robust strategies to predict and mitigate these operational uncertainties associated with the DER integration to ensure reliable power system operations and long-term network sustainability. In general, the grid is the go-to source when dealing with any type of uncertainty, however, this approach does not fully utilise the DER capabilities and moreover, carbon emissions are higher in the case of grid usage. Addressing the

above-mentioned issues, this chapter proposes a two-fold strategy to mitigate the impact of operational uncertainties in the DNs by leveraging DERs. This two-fold approach employs the concept of competition and cooperation among the neighbouring areas before, during, and after the uncertain event. The entire system is segmented into distinct stages, as shown in Fig. 5.1: data collection, energy modelling, uncertainty detection, and mitigation.

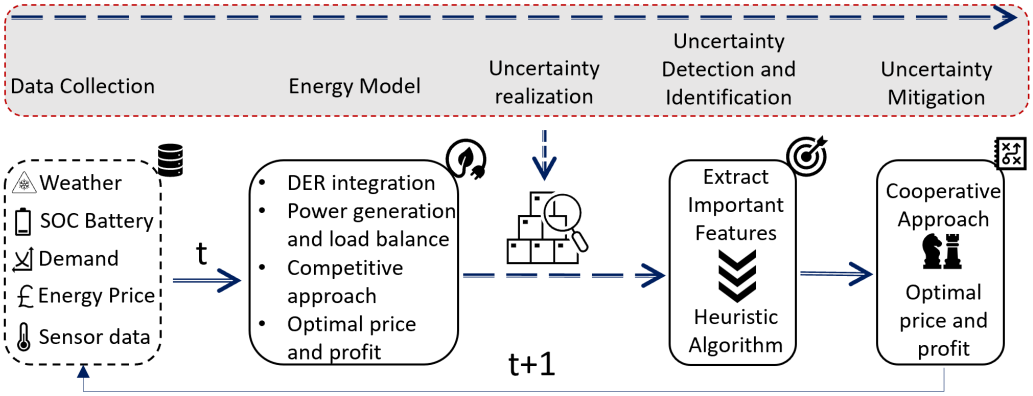

Figure 5.1: Research overview for the real-time uncertainty detection and mitigation

Initially, data is collected based on the weather conditions of various regions and subsequently fed into the energy model. The DERs are integrated into the energy model to compute the total power generation and load balance in the network at time t. A competitive strategy is used to cater to the load demand locally, thereby, minimising the dependence on the grid. Upon realising an uncertain event in the system, a heuristic algorithm is employed to identify its type. This information is then processed by a cooperative algorithm designed to mitigate the impact of the identified uncertainty on the system. A detailed description of the work carried out in these stages is given in Section 5.2. Considering the real-time problem described above, the major contributions of this chapter are as follows.

- A carbon-aware optimisation strategy for the energy network is proposed, utilising a competitive approach to determine optimal pricing during normal operations to minimise carbon emissions across the distribution network.

- An algorithm to detect and identify uncertain events within the energy network is designed by establishing hidden dependencies among the uncertain parameters using Bayesian networks which is further used to mitigate the impact of uncertainty.
- A novel cooperative strategy is proposed for the local areas mitigating the impacts of uncertainty by preventing the escalation of local problems into entire network disruptions, ensuring stable and reliable energy distribution.

The symbols used in this chapter are defined in Table 5.1.

5.1 System Model

Figure 5.2 illustrates the structure of the power system enabling a two-way flow of power, featuring a power generating sources transmitting energy through the transmission network to the DN as well as allowing consumers to both sell excess energy back to the grid and purchase energy when needed. Within the DN, DERs are integrated and connected to consumers, facilitating decentralised energy generation and consumption (modeled as per IEEE Std 1547-2018 [107]). Distribution system operators (DSOs) are responsible for ensuring a reliable power system from the transmission network to the consumers. In this study, as illustrated in Fig. 5.2, we consider two types of DSOs: the regional controller (RC) and the global controller (GC). The RC is responsible for managing energy requests from the local communities (LCs) and maintaining power reliability within small regional areas (A). The GC, on the other hand, oversees the overall management, operation, and control of the entire DN, handling all incoming and outgoing requests from the RC to ensure seamless network operations.

The total renewable energy generation $P^i_{GR}(t)$ at any time t in i^{th} area can be calculated as:

$$P^i_{GR}(t) = P^i_{pv}(t) + P^i_w(t) \tag{5.1}$$

Table 5.1: Table of symbols used in chapter 5

Symbol	Description
A_i	Area i
I	Intercept for energy demand calculation
C_i	Marginal cost to generate Q_i units of energy in the ith area (£/kWh)
$CE(t)$	Carbon footprints at any time instant (kg CO_2)
CI	Carbon intensity (kg CO_2/kWh)
D	Total energy demand (kW)
$E^f_{dis}(t)$	Energy discharged from the battery in area f at time t (kWh)
$E^f_{req}(t)$	Energy required by the faulty area at time t (kWh)
$E_{sales}(t)$	Total energy sold to the grid at time t (kWh)
$E_{total\_sup}(t)$	Total energy supplied by all areas at time t (kWh)
$G_{exp}(t)$	Expected power generation for each area at time interval t (kW)
$G_{rt}(t)$	Real-time power generation for each area at time interval t (kW)
$P^i_b(t)$	Battery power for the ith area at time t (kW)
$P^f_{dis}(t)$	Power discharge rate of the battery in the affected area f at time t (kW)
$P^i_{GR}(t)$	Total renewable generation at time t in the ith area (kW)
$P^i_{load}(t)$	Load demand of ith area at time t (kW)
P^f_{req}	Power demand of the faulty/uncertain area (kW)
$P^i_{pv}(t)$	Solar power generation of ith area at time t (kW)
$P^i_w(t)$	Wind power generation of ith area at time t (kW)
$p_r(t)$	Optimal price of energy in the market (£/kWh)
$p^i_r(t)$	Cooperative price offered by the selected areas (£/kWh)
$p^{grid}_r(t)$	Market price offered by grid (£/kWh)
Q_i	Quantity of energy produced by the ith area (kWh)
Q^{min}_i, Q^{max}_i	Minimum and maximum production of energy by the i^{th} area (kWh)
SOC_i	State of charge of the battery in the ith area (%)
SOC^{max}	Maximum state of charge of the battery (%)
SOC^{min}	Minimum state of charge of the battery (%)
α_i, β_i	Marginal cost coefficients for thermal power generation in ith area
e	Elasticity coefficient
γ_i	Fixed costs or capital costs in the ith area (£)
μ	Complementary slackness condition
k	Battery discharging coefficient
π_i	Profit of the ith area (£)
ρ	SOC threshold for discharging battery of affected area (%)
σ, ψ	SOC thresholds for discharging neighboring batteries (%)
φ^{min}_i, φ^{max}_i	Lagrange multipliers for inequality constraints
ξ	Profit margin of an area (%)

where $P^i_{pv}(t)$ and $P^i_w(t)$ are the solar and wind power generations of i^{th} area at time t.

The solar power $P^i_{pv}(t)$ generated by each solar panel within an area at time t is calculated using Eq. (3.1) [31]. The optimal location, capacity, and number of DERs in a particular area have been calculated beforehand using PSO discussed in

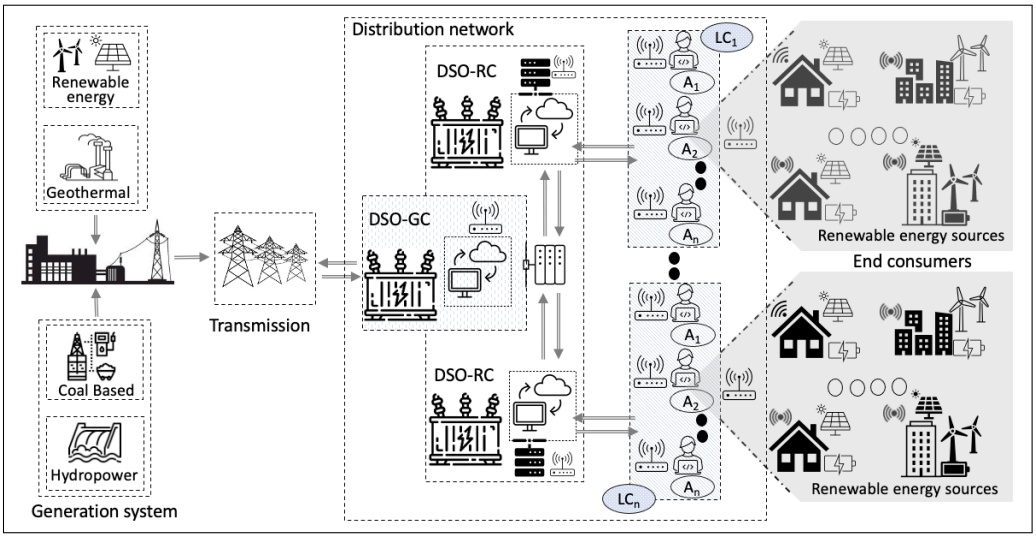

Figure 5.2: System model with DERs integrated DN

Chapter 3 [93]. Similarly, the wind power, $P_w^i(t)$, generated by each wind turbine within i^{th} area at time t is expressed using Eq. (3.2) [30].

The battery storage system, BESS, plays an important role in managing the consumer energy demand when the power generated from the DERs is not sufficient. BESS stores the energy during the surplus renewable energy generation and feeds the energy whenever required. The charging and discharging of the battery power for i^{th} area, $P_b^i(t)$, can be calculated using Eq. (3.3) [86].

The operational strategy used to simulate each area's energy system dynamics is indicated in Algorithm 5.1. The expected power generation, $P_{GR}^{exp}(t)$, for each area and at time interval t is calculated using the Eq. (5.1) and is compared with its real-time value, $P_{GR}^{rt}(t)$. If these values match, then a carbon-aware energy scheduling is performed, that manages the load demand of an area by using renewable energy generation or charging/discharging the battery. The excess generation from the neighboring area is sold to the deficient areas based on the price calculated using the competitive game model described in Section 5.2.1. If the real-time and expected values do not match, then an uncertainty detection and identification algorithm (Algorithm 5.3) is run as described in Section 5.2.2. If there is an uncertainty present in the system, then it is mitigated using the uncertainty mitigation

algorithm (Algorithm 5.4) detailed in Section 5.2.3.

Algorithm 5.1 Distribution Network System Operation

Input: Area Request: $i \in \{A\}, i = 1, 2, \ldots, n$
Output: Profit
for $(\forall i)$ **do**
    Compute: $P_{GR}^{exp}(t)$ using Eq. (5.1)
    if $(P_{GR}^{exp}(t) \simeq P_{GR}^{rt}(t))$ **then**
        Execute: ▷ Carbon-aware energy scheduling
        if $(P_{GR}^{i}(t) > P_{load}^{i}(t))$ **then**
            if $(SOC^{i}(t) < SOC_{\max}(t))$ **then**
                Battery Status (D) $\rightarrow$ *CHARGE*
            else
                Sell Energy $\rightarrow$ **Competitive Theory Approach** ▷ See Section 5.2.1
            end if
        else
            if $(SOC^{i}(t) > SOC_{\min}^{i})$ **then**
                Battery Status (D) $\rightarrow$ *DISCHARGED*
            else
                Use Competitive Theory Approach ▷ See Section 5.2.1
            end if
        end if
    else
        Call Function: $F = \mathrm{UDI}(i)$ ▷ See Algorithm 5.3
        if $(F == A_{\delta})$ **then**
            Call Function: $P = \mathrm{UM}(i)$ ▷ See Algorithm 5.4
        end if
        Update: $P_{G}^{exp} = P$ ▷ Check the condition
    end if
end for

The DN system model described in this section highlights the fundamental principles and equations governing energy distribution and generation within the network. To enhance the robustness and reliability of the DN, we propose a novel scheme that incorporates state transitions to manage the network's response to different phases of operation: healthy, fractured, and recovered. This proposed scheme is illustrated through a state transition diagram and detailed in the following section.

5.2 Proposed Scheme

The proposed scheme focuses on the DN's operation into three distinct phases as shown in Fig. 5.3. These are 1) Healthy (or Normal) Phase, 2) Fractured (or Uncertain) Phase, and 3) Recovered (or Mitigation) Phase. These phases are based on the behaviour of the system before and after the occurrence of uncertain events, providing a comprehensive framework for understanding and addressing system disruptions. The control actions for the three phases leverage three novel approaches

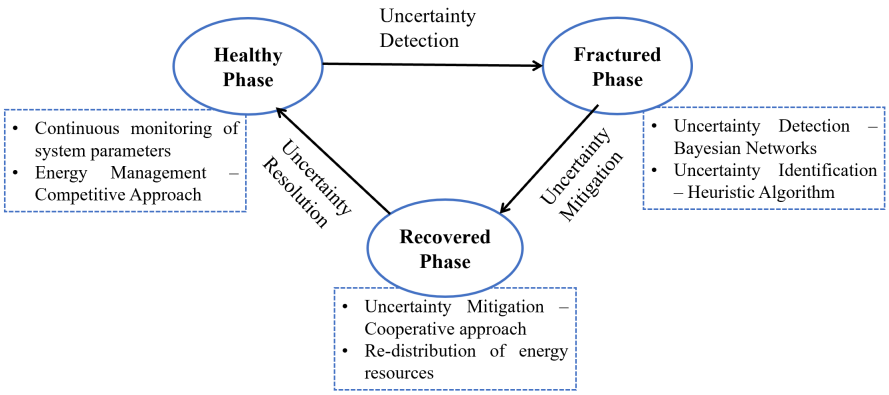

Figure 5.3: Phase transition diagram during the energy system operation

designed to ensure the reliability of the DN. These approaches not only maintain the network's reliability but also optimise regional profitability and minimise carbon emissions. In the healthy phase, the system operates under optimal conditions with efficient energy management and minimal carbon footprint. During the uncertain phase, an advanced Bayesian algorithm is employed to detect and mitigate the impacts of uncertainties, such as fluctuating renewable energy output or unexpected load variations. Finally, in the recovery phase, the system employs robust strategies to restore normal operations while continuing to optimise economic and environmental outcomes. A detailed description of the proposed approaches used in the three phases is as follows.

5.2.1 Healthy / Normal Phase

This phase signifies the desired and stable operational mode, where the power system is capable of meeting the consumer load demand. During normal operation of the DNs, a competitive energy-based demand-supply model (based on Cournot Game Theory) is employed to determine the optimal energy price offered by each area and their corresponding profits. All the areas would sell the surplus renewable energy to the neighbouring areas at the optimal market price before selling it to the grid. By leveraging competitive dynamics within the areas, this model seeks to minimise reliance on the grid, thus reducing grid purchases and subsequently decreasing the overall carbon footprints.

The market price of the energy depends on the demand for the energy in the market, and to compute its optimal value, a linear relationship is established between the demand (D) [108] and supply of the energy available in the market as given below.

$$D = I - e \cdot p \tag{5.2}$$

where p is the optimal market price of the energy, D is the total demand, e is the elasticity coefficient, and I is the intercept. To maintain the balance between total energy and demand, all the areas must fulfill the energy demand. Suppose there are n areas supplying the energy, D must be fulfilled by the total quantity Q of energy produced by the area as mentioned below:

$$D = \sum_{i=0}^{i=n} Q_i \tag{5.3}$$

During production of the energy by i^{th} area ($i = 1, 2, ..., n$), there is also a marginal cost, C_i, incurred to generate Q_i quantity of energy which is calculated by:

$$C_i = \alpha_i \cdot Q_i^2 + \beta_i \cdot Q_i + \gamma_i \tag{5.4}$$

where α_i and β_i are marginal cost coefficients for i^{th} area corresponding to thermal power generation, γ_i represents fixed costs or capital costs associated with renewable energy installations that are not directly proportional to the quantity

of energy generated Q_i. We utilised the Cournot Game model to simulate and analyse the energy transactions among suppliers. This model effectively represents and understands the dynamics of competing markets in this context [108].

5.2.1.1 Cournot Game Model

The main aim of an area participating in the energy ecosystem is to maximise its profit. The profit of i^{th} area (π_i) is calculated by the price quoted by an area in the market minus the marginal cost of the energy production as mentioned below:

$$\max_{(Q_i, i=1,2,\ldots,n)} \pi_i = p \cdot Q_i - C_i \tag{5.5}$$

$$s.t. \sum_{i=0}^{i=n} Q_i = I - e \cdot p \tag{5.6}$$

$$Q_i^{min} < Q_i < Q_i^{max} \tag{5.7}$$

where Q_i^{min}, Q_i^{max} are the minimum and maximum production of energy by the i^{th} area. The price p is calculated by using Eq. (5.6) as mentioned below:

$$p = \frac{I - \sum_{i=0}^{i=n} Q_i}{e} \tag{5.8}$$

The profit of i^{th} area is calculated by adding its revenue from the game model to the income from any contracts and then subtracting its generation costs. Formulating the Eq. 5.5 by substituting the value of p from Eq. 5.8 gives:

$$\max_{(Q_i, i=1,2,\ldots,n)} \pi = \frac{I - \sum_{i=0}^{i=n} Q_i}{e} \cdot (Q_i) - C_i \tag{5.9}$$

The price equilibrium is obtained by using the Kuhn-Karesh-Tucker (KKT) condition highlighted below:

$$\frac{\delta \pi_i}{\delta Q_1} = \frac{I - \sum_{i=0}^{i=n} Q_i}{e} - C_i' + \phi_i^{min} - \phi_i^{max} = 0 \tag{5.10}$$

where ϕ_i is the Lagrange multipliers associated with the inequality constraints. Substitute $\frac{I - \sum_{i=0}^{i=n} Q_i}{e}$ by p using Eq. 5.8,

$$\frac{\delta \pi_i}{\delta Q_1} = p - C_i' + \phi_i^{min} - \phi_i^{max} = 0 \tag{5.11}$$

$$s.t. \;\; p = C_i^{'} - \phi_i^{min} + \phi_i^{max} \tag{5.12}$$

$$\phi^{min} \geq 0, (Q_i - Q_i^{min}) \geq 0, \phi_i^{min}(Q_i - Q_i^{min}) = 0 \tag{5.13}$$

$$\phi^{max} \geq 0, (Q_i^{max} - Q_i) \geq 0, \phi_i^{max}(Q_i^{max} - Q_i) = 0 \tag{5.14}$$

5.2.1.2 Nash Equilibrium Solution

In this model, the areas $(A_1, A_2, \ldots, \mathrm{A}_n)$ submit their offers simultaneously to the RC to participate in the competition model. In this model, there is no cooperation among the participating areas. The utility/profit function is calculated based on the defined inequality constraints. In the defined model, the inequality constraints are defined to maximise the profit of the area and the energy consumer. The defined model works statically due to the non-cooperative behaviour of the participating areas. Due to the static model, the game is defined to maximise the profits of the areas, denoted as (A, π) and elaborated below:

- $A = \{A_1, A_2, \ldots, A_n\}$ are the areas participating in the defined model.
- $\pi = \{\pi_1, \pi_2, \ldots, \pi_n\}$ are the set of utility functions calculated to maximise the profit of the participating areas.

In this game, the areas have to calculate the profits concerning the value of Q. Considering the scenario of two areas, the utility function is calculated as below:

- In the utility matrix, π_1 and π_2 represent the profit of the A_1 and A_2 for a given combination of Q_1 and Q_2.
- The inequality constraints ϕ_{min} and ϕ_{max} are calculated using Lagrange multipliers as mentioned below:

$$\phi_{min} = \frac{\mu}{C_1} \tag{5.15}$$

$$\phi_{max} = \frac{\mu}{C_2} \tag{5.16}$$

  where, μ is the complementary slackness condition, and C_1, C_2 are the costs of the respective areas.

- The $\pi^{A}_{i/j}$ represents the profit function for i^{th}/j^{th} area corresponding to $A \in \{A_i, A_j\}$ with respect to the Q.

To reach the Nash equilibrium, the utility matrix to access the possible behaviours of the areas is depicted in Table 5.2.

Table 5.2: The Utility matrix of i^{th} area considering j^{th} area

	Area A_i	
	$Q_j = \min$	$Q_j = \max$
$Q_i = \min$	(π_i, π_j)	(π_i, π_j)
$Q_i = \max$	(π_i, π_j)	(π_i, π_j)

Each entry of the utility matrix (π_i, π_j) represents the profit of area i and area j based on the specific quantities of Q_i and Q_j.

5.2.1.3 A Case Study

To better understand the defined game model, we present a case study to calculate the Utility Matrix using collected data points from 10 different areas in the UK (which are discussed later). The Utility Matrix is calculated using two areas (the Gateshead and Longbenton areas) and the notations for which are defined in Table 5.3.

Table 5.3: Notation values in the Case Study

Notation	**Value**	**Description**
A_1	Gateshead	First area name
A_2	Longbenton	Second area name
D_{yr}	1	1st day of year data
C_1	0.1595	Cost of A_1
C_2	0.2102	Cost of A_2
Q_1	[0:15819]	Range of produced quantity by A_1
Q_2	[0:69115]	Range of produced quantity by A_2
ϕ_{min}	0	Inequality constraint
ϕ_{max}	0	Inequality constraint

- Source: $(C_1, C_2) \leftarrow$ [109], $(Q_1, Q_2, \phi_{min}, \phi_{max}) \leftarrow$*Simulation results*

- A_1 initiates the game procedure along with the A_2 and quotes 0.1595 costs per required unit to the consumer.
- In a similar pattern, A_2 quotes 0.2102 cost for the same requirement.
- The ϕ_{min} and ϕ_{max} is calculated as 0 using best response optimisation approach [110]. This could occur if the market price p is always greater than or equal to the total costs $C_1Q_1 + C_2Q_2$, leading to an inactive complementary slackness situation.
- The minimum and maximum range of the A_1 is highlighted as [0:15819] and A_2 as [0:69115] from the collected data points corresponding to Gateshead and Longbenton areas.
- The price p corresponding to both areas is calculated using Eq. (5.8), and the Utility Function (π) is calculated using Eq. (5.5).

The Utility matrix corresponding to both areas is mentioned in the Tables 5.4 and 5.5.

Table 5.4: The Utility matrix of A_1 area

Area A_1		
	$Q_2 = 0$	$Q_2 = 69115$
$Q_1 = 0$	0	0
$Q_1 = 15819$	3.9911*e^{07}	3.9911*e^{07}

Table 5.5: The Utility matrix of A_2 area

Area A_2		
	$Q_2 = 0$	$Q_2 = 69115$
$Q_1 = 0$	0	-0.0001*e^{08}
$Q_1 = 15819$	0	1.7437*e^{08}

5.2.2 Fractured / Uncertain Phase

This phase occurs when there is an uncertainty or abnormality observed within the system. In coordination with the competitive energy sharing model described in

Section 5.2.1, we employ a Bayesian approach [92] to effectively detect uncertain events within the distribution system. The BN is utilised to find the conditional probabilities among the uncertain variables computed using the complex Bayesian algorithm as given in Algorithm 5.2. It is a form of semi-naive Bayesian Learning that introduces a complex structure to capture inter-dependencies among variables, thereby alleviating the assumption of attribute independence made by the Bayes approach. Algorithm 5.2 aims to process and examine a complex BN for analysing power system data. It takes a data source file from algorithm 5.1 and other required parameters as inputs. The forwarded inputs are processed and specific performance metrics are given as output. At the initial phase, the nodes (θ) are sorted topologically in the form of a directed acyclic graph (ψ) to achieve the correct sequence for processing. Each node corresponding to a random variable (X_i) is checked to find if it has observed data; if not, it is estimated using rejection sampling. Bayesian parameter estimation ($BayesianParameEst()$) updates the conditional probability table (CPT) if the nodes θ do not have observed data. The algorithm calculates probabilities for specific performance metrics (e.g., **G** as solar radiation status and **V** as wind speed status) using the BN. It provides the calculated values to algorithm 5.3 for further processing. Therefore, based on the correlation among the different weather parameters, the important features are extracted, that are highly correlated to each other to reduce the computation burden while solving the DN equations.

Once an uncertain event is detected, a heuristic algorithm (described in Algorithm 5.3) is utilised for identifying the type of uncertainty. By combining the power of Bayesian inference with the heuristic algorithm, our approach ensures accurate and timely identification of critical events, thereby enabling proactive responses to mitigate their impact. In Algorithm 5.3, the LC at the regional level continuously monitors the real-time power sold, P^{rt}_{sold}, and purchased, P^{rt}_{pur}, from the grid for each area. Upon detecting a mismatch between real-time and expected power values, the LC conducts a thorough assessment of real-time power flows in each

Algorithm 5.2 Complex Bayesian Network Algorithm

Input:
  DS: Power system data source file
  P: Power system performance metrics data
  ψ: Directed acyclic graph
  θ: Nodes
  λ: Directed edges
  CPT: Conditional probability table
Output:
  $\mathbf{G}_{min}, \mathbf{G}_{max}, \mathbf{V}_{min}, \mathbf{V}_{max}$
function CBN(**DS**)
  $W \leftarrow$ `Sort`(θ in ψ) ▷ Topologically sort nodes in ψ
  for (each X_i and X_m in W) **do**
    if (X_i is observed in **DS**) **then**
      $X_i \leftarrow$ `Set`(**DS**)
    else
      $X_i \leftarrow$ `RejectionSample`($P(X_i|\text{Pa}(X_i), CPT)$)
    end if
    if (X_m is observed in **P**) **then**
      $X_m \leftarrow$ `Set`(**P**)
    else
      $X_m \leftarrow$ `RejectionSample`($P(X_m|\text{Pa}(X_m), CPT)$)
    end if
  end for
  for (each X_i and X_m in W) **do**
    if (X_i is not observed in **DS**) **then**
      $CPT \leftarrow$ `BayesianParameterEst`($X_i, \text{Pa}(X_i)$, **DS**)
    end if
    if (X_m is not observed in **P**) **then**
      $CPT \leftarrow$ `BayesianParameterEst`($X_m, \text{Pa}(X_m)$, **P**)
    end if
  end for
end function
G(Solar Radiation Status|min, max) = $\prod_i P(X_i|\text{Pa}(X_i), CPT)$
V(Wind Speed Status|min, max) = $\prod_i P(X_m|\text{Pa}(X_m), CPT)$

area. This assessment involves comparing the real-time powers generated from solar and wind sources (calculated using Equations (3.1) and (3.2), respectively) with their respective expected values ($P_{pv}^{exp}(t)$ and $P_{w}^{exp}(t)$), obtained from optimal energy scheduling of DERs at time t. If the power generation values align with

Algorithm 5.3 Uncertainty Detection and Identification Algorithm

Input:
  $G_{min,max}$, $V_{min,max}$
  i: Area Request
Output:
  A_δ: State of uncertainty in an area ▷ δ: Uncertainty
function UDI(i)
  if $(P_{PV}^{exp}(i) \neq P_{PV}^{rt}(i))$ **and** $(P_{PV}^{rt}(i) \notin (P_{PV}^{min}(i), P_{PV}^{max}(i)))$ **then**
    Assign $A_i \rightarrow A_\delta$ ▷ Data Uncertainty
  else if $(P_{PV}^{exp}(i) \neq P_{PV}^{rt}(i))$ **and** $(P_{PV}^{rt}(i) \in (P_{PV}^{min}(i), P_{PV}^{max}(i)))$ **then**
    Assign $A_i \rightarrow A_\delta$ ▷ Weather Uncertainty
  else if $(P_{w}^{exp}(i) \neq P_{w}^{rt}(i))$ **and** $(P_{w}^{rt}(i) \notin (P_{w}^{min}(i), P_{w}^{max}(i)))$ **then**
    Assign $A_i \rightarrow A_\delta$ ▷ Data Uncertainty
  else if $(P_{w}^{exp}(i) \neq P_{w}^{rt}(i))$ **and** $(P_{w}^{rt}(i) \in (P_{w}^{min}(i), P_{w}^{max}(i)))$ **then**
    Assign $A_i \rightarrow A_\delta$ ▷ Weather Uncertainty
  else if $(P_{load}^{exp} \neq P_{load}^{rt})$ **then**
    Assign $A_i \rightarrow A_\delta$ ▷ Behavioral Uncertainty
  else
    Send Signal: *Normal* $\xrightarrow{\text{ack}}$ GC ▷ GC: Global Controller
  end if
  return A_δ
end function

expectations, the LC proceeds with normal operations. However, if inconsistencies arise, the LC employs a Bayesian analysis to determine the probability distribution of G or v, and finds their respective ranges (G_{min}, G_{max}) or (v_{min}, v_{max}). Based on these, using the Eq. (3.1) and Eq. (3.2), the range of solar $(P_{PV}^{min}, P_{PV}^{max})$ and wind power $(P_{w}^{min}, P_{PV}^{w})$ generation can be calculated. If the real-time values fall inside this range, it indicates that the weather parameters are changed suddenly based on which a potential weather uncertainty is detected. Otherwise, the mismatch may be attributed to faulty data, which could stem from various sources such as faulty or dead sensors (erratic/uniform/zero readings from a sensor) and data manipulation (intentional alteration of data). If none of these, the uncertainty is attributed to the change in consumer behavior by comparing the expected (P_{load}^{exp}) and real-time

(P^{rt}_{load}) values of the consumer demand of an area. If neither of the above case exist, then the LC sends normal signal to the GC implying that there is no issue in their respective area.

Hence, using the BN approach, the hidden interdependencies among the weather parameters is established which is further utilised to detect and identifying the uncertainties using the heuristic approach.

5.2.3 Recovered / Mitigation Phase

Whenever an uncertain event is identified in an area a, we propose a novel cooperative strategy, to mitigate its adverse effects on the entire DN. This strategy is grounded in the notion that rather than operating in isolation to maximise their individual profit (as in the case of competitive strategy), all areas collaborate to address the issue at hand by pooling resources to support the affected area under uncertainty in minimising overall grid dependency and carbon footprints as described in Algorithm 5.4. Therefore, the objective during the uncertain situation is loss minimisation instead of profit maximisation.

In Algorithm 5.4, at each time instant, the total surplus energy of all areas sold to the grid is checked. If this energy is enough to meet the required load demand, then it is sold to the affected area at the optimal price as described in the competitive approach using Eq. (5.8). If the total energy sold to the grid ($\sum P_{sales}(t)$) is not enough, then the battery of the affected area (f) will be discharged according to the power discharge rate function depicted in Eq. (5.17) until its state of charge SOC^f is equal to a threshold value ($\rho = 30\%$).

$$P^f_{dis}(t) = \frac{\mathrm{d}SOC^f(t)}{\mathrm{d}t} = -k \cdot SOC^f(t) \tag{5.17}$$

where k is the battery discharging coefficient. Integrating the power discharge rate function over time determines the energy discharged using:

$$E^f_{dis}(t) = \int_{t_1}^{t} P^f_{dis}(t)\,\mathrm{d}t \tag{5.18}$$

Algorithm 5.4 Uncertainty Mitigation Algorithm

Input:
  Area Request: $i \in \{A\}, i = 1, 2, \ldots, n$; f $\leftarrow A_\delta$
  Set SOC thresholds: **Threshold1** $\rightarrow \rho$, **Threshold2** $\rightarrow \sigma$, **Threshold3** $\rightarrow \psi$
Output: Power purchased from grid: P_{grid}
function UM(i)
  Compute: P^f_{req}, P^f_{GR} ▷ f←faulty/uncertain area
  if ($P^f_{req} \geq P^f_{GR}$ **and** $SOC^f(t) > \rho$) **then**
    Discharge Battery ▷ until SOC reaches ρ
  else
    if ($\sum P^i_{sales}(t) > 0$) **then**
      if ($\sum P^i_{sales}(t) > P^f_{req}(t)$) **then**
        Apply Competitive Theory Approach ▷ Compute price
        $P^f_{rem}(t) = 0$
      else
        Calculate: $P^f_{rem}(t) = P^f_{req} - \sum P^i_{sales}(t)$
      end if
    else
      Assign: $P^f_{rem}(t) = P^f_{req}$
      if ($SOC^i(t) > \sigma$) **then**
        Compute: E^i_{dis} ▷ using Eq. (5.22)
        Discharge Battery ▷ until SOC reaches σ
        $P^f_{rem}(t) = P^f_{req} - \sum P^i_{dis}(t)$
      else if ($SOC^i > \psi$) **then**
        Compute: E^i_{dis} ▷ using Eq. (5.22)
        Discharge Battery ▷ until SOC reaches ψ
        $P^f_{rem}(t) = P^f_{req} - \sum P^i_{dis}(t)$
      else
        Assign: $P^f_{rem}(t) = P^f_{req}$
      end if
    end if
  end if
  $P_{\text{grid}} = P^f_{rem}(t)$
  return P_{grid}
end function

If the battery discharge is not sufficient to meet the load demand of that area, then the neighbouring areas with SOC^i $(i = 1, 2, \ldots, n; i \neq f)$ greater than the threshold ($\sigma = 60\%$) will discharge their batteries to meet the load of the energy-deficient area. The battery discharge of the neighbouring areas can be carried out in three possible ways.

- *Entire energy purchased from one area only:* If the chosen firm has sufficient battery storage, it can ensure uninterrupted energy supply to the affected area such that:

$$E^i_{\text{dis}}(t) \geq E^f_{req}(t) \tag{5.19}$$

  where $E^i_{\text{dis}}(t)$ is the energy discharged by i^{th} area at time t and $E^f_{req}(t)$ is the energy required by faulty (or uncertain) area at time t.

- *Equal energy purchase:* In this case, selected areas would discharge an equal amount of their battery storage to meet the required load demand represented below.

$$E^i_{\text{dis}}(t) = \frac{E^f_{req}(t)}{n} \tag{5.20}$$

  where n is the total number of areas selected whose $SOC^i > \sigma$ and $i \neq f$.

- *Proportionate energy sharing:* Proportionate energy sharing ensures that each area contributes based on its available capacity. Areas with greater battery storage contribute more, while those with smaller battery storage contribute proportionately less. The proportion of the required energy demand allocated to area i is depicted by:

$$Prop_i(t) = \frac{E^i_{avl}(t)}{E_{\text{total\_sup}}(t)} \tag{5.21}$$

  where $E_{\text{total\_sup}}$ is the total energy supplied by all areas and is calculated as $\sum_i E_i$, such that $i = 1, 2, \ldots, n; i \neq f$, and E_i be the energy supplied by the i^{th} area. The proportional energy allocated to i^{th} area in this case is given as:

$$E^i_{dis}(t) = Prop_i(t) \cdot E^f_{req}(t) \tag{5.22}$$

This case ensures fairness in the system and therefore is used as the default strategy in the proposed scheme for battery discharge in neighbouring areas.

If there is no area with $SOC^i > \sigma$, then check the areas with $SOC^i > \psi$, where $\psi \leq \sigma$ (and is set at 50%), and follow the same procedure for battery discharging as mentioned in the Eq. (5.21) and Eq. (5.22). The final step involves purchasing the energy from the grid E_{grid}, in case none of the neighbouring areas can meet the load demand of the affected area.

The cooperative strategy is designed such that even during an uncertain event while supporting the affected area to meet its load demand, the supplying areas do not incur any loss. The optimal price at any time t during uncertainty is calculated as:

$$p_r(t) = \begin{cases} p(t), & E_{sales}(t) \geq 0 \\ p_r^{grid}(t), & E_{sales}(t) \leq 0 \text{ or } \eta = 0 \\ p_r^i(t), & \eta \neq 0 \end{cases} \tag{5.23}$$

where $p(t)$ is the price calculated using Eq. (5.8), $p_r^{grid}(t)$ is the market price offered by the grid at time instant t, E_{sales} is the total energy sold to the grid ($E_{sales}(t) = \sum E_{sales}^i$; E_{sales}^i) is the energy sales of an individual area), η is the number of selected areas to supply energy and $p_r^i(t)$ is the cooperative price offered by the selected area to the affected area which is formulated using:

$$p_r^i(t) = \begin{cases} E_{grid}^i(t+1) \cdot p(t+1), & E_{grid}^i(t+1) \geq 0 \\ \xi \cdot E_{dis}^i(t) \cdot C^i(t), & otherwise \end{cases} \tag{5.24}$$

where ξ is the profit margin of an area, E_{grid}^i is the energy purchased by an area from the grid.

The associated carbon footprints (CE) at any time instant can be calculated using:

$$CE(t) = CI \cdot \sum_{i=1}^{n} E_{grid}^i(t) \tag{5.25}$$

where CI is the carbon intensity and E_{grid}^i is the energy purchased by i^{th} area from the grid.

5.3 Results and Discussion

The primary objective of this study is to analyse the behavior of an energy system in response to uncertain events and develop strategies to mitigate their impact, with a particular emphasis on reducing overall carbon footprints. To achieve this, we have considered nine regions (i.e., LCs) within England, each comprising multiple areas (denoted by A) as depicted in Fig. 5.4. One such LC (Newcastle) consisting of ten areas is highlighted in this figure. These areas are further equipped with DERs to meet their respective load demands.

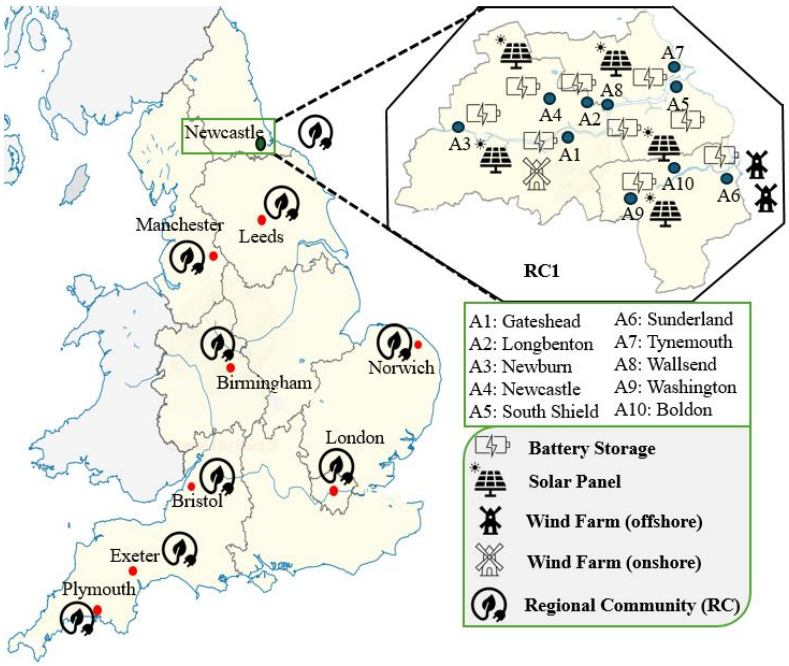

Figure 5.4: Considered areas of England for simulation

In our model, RC is responsible for managing incoming and outgoing energy requests within its respective LC, while the GC checks energy scheduling and coordination at the regional level. By focusing on reducing carbon footprints, the study aims to enhance the sustainability of the energy DN under uncertainty. For instance, when an uncertainty such as a sudden drop in renewable generation occurs, the RC would first seek to balance the energy deficit using stored renewable energy within the respective LC or by purchasing surplus renewable energy from

neighboring LCs. Only as a last resort would the AC draw energy from the main grid, thereby minimising the carbon impact.

Assumptions: To effectively simulate the system's behavior in handling uncertainties, the proposed study has made the following realistic assumptions.

- The types of uncertainties that can occur in the DN are:
  - *Weather Uncertainty:* It relates to sudden weather changes that deviate from predicted values.
  - *Data Uncertainty:* It depicts faulty sensors or equipment failures that can lead to malicious data being received at the RC.
  - *Behavioral Uncertainty:* It is associated with sudden increases/decreases in load demand at the consumer end.
- During normal operation, the excess generation areas must sell energy to energy-deficient areas before selling it to the grid to minimise the overall carbon footprints.
- During an uncertain event, all the areas in an LC would support the area under uncertainty by selling their excess generation. If there is no excess renewable energy generation in any area, these areas will discharge their batteries to support their neighbouring area under uncertainty.

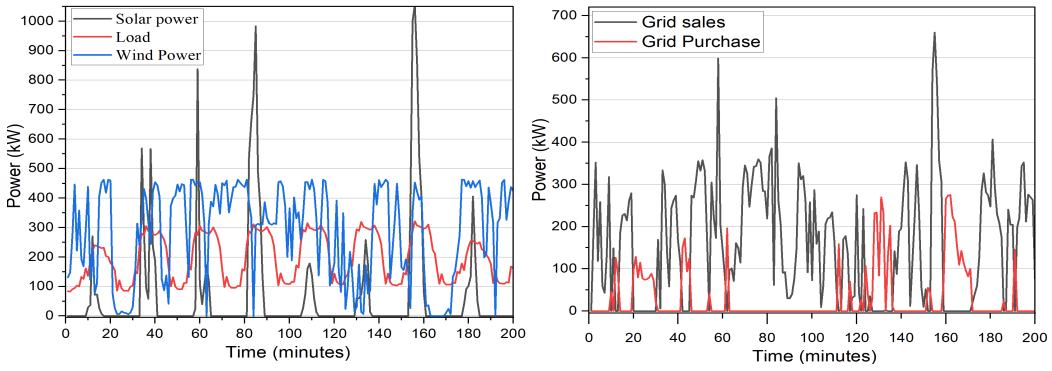

(a) (b)

Figure 5.5: Energy profile of an area (a) Power generation and load demand (b) Power sold and purchased from grid

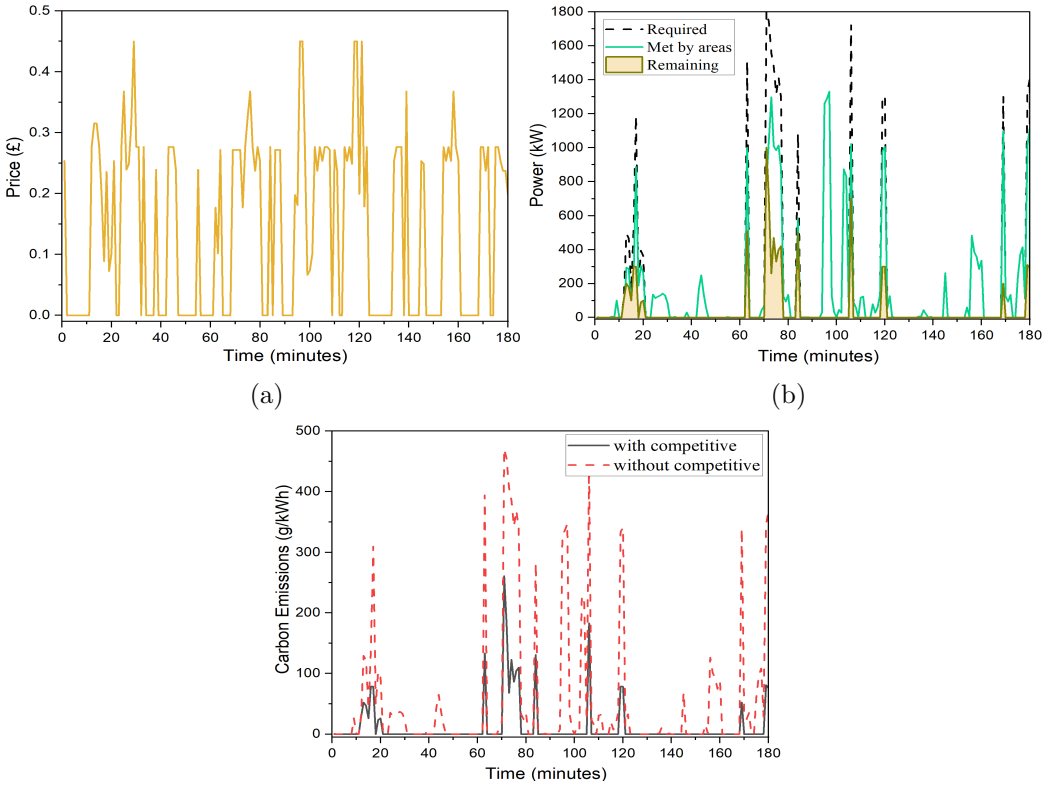

Figure 5.6: Healthy phase results (a) price offered by neighbouring area (b) energy demand met by areas (c) carbon emissions

5.3.1 Normal Phase

For normal operation, weather data was systematically collected for one year, spanning from Jan 01, 2023, to Dec 31, 2023 [102], from 10 distinct locations of Newcastle in CSV format. Each location's data is stored in a dedicated file and has 14 distinct meteorological parameters. The energy price data for energy sales and purchased is gathered from the UK's energy provider website [109]. It is assumed that the sensors deployed at each DER yield generation data estimated using Eq. (3.1) and Eq. (3.2) for solar and wind resources, respectively. The energy profile of one week for one area in Newcastle (i.e., Gateshead), is shown in Fig. 5.5. Fig. 5.5(a) depicts the wind and solar generation in this area as well as its overall load demand. Fig. 5.5(b) highlights the power purchased from the grid during low renewable energy generation and sold to the grid during high renewable energy

generation within the depicted time duration.

Furthermore, in the normal operational phase, all areas will be participating in the energy market based on their individual renewable energy generation. Fig. 5.6 shows the results based on the competitive approach for the entire region as described in Section 5.2.1 and the following inferences can be drawn. The market price offered by the areas with excess renewable energy generation is shown in Fig. 5.6(a). The zero price indicates that at that time instant there is no energy demand from the neighbouring areas and hence, no energy would be sold to any area. Fig. 5.6(b) shows the amount of energy met by the surplus renewable energy in the neighbouring areas using the competitive approach. When there is no surplus energy, the remaining energy demand is met by purchasing from the grid. The comparison of carbon footprints with and without using the competitive approach is highlighted in Fig. 5.6(c). As the major amount of energy demand is met by the excess generation of neighbouring areas, therefore, the proportion of energy purchased from the grid is reduced, resulting in a reduction in carbon emissions by approximately 80%.

5.3.2 Uncertainty Detection and Identification

To detect and identify the occurrence of uncertain events, the BN approach as described in Section 5.2.2 is utilised. A structured data discretisation process is implemented by employing a hierarchical method to convert the extensive dataset into finite states, thereby enhancing its tractability. The discretisation procedure serves to simplify the interpretation of real-world instances, obviating the necessity for specialised expertise. For instance, wind speed is discretised into three distinct states namely low, medium, and high (as shown in Fig. 5.7), providing a lucid framework to interpret the findings. The correlation between various parameter states along with their conditional probability is computed using a complex BN algorithm as discussed in algorithm 5.3. The correlation output of wind speed with other weather parameters is shown in Fig. 5.7 and the corresponding conditional

probability table is illustrated in Table 5.6. This relationship, modeled using a BN approach, is further utilised to find the range of uncertain parameters affected by the variations in other considered parameters.

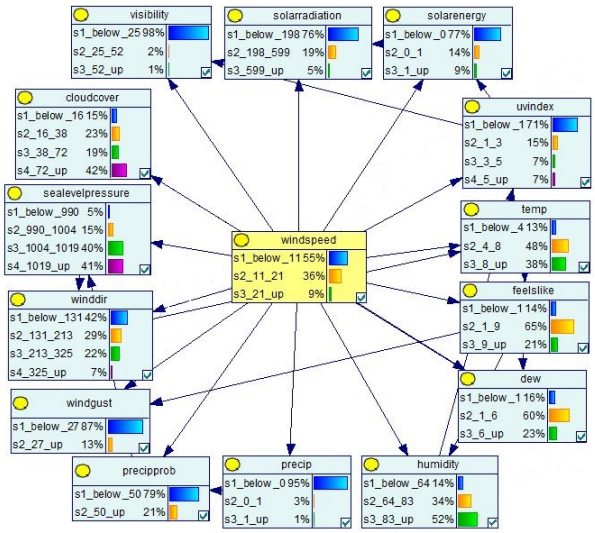

Figure 5.7: Dependence of wind speed on weather parameters

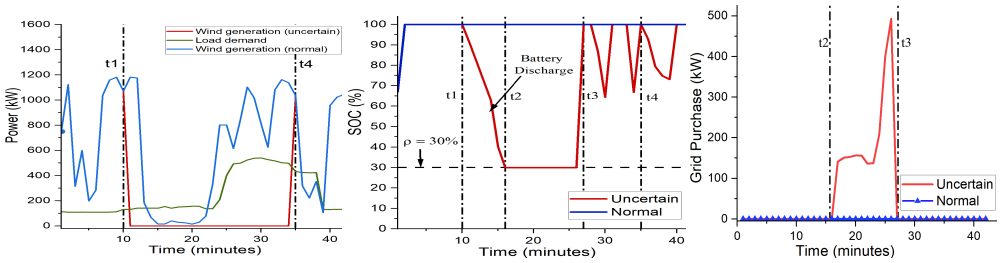

(a) (b) (c)

Figure 5.8: Impact of uncertainty on (a) wind generation (b) SOC of the battery (c) power purchase from grid

After computing the range of values for solar radiation and wind speed, their respective power generation in each area with the help of Eq. (3.1) and (3.2) are then computed and compared with their real-time values. We have chosen one

Table 5.6: CPT for windspeed and other weather parameters

windgust (%)	**windgust (<27)**	**windgust (>27)**	**windgust (>27)**
winddir (%)	**winddir (<131)**	**winddir (<131)**	**winddir (>325)**
sealevelpressure (%)	**sealevelpressure (<990)**	**sealevelpressure (<990)**	**sealevelpressure (<990)**
cloudcover (%)	**cloudcover (<16)**	**cloudcover (<16)**	**cloudcover (<16)**
windspeed (<11)	25%	2%	18%
windspeed (>11 & <21)	74%	75%	30%
windspeed (>21)	1%	23%	52%

specific area A5 (i.e., Southshields) from Fig. 5.4 to show the detailed impact of uncertainty. On detection of an uncertain event in A5, the type of uncertainty is identified using Algorithm 5.3. Based on the algorithm, the area A5 suffers from data uncertainty at time $t1$, due to which its measured wind generation becomes zero, which was resolved by time $t4$ as shown in Fig. 5.8(a). Consequently, the local energy supply is disrupted, prompting the utilisation of battery storage to meet the load demand that can be seen from decreasing the SOC of the battery in Fig. 5.8(b). After $t2$, the battery is discharged to its maximum capacity, the area becomes dependent either on the grid or other neighbouring areas to buy energy to meet the load demand. There is an increase in grid purchase from $t2$ to $t3$ to meet the load demand of A5 (Fig. 5.8(c)), which corresponds to no excess renewable generation available from neighboring areas. From $t3$ to $t4$, the grid purchases became zero, showing that there is excess renewable energy generation in the neighbouring areas which is purchased by A5 to meet its load demand and charge the battery until the uncertainty is resolved at $t4$.

5.3.3 Uncertainty Mitigation

Upon uncertain event detection in phase B, our research employs a cooperative strategy to address the uncertainty in affected areas and minimise its impact on the overall operation of the DN. The battery storage of area A5 with uncertain event along with the battery storage of all neighbouring areas is leveraged in the cooperative strategy as detailed in Section 5.2.3. In Fig. 5.9, SOC profiles of batteries from different areas selected using the algorithm 5.4 during uncertain situations are depicted. We compare two distinct scenarios where energy discharge from battery storage is managed equally and proportionately among selected areas to meet the load demand of the affected area. Fig. 5.9(a) shows the outcome when an equal amount of energy is drawn from the battery storage across all selected areas. When energy discharge is uniform across all areas, the SOC trajectory shows fluctuations and fails to reach its maximum capacity, indicative of sub-optimal

battery utilisation and potentially accelerated degradation. Fig. 5.9(b) showcases a strategic approach, distributing energy discharge in proportion to each area's capacity using the cooperative algorithm.

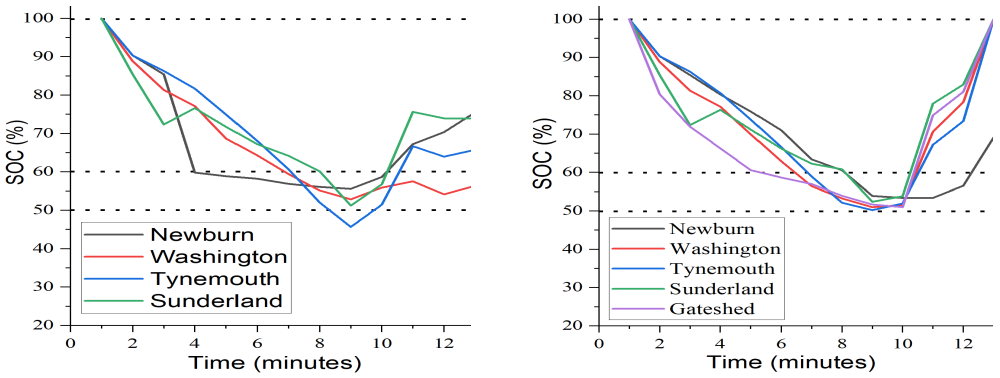

(a) (b)

Figure 5.9: SOC of different areas using cooperative approach when energy is shared (a) equally (b) proportionally

Under the proportionate energy discharge strategy, there is a smooth trend in the battery's discharge and recharge cycles. This smoother operational pattern hints at reduced battery degradation, attributed to the balanced and optimised utilisation of energy resources across the network.

We further extend our analysis to compare the overall profit and carbon emissions during uncertainty using three different strategies: competitive, cooperative-equal sharing, and cooperative-proportionate sharing as shown in Fig. 5.10.

Fig. 5.10(a) illustrates the overall profit during the uncertain period. The results indicate that the competitive algorithm achieves 16.4% higher profit as compared to the cooperative-proportionate sharing method. This is because the competitive strategy prioritises the maximisation of an individual area's profit. However, the higher profit comes at a significant environmental cost. Fig. 5.10(b) presents a comparison of carbon emissions among the three strategies. It demonstrates that the reduction in carbon emissions between the two methods ranges from 0% to 97% throughout the uncertain scenario considered, with an average reduction of 48.2% with the cooperative proportionate sharing method as compared to the competitive

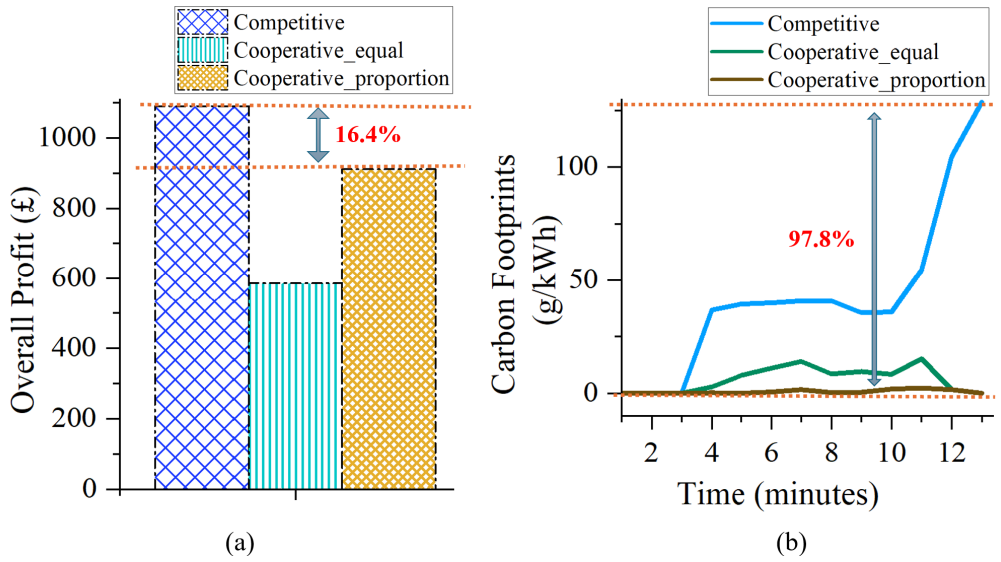

Figure 5.10: Comparison of different approaches under uncertainty for (a) overall profit (b) carbon footprints

approach.

Overall, the competitive algorithm is used under normal conditions to maximise immediate profits without overburdening the batteries. In contrast, the cooperative-proportionate strategy is employed during uncertainties, leveraging the battery storage capacities of neighboring areas to support the affected area. This two-fold approach ensures both the economic benefits and environmental sustainability of the energy system, optimising resource utilisation during normal operations, and enhancing reliability during uncertain conditions.

5.4 Summary

The integration of DERs into DNs introduces various uncertainties, such as unpredictable renewable energy outputs, fluctuating consumer energy demands, and data or equipment faults. In this study, we implemented a two-fold strategy to manage the system under normal and uncertain conditions. During normal operations, a competitive algorithm maximises profit and ensures efficient market functioning, along with cutting down carbon footprints to one-fifth. In contrast,

during uncertain conditions, a cooperative strategy with proportionate sharing stabilises the system by utilising the battery storage capacities of neighboring areas. Our results show that the cooperative-proportionate sharing method significantly reduces carbon emissions by a maximum of 97% compared to the competitive algorithm during uncertainty with an average reduction of 48.2%, while also ensuring a smoother SOC trend and reducing battery degradation. This approach balances economic and environmental outcomes, enhancing the reliability and sustainability of renewable-integrated DNs.

Chapter 6

Conclusion

6.1 Contribution

With renewable energy penetration in the energy systems, we can achieve the net-zero emissions target by 2050. However, replacing the existing energy system with renewable energy systems incurs challenges associated with cost, reliability and operational uncertainties. To address these challenges, this thesis presents a comprehensive carbon intelligent framework that after optimal placing the RESs in the energy network, models the uncertainties in the planning stage and handles the real-time uncertainties during the operational stage. Therefore, the following are the key contributions of the thesis:

- An optimal planning solution – a trade-off between cost and emissions for the considered residential and hybrid load is evaluated. The techno-economic-environmental analysis presented in this work highlights different feasible combinations of distinct energy sources that could be employed to power the UK's energy sector. The environmental analysis carried out suggested the dominance of installing wind turbines based on the weather profile of the area. The technical analysis deduced the amount of energy exchange between households and the grid, while the economic parameters advised the energy users about the profit and the payback period for the optimal case.

- Furthermore, after optimal planning, the thesis discusses the impact of uncertain weather events on real-time power system operations. The integration of DERs into DNs introduces various uncertainties, such as unpredictable renewable energy output, fluctuating consumer energy demands, and data or equipment faults. To reduce this impact during operational planning and energy scheduling, we proposed a robust and time-coordinated uncertainty modelling strategy based on BNs. TCS dynamically adapts to time-varying distributions and incorporates temporal correlations, offering improvements over traditional MCMC methods. The results show that TCS maintains minimal voltage deviation during extreme weather, increases energy sold to the grid, and accurately models weather parameters for better energy scheduling. This enhances system resilience and stability during uncertain events obtained from the proposed performance metrics, ensuring real-time robustness and reduced carbon emissions.

- As it is difficult to predict real-time uncertainties, therefore, a two-fold strategy to manage the system under normal and uncertain conditions is proposed. During normal operations, a competitive algorithm maximises profit and ensures efficient market functioning, along with cutting down carbon footprints to one-fifth. In contrast, during uncertain conditions, a cooperative strategy with proportionate sharing stabilises the system by utilising the battery storage capacities of neighboring areas. Our results show that the cooperative-proportionate sharing method significantly reduces carbon emissions by a maximum of 97% compared to the competitive algorithm during uncertainty with an average reduction of 48.2%, while also ensuring a smoother SOC trend and reducing battery degradation. This approach balances economic and environmental outcomes, enhancing the reliability and sustainability of renewable-integrated DNs.

6.2 Future work

The consumer load pattern modelling is highly unpredictable and challenging as it depends on a number of factors such as lifestyle, weather, holidays, family events, etc. In the future, the work will focus on accurate modelling of the uncertainty arising due to unpredictable consumer behavior at the planning stage and further reducing its impact on DN operations. Furthermore, the long-term and short-term impact of renewable energy integration with the grid on economic and environmental sustainability will be examined.

Moreover, the existing literature assumes deterministic charging patterns for electric vehicles (EVs). However, EV's charging and discharging patterns are dynamic in nature and are difficult to model. Therefore, the hybrid energy system considered in chapter 4 could be extended to integrate EVs along with the RESs in the DNs by using the probabilistic/stochastic modelling for EV's charging and discharging patterns.

The cooperative approach proposed in this thesis would be further extended to find the optimal storage reserve required by the communities such that the overall carbon emissions and cost of energy are minimised before, during and after an uncertain event without disturbing the usual operations of the DN.

Bibliography

[1] "Net zero by 2050: A roadmap for the global energy sector." 2021, [Online], Available: https://www.iea.org/events/net-zero-by-2050-a-roadmap-for-the-global-energy-system, [Accessed: May, 2022].

[2] V. Dhinakaran and S. A. Daniel, "New frontiers in solar power generation: A comprehensive review of solar power satellite schemes," in *2021 International Conference on Smart Generation Computing, Communication and Networking (SMART GENCON)*, pp. 1–5, Pune, India, 2021.

[3] "Shining brightly." 2022, [Online], Available: https://news.mit.edu/2011/energy-scale-part3-1026, [Accessed: October, 2022].

[4] P. Bojek, "Solar PV." 2022, [Online], Available: https://www.iea.org/reports/solar-pv, [Accessed: December, 2022].

[5] P. Zhao, C. Gu, D. Huo, Y. Shen, and I. Hernando-Gil, "Two-stage distributionally robust optimization for energy hub systems," *IEEE Transactions on Industrial Informatics*, vol. 16, no. 5, pp. 3460–3469, 2019.

[6] S. Grijalva, "Computational challenges and analysis under increasingly dynamic and uncertain electric power system conditions," in *2012 IEEE Power and Energy Society General Meeting*, pp. 1–2, San Diego, CA, USA, 2012.

[7] A. Jindal, "Data analytics of smart grid environment for efficient management of demand response," *Doctoral Thesis, Thapar University*, 2018. Available: `http://hdl.handle.net/10266/5405`.

[8] A. Jindal, N. Kumar, and G. S. Aujla, *Internet of Energy for Smart Cities: Machine Learning Models and Techniques*. CRC Press, 2021.

[9] H. Ritchie, M. Roser, and P. Rosado, "Renewable energy." 2024, [Online], Available: `https://ourworldindata.org/renewable-energy`, Accessed: March, 2024.

[10] H. Ritchie, M. Roser, and P. Rosado, "CO_2 and greenhouse gas emissions." 2023, [Online], Available: `https://ourworldindata.org/co2-and-other-greenhouse-gas-emissions`, [Accessed: June, 2023].

[11] D. Carver, "Who are the biggest emitters?." 2022, [Online], Available: `https://commonslibrary.parliament.uk/global-net-zero-commitments/`, [Accessed: May, 2022].

[12] "Powering up britain- net-zero growth plan." 2022, [Online], Available: https://assets.publishing.service.gov.uk/government/uploads/system/uploads/attachment_data/file/1147457/powering-up-britain-net-zero-growth-plan.pdf, [Accessed: May, 2023].

[13] T. Nation, "Introducing: the 32 companies joining net zero 2.0." 2022, [Online], Available: `https://technation.io/news/climate-tech-companies-net-zero-2021/`, [Accessed: July, 2022].

[14] H. Ritchie, P. Rosado, and M. Roser, "Breakdown of carbon dioxide, methane and nitrous oxide emissions by sector." 2020, [Online], Available: `https://ourworldindata.org/emissions-by-sector`, [Accessed: November, 2020].

[15] BBC, "Uk to finish with coal power after 142 years." 2024, [Online], Available: `https://www.bbc.co.uk/news/articles/c5y35qz73n8o`, [Accessed: August, 2024].

[16] Gov.UK, "Offshore wind net zero investment roadmap." 2023, [Online], Available: `https://www.gov.uk/government/publications/offshore-wind-net-zero-investment-roadmap`, [Accessed: September, 2023].

[17] "Massive expansion of renewable power opens door to achieving global tripling goal set at cop28." 2024, [Online], Available: https://www.iea.org/news/massive-expansion-of-renewable-power-opens-door-to-achieving-global-tripling-goal-set-at-cop28,[Accessed: May, 2024].

[18] F. Luo, Q. Bu, Z. Ye, Y. Yuan, L. Gao, and P. Lv, "Dynamic reconstruction strategy of distribution network based on uncertainty modeling and impact analysis of wind and photovoltaic power," *IEEE Access*, vol. 12, pp. 64069–64078, 2024.

[19] Q.-H. Wu, A. Bose, C. Singh, J. H. Chow, G. Mu, Y. Sun, Z. Liu, Z. Li, and Y. Liu, "Control and stability of large-scale power system with highly distributed renewable energy generation: Viewpoints from six aspects," *CSEE Journal of Power and Energy Systems*, vol. 9, no. 1, pp. 8–14, 2023.

[20] A. Jindal, A. K. Marnerides, A. Gouglidis, A. Mauthe, and D. Hutchison, "Communication standards for distributed renewable energy sources integration in future electricity distribution networks," in *ICASSP 2019-2019 IEEE International Conference on Acoustics, Speech and Signal Processing (ICASSP)*, pp. 8390–8393, Brighton, UK, 2019.

[21] L. Chen, L. Liu, Y. Peng, W. Chen, H. Huang, T. Wu, and X. Xu, "Distribution network operational risk assessment and early warning considering multi-risk factors," *IET Generation, Transmission & Distribution*, vol. 14, no. 16, pp. 3139–3149, 2020.

[22] D. P. Loucks and E. van Beek, *An Introduction to Probability, Statistics, and Uncertainty*, pp. 213–300. Cham: Springer International Publishing, 2017.

[23] A. Radovanović, R. Koningstein, I. Schneider, B. Chen, A. Duarte, B. Roy, D. Xiao, M. Haridasan, P. Hung, N. Care, *et al.*, "Carbon-aware computing for datacenters," *IEEE Transactions on Power Systems*, vol. 38, no. 2, pp. 1270–1280, 2022.

[24] D. Yi, X. Zhou, Y. Wen, and R. Tan, "Toward efficient compute-intensive job allocation for green data centers: A deep reinforcement learning approach," in *2019 IEEE 39th International Conference on Distributed Computing Systems (ICDCS)*, pp. 634–644, Dallas, Texas, USA, 2019.

[25] G. Smpokos, M. A. Elshatshat, A. Lioumpas, and I. Iliopoulos, "On the energy consumption forecasting of data centers based on weather conditions: Remote sensing and machine learning approach," in *2018 11th International Symposium on Communication Systems, Networks & Digital Signal Processing (CSNDSP)*, pp. 1–6, Budapest, Hungary, 2018.

[26] Y. Li, Y. Wen, D. Tao, and K. Guan, "Transforming cooling optimization for green data center via deep reinforcement learning," *IEEE transactions on cybernetics*, vol. 50, no. 5, pp. 2002–2013, 2019.

[27] J. Ramanujam and U. P. Singh, "Copper indium gallium selenide based solar cells–a review," *Energy & Environmental Science*, vol. 10, no. 6, pp. 1306–1319, 2017.

[28] G. D'Amico, F. Petroni, and S. Vergine, "Ramp rate limitation of wind power: An overview," *Energies*, vol. 15, no. 16, p. 5850, 2022.

[29] O. Krishan and S. Suhag, "Techno-economic analysis of a hybrid renewable energy system for an energy poor rural community," *Journal of Energy Storage*, vol. 23, pp. 305–319, 2019.

[30] T. Ma and M. S. Javed, "Integrated sizing of hybrid PV-wind-battery system for remote island considering the saturation of each renewable energy resource," *Energy conversion and management*, vol. 182, pp. 178–190, 2019.

[31] N. M. Kumar, S. S. Chopra, A. A. Chand, R. M. Elavarasan, and G. Shafiullah, "Hybrid renewable energy microgrid for a residential community: A techno-economic and environmental perspective in the context of the SDG7," *Sustainability*, vol. 12, no. 10, p. 3944, 2020.

[32] A. Mostafaeipour, A. Bidokhti, M.-B. Fakhrzad, A. Sadegheih, and Y. Z. Mehrjerdi, "A new model for the use of renewable electricity to reduce carbon dioxide emissions," *Energy*, vol. 238, p. 121602, 2022.

[33] R. Chopra, C. Magazzino, M. I. Shah, G. D. Sharma, A. Rao, and U. Shahzad, "The role of renewable energy and natural resources for sustainable agriculture in ASEAN countries: Do carbon emissions and deforestation affect agriculture productivity?," *Resources Policy*, vol. 76, p. 102578, 2022.

[34] M. Butturi, F. Lolli, M. Sellitto, E. Balugani, R. Gamberini, and B. Rimini, "Renewable energy in eco-industrial parks and urban-industrial symbiosis: A literature review and a conceptual synthesis," *Applied Energy*, vol. 255, p. 113825, 2019.

[35] S. M. Ali, A.-A. A. Mohamed, and A. Hemeida, "A pareto strategy based on multi-objective for optimal placement of distributed generation considering voltage stability," in *2019 International Conference on Innovative Trends in Computer Engineering (ITCE)*, pp. 498–504, Aswan, Egypt, 2019.

[36] S. Saha and V. Mukherjee, "A novel multi-objective modified symbiotic organisms search algorithm for optimal allocation of distributed generation in radial distribution system," *Neural Computing and Applications*, vol. 33, no. 6, pp. 1751–1771, 2021.

[37] O. Khoubseresht and H. Shayanfar, "The role of demand response in optimal sizing and siting of distribution energy resources in distribution network with time-varying load: An analytical approach," *Electric Power Systems Research*, vol. 180, p. 106100, 2020.

[38] A. A. Abou El-Ela, R. A. El-Sehiemy, and A. S. Abbas, "Optimal placement and sizing of distributed generation and capacitor banks in distribution systems using water cycle algorithm," *IEEE Systems Journal*, vol. 12, no. 4, pp. 3629–3636, 2018.

[39] A. Rastgou, J. Moshtagh, and S. Bahramara, "Improved harmony search algorithm for electrical distribution network expansion planning in the presence of distributed generators," *Energy*, vol. 151, pp. 178–202, 2018.

[40] M. A. Tolba, H. Rezk, V. Tulsky, A. A. Z. Diab, A. Y. Abdelaziz, and A. Vanin, "Impact of optimum allocation of renewable distributed generations on distribution networks based on different optimization algorithms," *Energies*, vol. 11, no. 1, p. 245, 2018.

[41] B. Poornazaryan, P. Karimyan, G. Gharehpetian, and M. Abedi, "Optimal allocation and sizing of dg units considering voltage stability, losses and load variations," *International Journal of Electrical Power & Energy Systems*, vol. 79, pp. 42–52, 2016.

[42] S. Pazouki, A. Mohsenzadeh, S. Ardalan, and M.-R. Haghifam, "Optimal place, size, and operation of combined heat and power in multi carrier energy networks considering network reliability, power loss, and voltage profile," *IET Generation, Transmission & Distribution*, vol. 10, no. 7, pp. 1615–1621, 2016.

[43] W. Liu, H. Xu, S. Niu, and J. Xie, "Optimal distributed generator allocation method considering voltage control cost," *Sustainability*, vol. 8, no. 2, p. 193, 2016.

[44] M. Kefayat, A. L. Ara, and S. N. Niaki, "A hybrid of ant colony optimization and artificial bee colony algorithm for probabilistic optimal placement and sizing of distributed energy resources," *Energy Conversion and Management*, vol. 92, pp. 149–161, 2015.

[45] H. Louie and K. Strunz, "Hierarchical multiobjective optimization for independent system operators (isos) in electricity markets," *IEEE Transactions on Power Systems*, vol. 21, no. 4, pp. 1583–1591, 2006.

[46] L. F. Ochoa, A. Padilha-Feltrin, and G. P. Harrison, "Evaluating distributed time-varying generation through a multiobjective index," *IEEE Transactions on Power Delivery*, vol. 23, no. 2, pp. 1132–1138, 2008.

[47] L. F. Ochoa, C. J. Dent, and G. P. Harrison, "Distribution network capacity assessment: Variable dg and active networks," *IEEE Transactions on Power Systems*, vol. 25, no. 1, pp. 87–95, 2009.

[48] P. Denholm and M. Hand, "Grid flexibility and storage required to achieve very high penetration of variable renewable electricity," *Energy Policy*, vol. 39, no. 3, pp. 1817–1830, 2011.

[49] S. You, C. Traeholt, and B. Poulsen, "A market-based virtual power plant," in *2009 International Conference on Clean Electrical Power*, pp. 460–465, Capri, Italy, 2009.

[50] A. Zakaria, F. B. Ismail, M. H. Lipu, and M. A. Hannan, "Uncertainty models for stochastic optimization in renewable energy applications," *Renewable Energy*, vol. 145, pp. 1543–1571, 2020.

[51] A. Qureshi, R. Weber, H. Balakrishnan, J. Guttag, and B. Maggs, "Cutting the electric bill for internet-scale systems," in *Proceedings of the ACM SIGCOMM 2009 conference on Data communication*, pp. 123–134, Barcelona, Spain, 2009.

[52] G. S. Aujla and N. Kumar, "Mensus: An efficient scheme for energy management with sustainability of cloud data centers in edge–cloud environment," *Future Generation Computer Systems*, vol. 86, pp. 1279–1300, 2018.

[53] S. Jebaraj and S. Iniyan, "A review of energy models," *Renewable and sustainable energy reviews*, vol. 10, no. 4, pp. 281–311, 2006.

[54] G. B. Choi, S. G. Lee, and J. M. Lee, "Multi-period energy planning model under uncertainty in market prices and demands of energy resources: A case study of korea power system," *Chemical Engineering Research and Design*, vol. 114, pp. 341–358, 2016.

[55] B. Alizadeh and S. Jadid, "Uncertainty handling in power system expansion planning under a robust multi-objective framework," *IET Generation, Transmission & Distribution*, vol. 8, no. 12, pp. 2012–2026, 2014.

[56] M. Alhazmi, P. Dehghanian, S. Wang, and B. Shinde, "Power grid optimal topology control considering correlations of system uncertainties," *IEEE Transactions on Industry Applications*, vol. 55, no. 6, pp. 5594–5604, 2019.

[57] O. Onojo, G. Chukwudebe, E. Okafor, and S. Ogbogu, "Feasibility investigation of a hybrid renewable energy system as a back up power supply for an ict building in nigeria," *Academic Research International*, vol. 4, no. 3, p. 149, 2013.

[58] R. Nürnberg and W. Römisch, "A two-stage planning model for power scheduling in a hydro-thermal system under uncertainty," *Optimization and Engineering*, vol. 3, pp. 355–378, 2002.

[59] K. N. Hasan, R. Preece, and J. V. Milanović, "Existing approaches and trends in uncertainty modelling and probabilistic stability analysis of power systems with renewable generation," *Renewable and Sustainable Energy Reviews*, vol. 101, pp. 168–180, 2019.

[60] K. H. M. Azmi, N. A. M. Radzi, N. A. Azhar, F. S. Samidi, I. T. Zulkifli, and A. M. Zainal, "Active electric distribution network: applications, challenges, and opportunities," *IEEE Access*, vol. 10, pp. 134655–134689, 2022.

[61] C. C. G. Rodríguez and S. Servigne, "Managing sensor data uncertainty: a data quality approach," *International Journal of Agricultural and Environmental Information Systems*, vol. 4, no. 1, pp. 35–54, 2013.

[62] N. Kang, R. Bhattarai, J. T. Reilly, and S. Ahmed, "Impact of high penetration distributed energy resources on the bulk electric system," tech. rep., Argonne National Lab.(ANL), Argonne, IL (United States); Reilly Associates …, 2021.

[63] A. Hentunen, J. Forsströmm, and V. Mukherjee, "Smart system of renewable energy storage based on integrated EVs and batteries to empower mobile, distributed and centralised energy storage in the distribution grid," *Horizon*, 2020.

[64] Q. Shi, W. Liu, B. Zeng, H. Hui, and F. Li, "Enhancing distribution system resilience against extreme weather events: Concept review, algorithm summary, and future vision," *International Journal of Electrical Power & Energy Systems*, vol. 138, p. 107860, 2022.

[65] E. F. Bødal, P. C. Del Granado, H. Farahmand, M. Korpås, P. Olivella, I. Munné, and P. Lloret, "Challenges in distribution grid with high penetration of renewables," *NTNU Open*, 2018, [Online], Available: http://hdl.handle.net/11250/2589060.

[66] X. Cao, J. Wang, and B. Zeng, "A chance constrained information-gap decision model for multi-period microgrid planning," *IEEE Transactions on Power Systems*, vol. 33, no. 3, pp. 2684–2695, 2017.

[67] Y. Jiang, C. Wan, C. Chen, M. Shahidehpour, and Y. Song, "A hybrid stochastic-interval operation strategy for multi-energy microgrids," *IEEE Transactions on Smart Grid*, vol. 11, no. 1, pp. 440–456, 2019.

[68] U. Oh, Y. Lee, J. Choi, and R. Karki, "Reliability evaluation of power system considering wind generators coordinated with multi-energy storage systems," *IET Generation, Transmission & Distribution*, vol. 14, no. 5, pp. 786–796, 2020.

[69] H. Fan, C. Wang, L. Liu, and X. Li, "Review of uncertainty modeling for optimal operation of integrated energy system," *Frontiers in energy research*, vol. 9, p. 641337, 2022.

[70] M. Aien, A. Hajebrahimi, and M. Fotuhi-Firuzabad, "A comprehensive review on uncertainty modeling techniques in power system studies," *Renewable and Sustainable Energy Reviews*, vol. 57, pp. 1077–1089, 2016.

[71] A. K. Khamees, A. Y. Abdelaziz, M. R. Eskaros, M. A. Attia, and A. O. Badr, "The mixture of probability distribution functions for wind and photovoltaic power systems using a metaheuristic method," *Processes*, vol. 10, no. 11, p. 2446, 2022.

[72] T. Ding, Q. Yang, Y. Yang, C. Li, Z. Bie, and F. Blaabjerg, "A data-driven stochastic reactive power optimization considering uncertainties in active distribution networks and decomposition method," *IEEE Transactions on Smart Grid*, vol. 9, no. 5, pp. 4994–5004, 2017.

[73] R. Khodabakhsh and S. Sirouspour, "Optimal control of energy storage in a microgrid by minimizing conditional value-at-risk," *IEEE Transactions on Sustainable Energy*, vol. 7, no. 3, pp. 1264–1273, 2016.

[74] T. Su, J. Zhao, Y. Pei, and F. Ding, "Probabilistic physics-informed graph convolutional network for active distribution system voltage prediction," *IEEE Transactions on Power Systems*, vol. 38, no. 6, pp. 5969–5972, 2023.

[75] S. Hosseini and M. Sarder, "Development of a bayesian network model for optimal site selection of electric vehicle charging station," *International Journal of Electrical Power & Energy Systems*, vol. 105, pp. 110–122, 2019.

[76] T. Adedipe, M. Shafiee, and E. Zio, "Bayesian network modelling for the wind energy industry: An overview," *Reliability Engineering & System Safety*, vol. 202, p. 107053, 2020.

[77] M. A. Rahim, "Unveiling weather-induced blackouts: A ten-year analysis with deep learning-driven power resilience enhancement," *IEEE Access*, vol. 12, pp. 62958–62963, 2024.

[78] C. Pan *et al.*, "Modeling the reserve capacity of wind power and the inherent decision-dependent uncertainty in the power system economic dispatch," *IEEE Transactions on Power Systems*, vol. 38, no. 5, pp. 4404–4417, 2023.

[79] C. Zhu, Y. Zhang, Z. Yan, and J. Zhu, "A nested mcmc method incorporated with atmospheric process decomposition for photovoltaic power simulation," *IEEE Transactions on Sustainable Energy*, vol. 11, no. 4, pp. 2972–2984, 2020.

[80] X. Lin *et al.*, "Application of joint raw moments-based probabilistic power flow analysis for hybrid ac/vsc-mtdc power systems," *IEEE Transactions on Power Systems*, vol. 37, no. 2, pp. 1399–1412, 2022.

[81] H. Wang, Z. Yan, M. Shahidehpour, Q. Zhou, and X. Xu, "Optimal energy storage allocation for mitigating the unbalance in active distribution network via uncertainty quantification," *IEEE Transactions on Sustainable Energy*, vol. 12, no. 1, pp. 303–313, 2021.

[82] Á. Paredes, J. A. Aguado, and P. Rodríguez, "Uncertainty-aware trading of congestion and imbalance mitigation services for multi-dso local flexibility markets," *IEEE Transactions on Sustainable Energy*, vol. 14, no. 4, pp. 2133–2146, 2023.

[83] H. Ritchie, M. Roser, and P. Rosado, "CO_2 and greenhouse gas emissions." 2020, [Online], Available:`https://ourworldindata.org/co2-and-other-greenhouse-gas-emissions`, [Accessed: January, 2023].

[84] G. Piggott, "Electricity consumption in a sample of london households." 2022, [Online], Available:`https://data.london.gov.uk/blog/`

`electricity-consumption-in-a-sample-of-london-households`, [Accessed: May, 2022], 2015.

[85] REopt, "Renewable energy integration and optimisation." 2023, [Online], Available: `https://www.nrel.gov/reopt/`, [Accessed: June, 2023].

[86] R. J. J. Molu, S. R. D. Naoussi, P. Wira, W. F. Mbasso, S. T. Kenfack, B. K. Das, E. Ali, M. J. Alshareef, and S. S. Ghoneim, "Optimizing technical and economic aspects of off-grid hybrid renewable systems: A case study of manoka island, cameroon," *IEEE Access*, vol. 11, pp. 130909–130930, 2023.

[87] Energy & Industrial Strategy, "Energy bills support factsheet." 2022, [Online], Available:`https://www.gov.uk/government/publications/energy-bills-support`, [Accessed: November, 2022].

[88] N.-C. Yang and C.-H. Tseng, "Adaptive convergence enhancement strategies for newton–raphson power flow solutions in distribution networks," *IET Generation, Transmission & Distribution*, vol. 18, no. 13, pp. 2339–2352, 2024.

[89] H. Energy, "Homer software for optimisation." 2022, [Online], Available: `https://homerenergy.com/`, [Accessed: May, 2022].

[90] L. Xu *et al.*, "Resilience of renewable power systems under climate risks," *Nature Reviews Electrical Engineering*, vol. 1, no. 1, pp. 53–66, 2024.

[91] K. Micek, "California utilities work to restore power after tropical storm hilary." 2023, [Online], Available: https://www.spglobal.com/commodityinsights/en/market-insights/latest-news/electric-power/082123-california-utilities-work-to-restore-power-related-to-tropical-storm-hilary, [Accessed: November, 2023].

[92] A. Garg, G. S. Aujla, and H. Sun, "Analyzing impact of data uncertainty in distributed energy resources using bayesian networks," in *2023 IEEE Interna-*

tional Conference on Communications, Control, and Computing Technologies for Smart Grids (SmartGridComm), pp. 1–6, Glassgow, Scotland, UK, 2023.

[93] A. Garg, G. S. Aujla, and H. Sun, "Techno-economic-environmental analysis for net-zero sustainable residential buildings," in *2023 IEEE PES Innovative Smart Grid Technologies Europe (ISGT EUROPE)*, pp. 1–5, Grenoble, France, 2023.

[94] B. Han, Y. Zahraoui, M. Mubin, S. Mekhilef, M. Seyedmahmoudian, and A. Stojcevski, "Home energy management systems: A review of the concept, architecture, and scheduling strategies," *IEEE Access*, vol. 11, pp. 19999–20025, 2023.

[95] X. Liu, D. Ai, S. Wang, H. Liu, and T. Yin, "Medium and long-term optimal scheduling for community integrated energy system with hydrogen energy storage," in *2023 4th International Conference on Advanced Electrical and Energy Systems (AEES)*, pp. 812–818, Shanghai, China, 2023.

[96] M. Ertem, "Renewable energy-aware machine scheduling under intermittent energy supply," *IEEE Access*, vol. 12, pp. 23613–23625, 2024.

[97] P. K. Saha, N. Chakraborty, A. Mondal, and S. Mondal, "Intelligent real-time utilization of hybrid energy resources for cost optimization in smart microgrids," *IEEE Systems Journal*, vol. 18, no. 1, pp. 186–197, 2024.

[98] S. Sharma, Y. Xu, A. Verma, and B. K. Panigrahi, "Time-coordinated multienergy management of smart buildings under uncertainties," *IEEE Transactions on Industrial Informatics*, vol. 15, no. 8, pp. 4788–4798, 2019.

[99] S. M. Shawon, X. Liang, and M. Janbakhsh, "Optimal placement of distributed generation units for microgrid planning in distribution networks," *IEEE Transactions on Industry Applications*, vol. 59, no. 3, pp. 2785–2795, 2023.

[100] "Increasing time granularity in electricity markets." 2019, [Online], Available: https://www.irena.org/-/media/Files/IRENA/Agency/Publication/2019/Feb/IRENA$_{I}ncreasing_{t}ime_{g}ranularity_{2}019.$

[101] S. H. Dolatabadi, M. Ghorbanian, P. Siano, and N. D. Hatziargyriou, "An enhanced ieee 33 bus benchmark test system for distribution system studies," *IEEE Transactions on Power Systems*, vol. 36, no. 3, pp. 2565–2572, 2021.

[102] "Weather data." 2023, [Online], Available:`https://www.visualcrossing.com/weather/weather-data-services`, [Accessed: March, 2023].

[103] M. Kendon, "Storm debi." 2023, [Online], Available: `https://www.metoffice.gov.uk/binaries/content/assets/metofficegovuk/pdf/weather/learn-about/uk-past-events/interesting/2023/2023_10_storm_debi.pdf`, [Accessed: January, 2024].

[104] C. Karras, A. Karras, M. Avlonitis, and S. Sioutas, *An Overview of MCMC Methods: From Theory to Applications*, p. 319–332. 06 2022.

[105] X. Wang, S. Li, and M. Iqbal, "Live power generation predictions via ai-driven resilient systems in smart microgrids," *IEEE Transactions on Consumer Electronics*, vol. 70, no. 1, pp. 3875–3884, 2024.

[106] "Most of bangladesh left without power after national grid failure." 2023, [Online], Available: `https://edition.cnn.com/2022/10/04/asia/bangladesh-blackouts-power-grid-failure-intl/index.html/`, [Accessed: January, 2024].

[107] "IEEE standard for interconnection and interoperability of distributed energy resources with associated electric power systems interfaces," *IEEE Std 1547-2018 (Revision of IEEE Std 1547-2003)*, pp. 1–138, 2018.

[108] R. Deng, Z. Yang, F. Hou, M.-Y. Chow, and J. Chen, "Distributed real-time demand response in multiseller–multibuyer smart distribution grid," *IEEE Transactions on Power Systems*, vol. 30, no. 5, pp. 2364–2374, 2015.

[109] "Energy prices." 2024, [Online], Available: /urlhttps://octopus.energy/octopus-smart-tariffs/, [Accessed: July, 2024].

[110] D. Dragone, L. Lambertini, and A. Palestini, "Static and dynamic best-response potential functions for the non-linear cournot game," *Optimization*, vol. 61, no. 11, pp. 1283–1293, 2012.